ISTANBUL TECHNICAL UNIVERSITY ★ GRADUATE SCHOOL OF SCIENCE ENGINEERING AND TECHNOLOGY

INVESTIGATING ALLOSTERIC SITES THAT ARE CRITICAL FOR ATPASE ACTIVATION IN HSP70 MOLECULAR CHAPERONE, DNAK, WHEN STIMULATED BY A SUBSTRATE

M.Sc. THESIS

Irem AVCILAR

Department of Advanced Technologies

Molecular Biology-Genetics and Biotechnology Programme

JANUARY 2012

ISTANBUL TECHNICAL UNIVERSITY ★ GRADUATE SCHOOL OF SCIENCE ENGINEERING AND TECHNOLOGY

INVESTIGATING ALLOSTERIC SITES THAT ARE CRITICAL FOR ATPASE ACTIVATION IN HSP70 MOLECULAR CHAPERONE, DNAK, WHEN STIMULATED BY A SUBSTRATE

M.Sc. THESIS

Irem AVCILAR
(521091093)

Department of Advanced Technologies

Molecular Biology-Genetics and Biotechnology Programme

Thesis Advisor: Assist. Prof. Dr. Gizem DINLER DOGANAY

JANUARY 2012

İSTANBUL TEKNİK ÜNİVERSİTESİ ★ FEN BİLİMLERİ ENSTİTÜSÜ

Escherichia coli HSP70 MOLEKÜLER ŞAPERON HOMOLOĞU DNAK PROTEİNİNDE ATPaz AKTİVİTESİNDEKİ ÖNEMLİ ALLOSTERİK BÖLGELERİN ARAŞTIRILMASI

YÜKSEK LİSANS TEZİ

İrem AVCILAR
(521091093)

İleri Teknolojiler Anabilim Dalı

Moleküler Biyoloji-Genetik ve Biyoteknoloji Programı

Tez Danışmanı: Yrd. Doç. Dr. Gizem DİNLER DOĞANAY

OCAK 2012

İrem AVCILAR, a **M.Sc.** student of ITU **Graduate School of Science Engineering and Technology** student ID **521091093**, successfully defended the thesis entitled **"INVESTIGATING ALLOSTERIC SITES THAT ARE CRITICAL FOR ATPASE ACTIVATION IN HSP70 MOLECULAR CHAPERONE, DNAK, WHEN STIMULATED BY A SUBSTRATE"**, which she prepared after fulfilling the requirements specified in the associated legislations, before the jury whose signatures are below.

Thesis Advisor : Assist. Prof. Dr. Gizem DİNLER DOĞANAY .....
İstanbul Technical University

Jury Members : Assist. Prof. Dr. Bülent BALTA .....
İstanbul Technical University

Assoc. Prof. Dr. Berna SARIYAR AKBULUT .....
Marmara University

Date of Submission : 19 November 2011
Date of Defense : 26 January 2012

To my family and friends,

FOREWORD

I would like to thank my supervisior, Gizem DİNLER DOĞANAY for her guidance and great support in this study. She gave me the oppurtunity to be involved in this project with her excellent encouragement.

I would like to thank TÜBİTAK (The Scientific and Technical Research Council of Turkey) to support financially in my first step of academic career and to finance this project whose number is 110T434.

I also thank all my colleagues, especially Umut GÜNSEL, for their help in the laboratory work and for their friendship in my life.

I would also thank Sibel ÇETİNEL and Burak ÇALIŞKAN for their helpness for my thesis and friendship. I feel lucky to benefit from their experience and I have really learned much more things about the procedures of the thesis.

I also thank the colleagues who share the laboratory, Aslı KİREÇTEPE, Timuçin AVŞAR, Şule ERDEMİR, Gökçe ÇELİKYAPI ERDEM, Ceren ALKIM, Can HOLYAVKİN, Nazlı KOCAEFE, Koray KIRIMTAY, Meryem MENEKŞE and Havva Esra BIYIK for their help and friendliness.

I am greatful to my dear friends, Gökhan KÜÇÜKGÖZE, Süha AKAN, Deniz Tanıl YÜCESOY, Şerif KARABULUT and Nurcan VARDAR for their motivation not only in the school time but also in my daily life. They always cheered me up when I felt upset, exhausted and annoyed. I am sure that they are always with me in my whole life.

Lastly, I would like thank my family, my father İbrahim AVCILAR, my mother Nebahat AVCILAR, my brother Emre AVCILAR for their endless support, unlimited love and reliance for all the time. The important thing is that they have encouraged me all the time, not only in the school life.

December 2011 İrem AVCILAR

TABLE OF CONTENTS

Page

ABBREVIATIONS

ADP : Adenosine diphosphate
ATP : Adenosine triphosphate
Apaf-1 : Apoptotic protease activating factor 1
APS : Ammonium persulfate
bHsc70 : Consitutively expressed Hsp70 homolog in bovine
CARD : Caspase recruitment domain
CD : Circular dichroism
dATP : Deoxyadenosine triphosphate
dCTP : Deoxycytidine triphosphate
DEAE : Diethylaminoethyl
dGTP : Deoxyguanosine triphosphate
DnaJ : Hsp40 homolog of *Escherichia coli*
DnaK : Hsp70 homolog of *Escherichia coli*
DTT : Dithiothreitol
dTTP : Deoxythymidine triphospate
EDTA : Ethylenediaminetetraacetic acid
ERα : Estrogen reseptor α
GrpE : Nucleotide exchange factor homolog in *E. coli*
HCl : Hydrocloric acid
hHsp70 : human Hsp70
Hsp60 : Heat shock protein 60
Hsp70 : Heat shock protein 70
Hsp90 : Heat shock protein 90
Hsp110 : Heat shock protein 110
IPTG : Isopropyl β-D-1-thiogalactopyranoside
NAD : Nicotinamide adenine dinucleotide
NADH : Nicotinamide adenine dinucleotide hydrate
NBD : Nucleotide binding domain
NEF : Nucleotide exchange factor
NMR : Nuclear magnetic resonance
OD : Optical density
PCR : Polymerase chain reaction
PDB : Protein data bank
PEP : Phosphoenolpyruvic acid
PMSF : Phenylmethanesulfonylfluoride
RDC : Residual dipolar coupling
SBD : Substrate binding domain
SDS-PAGE : Sodium dodecyl sulfate polyacrylamide gel electrophoresis
TEMED : Tetramethylethylenediamine
TROSY : Transverse relaxation optimized spectroscopy
wt : Wild type

LIST OF TABLES

Page

LIST OF FIGURES

Page

INVESTIGATING ALLOSTERIC SITES THAT ARE CRITICAL FOR ATPASE ACTIVATION IN HSP70 MOLECULAR CHAPERONE, DNAK, WHEN STIMULATED BY A SUBSTRATE

SUMMARY

Hsp70 chaperones play important roles in cells including protein folding, trafficking, degradation and enabling survival under stress conditions. DnaK is an *Echerichia coli* Hsp70 homolog comprising a 44 kDa ATPase domain (NBD) and a 25 kDa substrate-binding domain (SBD). DnaK has two nucleotide substrate-affinity states: In the ATP-bound state, substrate binding and release occur rapidly with low substrate-affinity, whereas in the ADP-bound state, slower substrate binding and release kinetics are observed with high substrate-affinity. Communication between the two domains is essential for chaperone function and is mediated via a conserved flexible hydrophobic linker region (^{384}GDVKDVLLL^{392}). Previous studies showed that truncated DnaK(1-392), containing the ATPase domain and the entire linker region, mimics the substrate-stimulated form of full-length DnaK, and also similar pH dependent ATPase profiles are observed for both proteins. Using this knowledge we aimed to understand the allosteric mechanism underlying the substrate binding effects to the ATPase domain by pinpointing the putative residues that are present in this path using DnaK(1-392). To this end, certain mutations were introduced at the DnaK(1-392) construct and their effects on the activity and stability of the ATPase domain were studied. We found that replacement mutations of histidine at position 226 to either alanine or phenylalanine caused 3-fold enhancement in the ATPase rates for pH values between 5.5 to 8.5. A similar result was obtained for threonine 225 to aspartic acid replacement mutation. These results suggest that H226 and T225 sites are important for the opening and closing of the ATPase domain since rate for this ATPase domain construct is dictated by conformational changes. In addition, observation of lowered stability of the ATPase domain by H226 mutation supports our activity results. An interesting result came from the mutational study done on aspartic acid 85. Replacement of D85 to either alanine or glutamic acid caused a dramatic loss of pH-dependence of ATPase activity, and displayed a DnaK(1-388) type activity profile. This result suggests that linker stimulated ATPase was lost by this mutation, revealing D85 as an allosteric site. In addition, replacement mutation of R71 showed 1.5 fold increased ATPase rate with a bell-shaped ATPase profile similar to DnaK(1-392) and replacement mutation of H295 revealed similar ATPase rate to compared DnaK(1-392) with slightly shifted bell-shaped ATPase profile. Overall, our study revealed T225 and H226 as important sites in the ATPase mechanism, and D85 as a critical point for ATPase activation at the linker stimulated form.

Escherichia coli HSP70 MOLEKÜLER ŞAPERON HOMOLOĞU DNAK PROTEİNİNDE ATPaz AKTİVİTESİNDEKİ ÖNEMLİ ALLOSTERİK BÖLGELERİN ARAŞTIRILMASI

ÖZET

70 kDa ısı şoku proteinleri (Hsp70) yeni sentezlenen proteinlere bağlanarak onları agregasyon ve denatürasyondan koruyan proteinlerdir. Ayrıca yanlış katlanmış proteinlerin yeniden katlanmasında ve protein translokasyonunda görev alırlar. Stres koşullarında, örneğin; artan sıcaklık, ağır metal ve oksitleyici içeren çevre koşullarında, anlatımları indüklenir. *Escherichia coli* Hsp70 homoloğu DnaK N-terminalinde 45 kDa boyutunda ATPaz bölgesi ve C-terminalinde 25 kDa boyutunda substrat bağlanma bölgesi içerir. Bu iki parçanın birbirleri ile etkileşimi ATP hidrolizi kontrolünde gerçekleşir. ATP bağlanmasıyla substratın bağlanıp ayrılma hızında artış gözlenir ve substrata olan affinite azalır. ATP'nin ADP'ye hidroliziyle, substratın bağlanıp ayrılma hızı azalır ve substrat affinitesi artar. Bu döngünün kontrolünde hidrofobik, esnek ve evrimsel süreçte korunmuş bağlayıcı bölgenin ("linker region") rolü büyüktür.

Yapılan birçok çalışmada, Hsp70'nin Alzehimer, Parkinson ve Hungtinton gibi nörodejeneratif hastalıklarla ilişkisi ortaya koyulmuştur. Amiloid benzeri yapılar nörodejeneratif hastalıklarda sinir sisteminde birikerek önemli sorunlara yol açmaktadır. Hsp70 aktivitesinin beta amiloid birikimini önlediği bulunmuştur (Duo ve diğ., 2003; Labrador-Garrido ve diğ., 2011, Warrick ve diğ., 1999; Chai ve diğ.,1999) Ayrıca, model organizmalarla yapılan çalışmalarda, yüksek düzeyde üretilen Hsp70 Alzehimer hastalığında yanlış katlanan tau proteininin çözünürlüğünü arttırmıştır (Duo ve diğ., 2003). Hsp70'in Parkinson hastalığının sebebi α-sinüklein proteininin agregasyonu ve toksisitesine karşı koruyucu rol oynadığı saptanmıştır (Labrador-Garrido ve diğ., 2011). Bunun yanında, Hsp70 apoptoz yolağında caspaz-9'un aktivasyonunu önleyerek anti apoptotik bir rol üstlenmektedir (Saleh ve diğ., 2000). Meme, serviks, böbrek, akciğer, kemik ve yumurtalık kanserlerinde Hsp70'in yüksek düzeyde ekspresyonu gözlenmiştir (Jaattela, 1999). Birçok kanser çeşidiyle olan bağlantısı, Hsp70'in hücre siklusundaki önemini ortaya koymaktadır. Hsp70'in allosterik yapısının aydınlatılması, nörodejeneratif hastalıklarda ve birçok kanser türünde yeni ilaçların geliştirilmesine olanak sağlayabilir.

Hsp70 ATPaz bölgesinin I ve II olarak iki lobdan oluştuğu ve bu lobların ikişer alt bölgeye (IA, IIA, IB, IIB) ayrıldığı bilinmektedir. ATP bağlanma bölgesi bu lobların arasında bulunur. Hsp70 substrat bağlama bölgesi β-alt bölge ve α-alt bölge olmak üzere iki kısımdan oluşur. β-alt bölgesi sekiz β-tabakadan oluşur ve substrat bağlama yarığı β-alt bölgesinde bulunur. α-alt bölge 5 heliks yapıdan oluşur ve substrat bağlanması sırasında α-alt bölge kapak gibi görev alır (Zhu ve diğ., 1999).

Yapılan çalışmalarda, bHsc70'te ATP hidrolizinde önemli rol oynayan dört amino asit; D10, E175, D199 ve D206 bulunmuştur (Flaherty ve diğ., 1994). ADP ve Pi bağlı bHsc70 ATPaz bölgesi kristal yapısında, Pi'nin K71 ile tuz köprüsü oluşturduğu ve T13, T204 rezidüleriyle hidrojen bağı oluşturduğu görülmüştür.

Ayrıca bHsc70'te mutasyon analizleriyle, hidroliz yolağında K71 amino asitinin anahtar rol oynadığı bulunmuştur (O'Brien ve diğ., 1996). K71 mutantlarında ATP'nin bağlandığı fakat hidrolize olamadığı görülmüştür. bHsc70'te T13 ile ilgili çalışmalarda, 13. pozisyondaki treoninin hidroksil grubunun ATP ile indüklenmiş konformasyonal değişimde önemli rol oynadığı görülmüştür (Sousa ve McKay, 1998). DnaK'da T199 amino asitinin mutasyona uğratılmasıyla ATP hidrolizinin gerçekleşmediği fakat iki bölge arasındaki allosterik iletişimin kurulduğu gözlenmiştir (McCarty ve Walker, 1991).

DnaK tüm dizim kristal yapıları ATPaz bölgesi ve substrat bağlanma bölgesi arasındaki etkileşimin anlaşılmasında önemli bilgiler vermektedir (Jiang ve diğ., 2005). Nükleotid ve substrat bağlı olmayan bHsp70 kristal yapısında, iki bölgenin birbirleriyle altı direkt veya su molekülü yardımıyla hidrojen bağı oluşturduğu gözlenmiştir. Fakat bu kristal yapıda, substrat bağlama bölgesindeki 84 amino asitlik kısım yoktur. Mutant bHsc70 proteinlerinde yapılan proteoliz, triptofan floresans and ATPaz hızı analizleriyle D152, D216, V388, L393, I515, V519 ve E530 amino asitlerinin allosterik iletişimde önemli rol oynadığı bulunmuştur. Bu kristal yapıda bağlayıcı bölgenin bir yere bağlı olmadan, ortada olduğu görülmektedir (Jiang ve diğ., 2005).

Hsp70'in ATP bağlı kristal yapısı çözülememiştir; fakat Hsp110/Sse'nin ATP bağlı formu önemli bilgiler vermektedir (Liu ve Hendrickson, 2007). ATP bağlanmasıyla subsrat bağlama bölgesi loblarının substrat bağlama yarığını açığa çıkartarak, birbirlerinden ayrıldığı anlaşılmıştır. Bağlayıcı bölgede bulunan D396 amino asitinin N173 ve P426 ile hidrojen bağı oluşturması, bağlayıcı bölgenin allosterik mekanizmada önemli rol oynadığını göstermektedir.

Son yıllardaki çalışmalarda, DnaK'nın ADP bağlı kristal yapısında substrat bağlama bölgesi ve ATPaz bölgesinin birbirlerinden bağımsız olarak hareket ettikleri görülmüştür (Bertelsan ve diğ., 2009). HNCO analizleriyle, substrat bağlama bölgesinin iki ayrı alt bölgesinin tek birim gibi beraber hareket ettikleri anlaşılmıştır. RDC ("residual dipolar coupling") analizleri IIB ATPaz alt bölgesinin diğer ATPaz alt bölgelerinden (IA, IB, IIA) 20º'lik farklı pozisyonda olduğunu ortaya çıkarmıştır. Aynı zamanda, nükleotid değişim faktörünün bağlanmasıyla IIB alt bölgesi konformasyonunda 14º'lik bir farklılık gözlenir (Sondermann ve diğ., 2001)

Bertelsan ve arkadaşlarının yaptığı çalışmada, C terminalden 33 amino asiti bulunmayan DnaK yapısı aydınlatılmış ve tüm dizim DnaK ile aynı otohidroliz hızı ve substrat tarafından indüklenmiş ATPaz aktivitesine sahip olduğu görülmüştür. Bu sonuç, bu 33 amino asitlik bölgenin DnaK'in fonksiyonunda önemli bir rolü olmadığını göstermektedir (Bertelsan ve diğ., 2009).

Allosterik mekanizmanın regülasyonunda bağlayıcı bölge önemli rol oynamaktadır. DnaK'de bağlayıcı bölgede yapılan mutasyonlarda (^{389}AAAA^{392} ve ^{389}VDDL^{392}) allosterik iletişimin gerçekleşmediği gözlenmiştir (Laufen ve diğ., 1999). Swain ve arkadaşları, ATPaz bölgesi ve bağlayıcı bölgenin tamamını içeren (^{384}GDVKDVLLL^{392}), fakat substrat bağlayıcı bölgeyi içermeyen Dna(1-392) proteinin ATPaz aktivitesinin ve pH'ya bağlı ATPaz profilinin substrat tarafından indüklenmiş tüm dizim DnaK aktivitesine ve profiline benzer olduğunu bulmuşlardır (Swain ve diğ., 2007). Aynı çalışmada, ATPaz bölgesi ve bağlayıcı bölgenin (^{384}GDVKD^{388}) bir kısmını içeren DnaK(1-388) proteinin ATPaz aktivitesinin ve pH'ya bağlı ATPaz profilinin substrat tarafından indüklememiş tüm dizim DnaK aktivitesine ve profiline benzer olduğu görülmüştür. NMR analizleriyle DnaK(1-392)

yapısında VLLL sekansının IA ave IIA arasındaki hidrofobik yarığa bağlandığı bulunmuştur. DnaK(1-392) dizimi konformasyonu, substrat tarafından indüklenmiş tüm dizim DnaK konformasyonuna benzediği için bu çalışmada DnaK(1-392) dizimi ile çalışmayı tercih ettik. Böylece, substrat bağlanmasıyla tetiklenen ATPaz bölgesindeki etkileşimleri ortaya çıkarmayı amaçladık.

Bu çalışmada, DnaK(1-392) diziminde R71, D85, T225, H226 ve H295 pozisyonlarındaki amino asitler mutasyona uğratıldı. Elde edilen R71A, D85A, D85E, T225D, H226A, H226F ve H295D nokta mutasyonlarını taşıyan plazmitler, genomunda *dnaK* geni bulunmayan *Escherichia coli* BB1553 hücrelerine transformasyon yöntemiyle aktarıldı. IPTG ile indüksiyon yapılarak, mutant proteinleri taşıyan genomlar elde edildi. Art arda uygulanan anyon değişim ve affinite kromagrafi yöntemleriyle mutant proteinler saflaştırıldı. Affinite kromatografi yönteminde DnaK'nın ATP'ye bağlanma özelliği kullanıldı. Farklı pH değerlerinde ATPaz aktiviteleri ölçüldü. Circular dichroism (CD) yöntemi kullanılarak H226A ve H226F proteinlerinin ikincil yapıları ve kararlılıkları ("stability") DnaK(1-392) proteiniyle karşılaştırılmalı olarak saptandı.

Öncelikle DnaK(1-392) proteininin ATPaz aktivitesi ölçüldü ve Swain ve arkadaşlarının bulduğu verilerle paralellik gösterdiği görüldü (Swain ve diğ., 2007). D85 mutasyonu ile ATPaz aktivitesinde DnaK(1-392)'ye göre önemli bir düşüş gözlendi. Aynı zamanda pH'ya bağlı ATPaz profilinin kaybolduğu ve substrat tarafından indüklenmemiş DnaK(1-388) ATPaz profiline benzediği görülmüştür. Bu sonuç, substrat bağlanmasıyla tetiklenen ATPaz bölgesindeki konformasyonal değişimde D85 residüsünün katalitik bir rolü olabileceğini göstermektedir.

T225D, H226F ve H226A mutasyonlarında ATPaz aktivitesi, DnaK(1-392) aktivitesine göre 3 kat artmış, fakat pH'ya bağlı ATPaz profilinin DnaK(1-392) benzer olduğu görülmüştür. Bu mutasyonlarla ATPaz bölgesinin açılıp kapanma hızının arttığı anlaşılmıştır.

CD spektroskopi kullanılarak proteinin ikincil yapısı ve kararlılığı ile ilgili önemli bilgiler edinmek mümkündür. Sağ-dönümlü ve sol-dönümlü dairesel polimerize ışığın, proteinin peptit bağları tarafından absorbsiyonu ile eliptiklik ("ellipticity") değeri bulunur. α-heliks, β-tabaka ve düzensiz sargı ("random coil") yapılarının CD spekrumundaki (190 nm-250 nm) karakteristik grafiklerinden proteinin ikincil yapısı hakkında bilgi sağlanabilir. DnaK(1-392), DnaK(1-392) H226F ve DnaK(1-392) H226A proteinlerinin 200-250 nm spektrumda pH 7 ve pH 8'de eliptiklik değerleri hesaplanmıştır. pH 8'de DnaK(1-392) H226F ve DnaK(1-392) H226A mutant proteinlerinin DnaK(1-392)'ye göre daha helikal bir yapıya sahip olduğu saptanmıştır. Artan sıcaklık ile DnaK(1-392) H226F ve DnaK(1-392) H226A mutant proteinlerinin kararlılığı pH 7 ve 8'de ölçülmüştür. DnaK(1-392) proteinin kararlılığında pH 7 ve pH 8'de bir farklılık gözlenmiş ve pH 7'de proteinin daha kararlı bir yapıya sahip olduğu bulunmuştur. DnaK(1-392) H226F ve DnaK(1-392) H226A mutant proteinlerde pH 7 ve 8 grafiğin y ekseninde sola doğru kaydığı gözlenmiştir. Böylece, H226A ve H226F mutasyonlarının proteinin kararlılığına etki ettiği bulunmuştur.

71. pozisyondaki arjinin mutasyona uğratılarak ATPaz aktivitesi pH'ya bağlı olarak ölçülmüştür. Bu mutasyonla ATPaz aktivitesi 1.5 kat artmış ve pH'ya bağlı ATPaz profili değişmemiştir. Ayrıca, 295. pozisyondaki histidin amino asitinin mutasyonu ile ATPaz hızı DnaK(1-392)'ye benzerlik göstermiş fakat; pH'ya bağlı ATPaz profili

hafifçe sağa kaymıştır. Bu mutasyonların mekanizmalarının anlaşılmasında çalışmalar devam etmektedir.
Sonuç olarak, bu çalışmada T225 ve H226 residülerinin ATPaz mekanizması için önemli olduğu ve D85 residüsünün bağlayıcı tarafından stimule olmuş ATPaz aktivesinde rol oynadığı bulunmuştur.

1. INTRODUCTION

Molecular chaperones are proteins that play roles in the folding of newly synthesized proteins, refolding of denatured proteins, protein trafficking and protein translocation under normal cell conditions. Their expression are induced by increasing temperature and also by other environmental stress conditions such as the presence of heavy metals, organics, oxidants. Molecular chaperones work as a network comprising Hsp60s, Hsp70s, Hsp90s, Hsp110s and small Hsps.

One of the major member of molecular chaperones is Hsp70. The annotation of Hsp70 comes from the first letters of "heat shock protein" and the number stands for the molecular weight of the protein. The members of Hsp70 are found in the cytosol of bacteria and in the endoplasmic reticulum, mitochondria, nucleus and chloroplast of eukaryotes. The constitutively expressed Hsp70 homolog is named Hsc70.

1.1 Roles of Hsp70 in Diseases

Hsp70s have important roles under normal and stress conditions in the cell. When a protein is synthesized, the hydrophobic regions tend to interact with each other and form aggregated molecule unless the process is controlled by Hsp70s. Due to this ability of Hsp70s, they are referred as "folders" (Mayer and Bukau, 2005; Hartl and Hayer-Hartl, 2002; Schlesinger, 1990).

The other effect of Hsp70s is that they recognize denatured proteins, and assist their renaturation or degradation**.** In the crowded macromolecular environment of the cell, Hsp70s protect aggregation prone or misfolded proteins by holding onto their exposed hydrophobic regions. On account of this ability of Hsp70s are referred as "holders".

During translocation, folded conformations of proteins prevent the passage through membrane, by the help of Hsp70s, client proteins are kept unfolded while crossing the membrane.

Hsp70s rescue proteins from aggregation. In certain pathological conditions, though, Hsps are not adequate to prevent misfolded proteins. Misfolding of certain proteins, such as; tau in Alzheimer's disease; α-synuclein in Parkinson's disease; huntington in Huntington's disease; ataxin 1, 2, 3 in Spinocerebellar ataxia 1, 2, 3, form amyloid-like structures with detergent insolubility, high β-sheet content and protease resistance. It is reported that Hsp70 activity inhibits β-amyloid accumulation in these pathological conditions (Dou *et al.*, 2003, Labrador-Garrido *et al.*, 2011, Warrick et al, 1999, Chai *et al.*, 1999). For instance, one study on the model organisms showed that increased level of Hsp70 promotes tau solubility and reduce tau hyperphosphorylation in Alzheimer's disease (Dou *et al.*, 2002). Another study including again animal models in Parkinson's disease revealed that Hsp70 has a protective effect against α-synuclein aggregation and toxicity (Labrador-Garrido *et al.*, 2011). In addition, it is found that overexpression of Hsp70s reduces polyglutamine aggregation and toxicity in transfected cells and a model organism of *Drosophila melanogaster* (Warrick *et al.*, 1999; Chai *et al.*, 1999). A polyglutamine tract, a protein portion contains a sequence of several glutamine units, becomes too long by mutations that results the formation of abnormal protein folding in some neurodegenerative diseases, such as Huntington's, Spinocerebellar ataxia, Dentatorubral-pallidoluysian atrophy, spinal bulbar muscular atrophy. (Warrick *et al.*, 1999; Chai *et al.*, 1999).

In apoptosis, mitochondrial membrane is disrupted by an apoptotic stimuli causing the release of cytochrome c into cytoplasm. Cytochrome c binds to apoptotic-protease-activating factor 1 (Apaf-1) and this heteromeric complex activates procaspase-9 by ATP/dATP manner. Active caspase-9 triggers the activation of caspase-3 and subsequently caspase cascade becomes active. Hsp70 has an anti-apoptotic role in this pathway (Saleh *et al.*, 2000). It binds to caspase recruitment domain (CARD) of Apaf1 in an ATP-dependent manner, and prevents interactions between procaspase-9 and Apaf1 (Saleh *et al.*, 2000).

Hsp70 has an important role not only in protein folding, but also in cell cycle and cancer. The alteration of the levels of Hsp70 causes loss of cell growth control and apoptosis (Jolly and Morimoto, 2000). The overexpression of Hsp70 is detected in breast, cervix, kidney, lung, leukemia, osteosarcoma and ovary cancers (Jaattela, 1999). Hsp70 is correlated with poor tumor differentiation in breast, ovary and oral

epithelium cancer; increased cell proliferation in breast, uterine cervix and lung cancer; lymph node metastasis in breast and colon cancer; increased tumor size in uterine cervix cancer (Ciocca and Calderwood, 2005). It was detected that Hsp70 is associated with estrogen reseptor α (ERα) in breast cancer and it may enhance ERα activity (Ciocca and Calderwood, 2005).

1.2 Structure and Mechanism of Hsp70s Family

All Hsp70 proteins consist of two functional domains. DnaK, the *Escherichia coli* (*E. coli*) homolog of Hsp70, is composed of a 44 kDa N-terminal nucleotide-binding domain (NBD), also named ATPase domain, and a 25 kDa C-terminal substrate binding domain (SBD). Hsp70s performs the folding process by binding to client protein repeatedly, and this process is controlled by ATP hydrolysis. In the ATP-bound state, the substrate binding and release occur rapidly and affinity of the substrate is lower compared to that of the ADP-bound state (Schmid *et al.*, 1994). On the contrary, in the ADP-bound state, high affinity and slow exchange for substrate are observed. Substrates bind to "open" peptide binding cleft, afterwards ATP hydrolysis triggers to close peptide binding cleft, leading stabilization the interaction between substrate and SBD. The cycle is repeated until the client protein is folded completely (Figure 1.1).

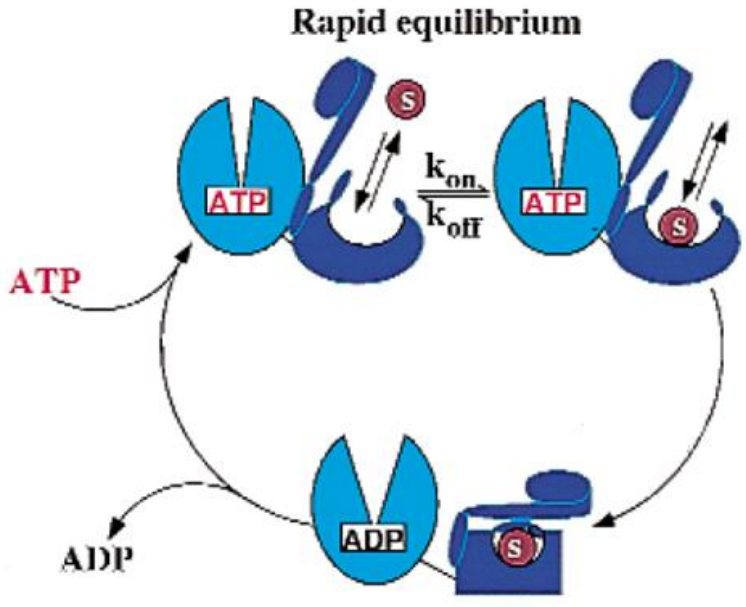

Figure 1.1 : The cycle of Hsp70 machinery. ATP binding triggers an enhanced substrate on and off rate, however slow exchange for substrate is observed by hydrolysis of ATP to ADP (Mayer *et al.*, 2000).

1.2.1 The structure of hsp70 family

The first time two-domain Hsp70 family structure was solved in the both nucleotide and substrate-free state (Jiang *et al.*, 2005). The crystal structure of two domain bovine Hsc70 (bHsc70) (1-554), NBD and truncated SBD, was obtained by the introduction of E213A and D214A mutations (Jiang *et al.*, 2005). The helix α of SBD connects the groove between lobes of NBD by six direct or water-mediated hydrogen bonds and five ionic interactions (Jiang *et al.*, 2005). Additional mutational analysis in this study showed that D152, L393 and V388 are important in the protection of linker against proteolysis in the presence of ATP (Jiang *et al.*, 2005). Mutations on the positions of D152, D216, V388, L393, I515 and V519 affect the quenching of tryptophan fluorescence by ATP binding, suggesting that these residues are important for allosteric coupling (Jiang *et al.*, 2005). Replacement of E530 decreases the ATPase rate, suggesting a role for this residue in the allosteric communication (Figure 1.2). This crystal structure of bHsc70 revealed that linker conformation is the solvent exposed form in the nucleotide and substrate-free state (Jiang *et al.*, 2005).

The crystal structure of ATP-bound full-length Hsp70 is not known, but cytosolic Hsp110/Sse1 crystal structure was solved in the complex of ATP-Mg^{2+}-K^{+} by X-ray crystallography (Liu and Hendrickson, 2007). This study is important to understand the ATP bound conformation in the two domain structure. Sse1 has almost 35 percent sequence identity with NBD of Hsp70 and it is a potent nucleotide exchange factor (NEF) for yeast Hsp70s, Ssa1 and Ssa2. Sse1 can be named as a "holdase" because of the fact that it blocks aggregation of denatured proteins *in vitro* but does not actively refold proteins. Unlike Hsp70, intrinsic ATPase activity of Sse1 is very low. The crystal structure showed that NBD lobes of Sse1 rotate against one another by almost 25º to expose the binding sites for interdomain linker and β-subdomain of SBD. Lobes of SBD dissociate to expose conserved peptide binding site upon ATP binding. In this structure, Pγ is coordinated with catalytically crucial D174 by Mg^{2+} and form hydrogen bonds with T176 and R154 (Liu and Hendrickson, 2007). D396 in linker connects with N173 and P426 by forming hydrogen bonds (Liu and Hendrickson, 2007). The interactions are highly important for both Sse1 and DnaK. The interactions revealed the linkers role in the allosteric mechanism of Hsp70s (Liu and Hendrickson, 2007).

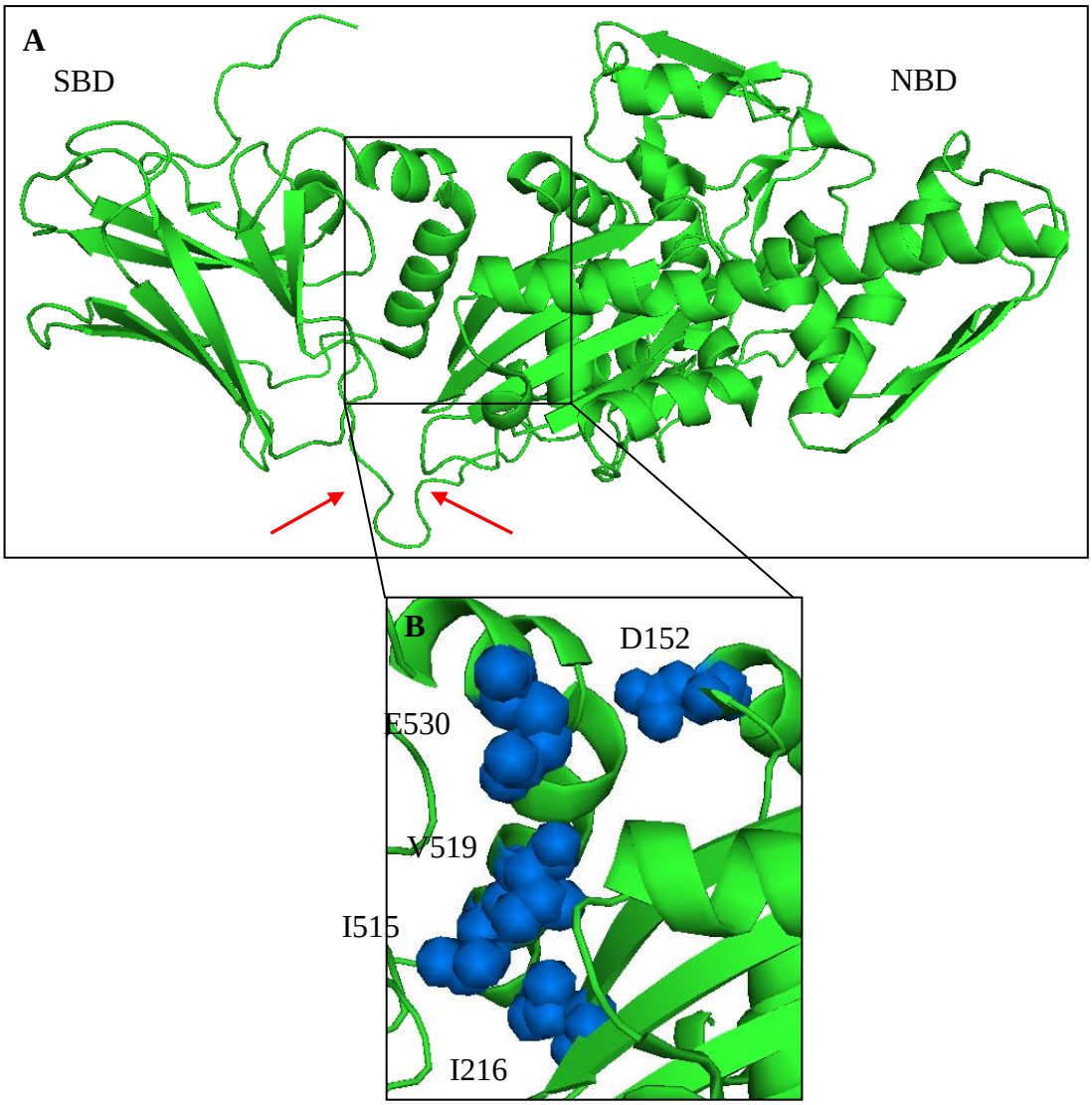

Figure 1.2 : The structure of bHsc70 and important amino acids for interaction of NBD and SBD. A)The structure of full-length bHsc70. The linker region is shown by red arrows. (PDB code: 1YUW) B) Important amino acids of the interdomain coupling between the NBD and SBD in the obtained crystal (Jiang *et al.*, 2005).

In recent years, more information about the structures of Hsp70 complexed with substrate was revealed in the ADP-bound state (Bertelsan *et al.*, 2009). In the study of full-length DnaK structure, NMR residual coupling and spin labeling methods showed that NBD, SBD and the linker move relatively independently in the ADP state, showing to loose association of domains (Bertelsan *et al.*, 2009). NBD and SBD have little or no contact and they can move in cones of ±35º in comparison with each other (Bertelsan *et al.*, 2009). Linker region is flexible and has a random coil conformation in the ADP/substrate bound state. The HNCO data shows that BETA (residues from 390 to 510) and LID (residues form 510 to 638) region move together

and act as a rigid unit (Bertelsan *et al.*, 2009). Besides, residual dipolar coupling (RDC) analysis revealed that IA, IB and IIA subdomains of NBD are similarly oriented and IIB subdomain of NBD differs from these by 20º (Bertelsan *et al.*, 2009). On the other hand, DnaK(1-605) and full-length DnaK structures are completely overlapped in aqueous solution in ADP/substrate bound state (Bertelsan *et al.*, 2009). In addition, DnaK(1-605) construct showed wild type autohydrolysis rate and substrate stimulated ATPase activity. This result shows that 33-amino acid in the C-terminus is not critical for the function in the cycle of DnaK (Bertelsan *et al.*, 2009). This study revealed that the linker is not bound to the NBD of full-length DnaK in the ADP-bound state, the two domains act independently but they are connected by a short flexible linker (Bertelsan *et al.*, 2009).

1.2.1.1 The nucleotide binding domain

Previous studies revealed the crystal structures of NBD; such as NBD of DnaK interacting with GrpE in nucleotide-free form (Harrison *et al.*, 1997), NBD of bHsc70 (Flaherty *et al.*, 1990; Flaherty *et al.*, 1994; Wilbanks and McKay**,** 1995; Sondermann *et al.*, 2001) and NBD of human Hsp70 (hHsp70) (Harrison *et al.*, 1997; Sriram *et al.*, 1997; Shida *et al.*, 2010). All of these structures revealed that NBD consists of two equal-sized lobes which are lobe I and lobe II each composing of two subdomains (IA, IIA, IB, IIB). Both IA and IIA subdomains consist of β-sheet, which contains five strand, flanked by α helices, showing similar topology, inspite of their weak sequence similarity. Subdomains of IB and IIB have different combination of helices and β-sheets (Flaherty *et al.*, 1990; Harrison *et al.*,1997). There is an ATP binding cleft between the lobes.

The bHsc70 and hHsp70 protein sequences are highly conserved, therefore structural similarity is remarkable for these proteins (Figure 1.3). Some substitutions are identified, for example the position of 7 and 18 amino acids are valine in bHsc70, whereas isoleusine in hHsp70. It is prominent that two additional amino acids are protruded on C and N termini in hHsp70 (Wilbanks and McKay**,** 1995; Sriram *et al.*, 1997).

The ATP hydrolysis requires divalent and monovalent ions in NBD. There are metal ion binding sites in the active site of the NBD in Hsp70s. The crystal structure revealed that Mg^{2+} divalent cation is more effective than the ions having either larger

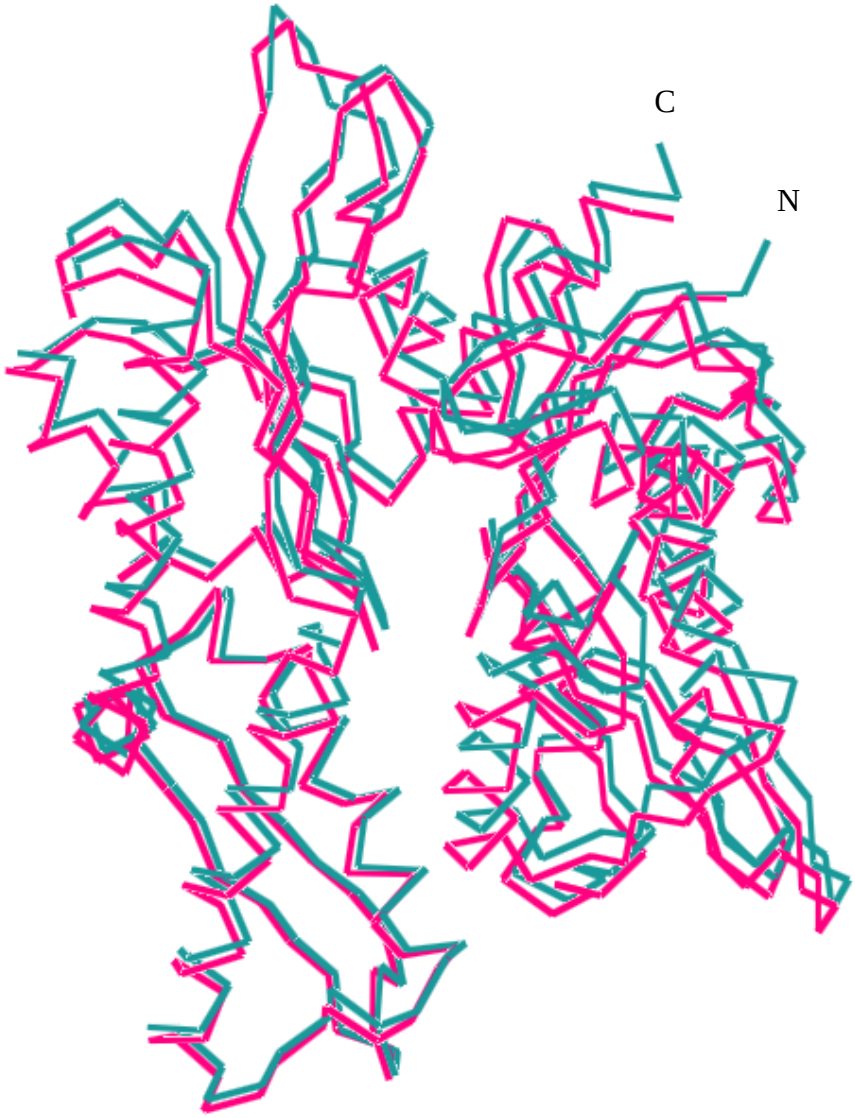

Figure 1.3 : The superposition of bHsc70 and hHsp70. hHsp70 is shown in blue, bHsc70 in pink. (PDB code:1S3X for hHsp70 and PDB code: 1HPM for bHsc70)

or smaller ionic radius in bHsc70, however Ca^{2+} is optimum in hHsp70. bHsc70 has one Mg^{2+} binding site in the active site, as well as two K^{+} cations binding sites (Wilbanks and McKay**,** 1995). The K^{+} ion is presented between the protein and the β-phosphate of Mg-ADP complex and the other K^{+} ion is located between the protein and Pi (Wilbanks and McKay**,** 1995). In this structure, many water molecules are presented (Wilbanks and McKay**,** 1995) (Figure 1.4). On the other hand, hHsp70 has two binding sites for two divalent cations (Sriram *et al.*, 1997). One of binding sites is located in the similar site as was observed for Mg^{2+} binding in bHsc70. The second Ca^{2+} ion is presented at the protein surface by the coordination of E231, D232 and H227 (Sriram *et al.*, 1997) (Figure 1.5).

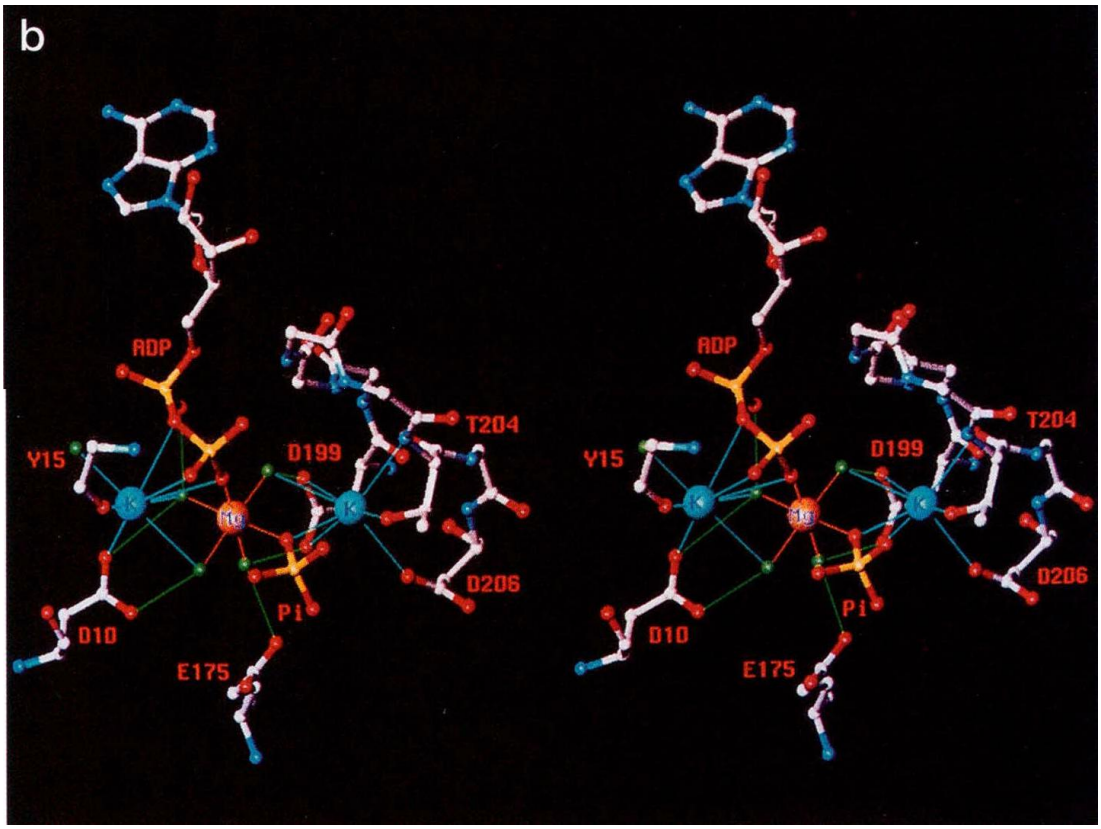

Figure 1.4 : Ball and stick model of K^+ and Mg^{2+} cations in the active site of bHsc. Carbon is shown in white, nitrogen in blue, non-water oxygen in red, water oxygen in green, phosphorus in yellow, magnesium in orange, potassium in turquoise (adopted from Wilbanks and McKay**,** 1995).

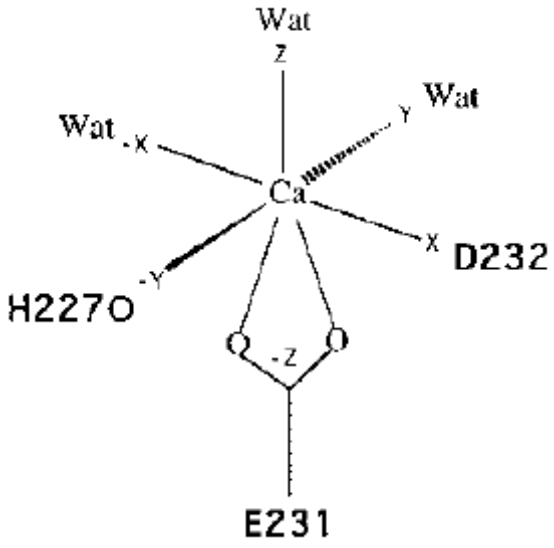

Figure 1.5 : Schematic diagram of the second site of Ca^{2+} in hHsp70 (Sriram *et al.*,1994).

It is certain that hydrolysis of ATP is crucial for Hsp70s. Studies showed that four acidic residues (D10, E175, D199, D206) are important for ATP hydrolysis in

bHsc70 (Flaherty *et al.*, 1994). The NBD crystal structures containing point mutations were obtained (ATP-bound crystal structures for D10 and D199, ADP-bound for E175 and D206). Mutant structures for E175 and D206 were superimposed with full-length protein in the MgADP+Pi bound state (Flaherty *et al.*, 1994). In MgADP+Pi-bound NBD structure, H_2O molecules are ligated by the carboxyl of D10 and D199, also E175 forms a weak hydrogen bond with H_2O, besides Pi forms a salt bridge to K71 and hydrogen bonds with hydroxyl groups of T13 and T204 (Flaherty *et al.*, 1994). At the intermediate step of hydrolysis, ATP forms a β,γ-bidendate complex with Mg^{2+} ion (Flaherty *et al.*, 1994). In the hydrolysis pathway, γ-phosphate of ATP forms hydrogen bond with T13 and backbone amide nitrogens of G202 and G203 and a H_2O or an OH ion attacks the γ phosphate (Flaherty *et al.*, 1994). In the hydrolysis, γ-phosphate moves almost 3,4 Å (Flaherty *et al.*, 1994). K71 has a switch role in this pathway (O'Brien *et al.*, 1996). In the mutant (K71E, K71A, K71M) NBD of bHsc70 structures, ATP is bound but not hydrolyzable. In these mutant protein structures, additional K^+ ion was detected instead of a H_2O molecule in the full-length protein (Wilbanks and McKay**,** 1995). It can be thought that the third K^+ ion is displaced by a H_2O molecule after hydrolysis but before ADP or Pi release (Wilbanks and McKay**,** 1995).

In DnaK structure, the homodimer GrpE binds to NBD of DnaK asymmetrically, therefore the stoichiometry is 1:2 (Harrison *et al.*, 1997). The mutant form of GrpE (G122D) was used because it is the temperature-sensitive phenotype but this mutation does not affect the binding of DnaK (Harrison *et al.*, 1997). GrpE binds to DnaK from the β-sheet of IB and IIB subdomains with non-polar, polar and salt-bridge interactions (Harrison *et al.*, 1997). Binding of GrpE induces a conformational rearrangement of the IIB subdomain of NBD of DnaK. GrpE elongated structure is critical for binding (Harrison *et al.*, 1997).

The Bag-bound hHsc70 crystal structure revealed that binding of Bag-1 induces an opening of nucleotide-binding cleft (Sondermann *et al.*, 2001). Bag-1 and GrpE binds to IB and IIB of NBD in spite of their unrelated structures. Residues T13, T14, T15 of subdomain IA and E268, K271, S275 of subdomain IIB are presented in different localization to compare nucleotide-bound states, showing that binding of Bag-1 to ADP-bound hHsc70 results opening of nucleotide-binding cleft (Sondermann *et al.*, 2001). When Bag-bound hHsc70 in the nucleotide-free state and

Hsc70 in the ATP-bound states are superimposed, the movement of IIB subdomain is measured as 14º (Sondermann *et al.*, 2001). This means that binding of ATP induces the movement of IIB subdomain 14º (Figure 1.6) (Sondermann *et al.*, 2001).

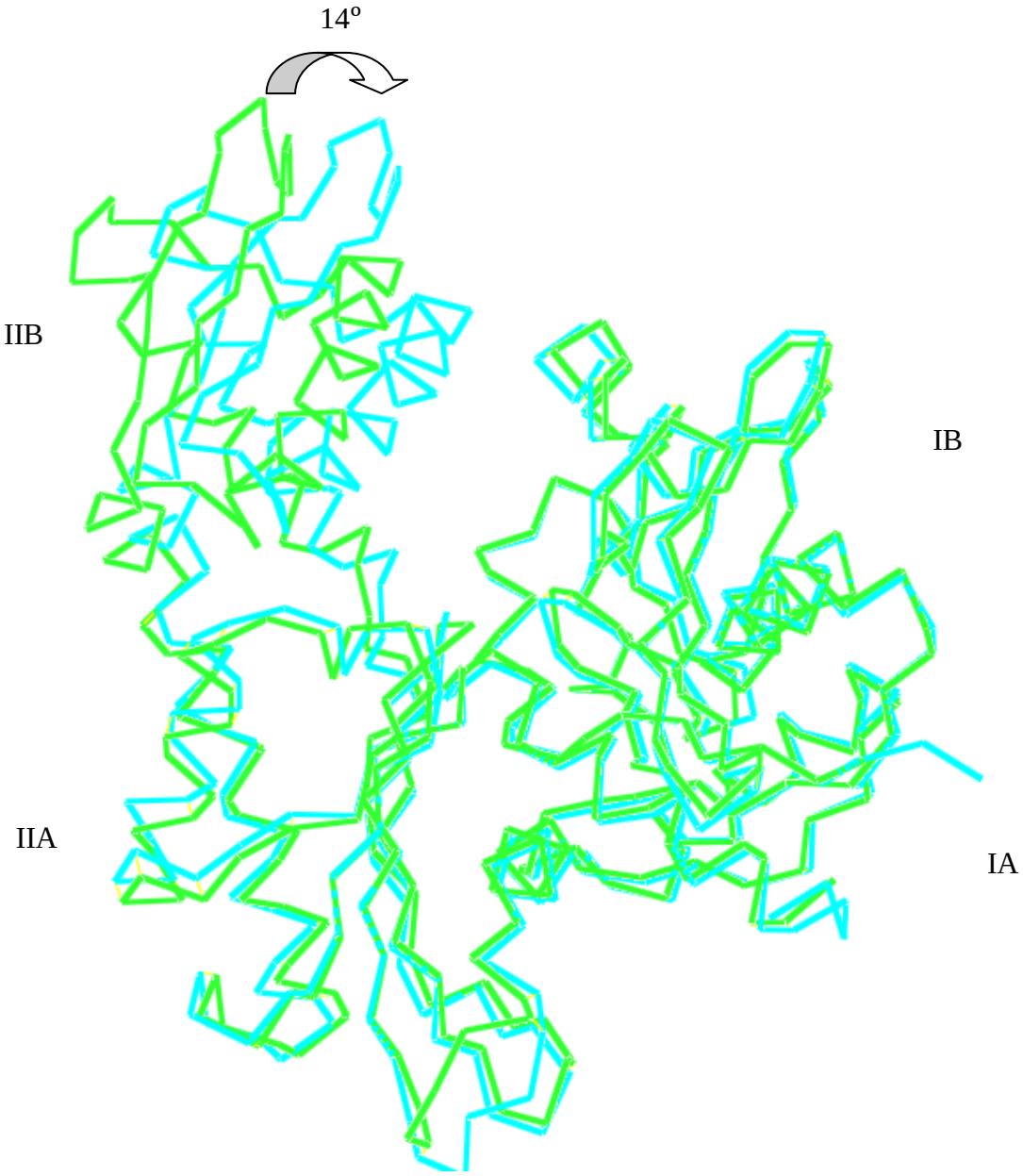

Figure 1.6 : Superimposed Bag-bound NBD of Hsc70 in the nucleotide-free state (PDB code: 3HSC) and NBD of Hsc70 in the ATP-bound state (PDB code: 1HX1). 14º rotation of IIB subdomain is shown by an arrow, Hsc70 in the nucleotide-free state is shown in green and ATP-bound Hsc70 in cyan (Sondermann *et al.*, 2001).

The crystal structure of hHsp70 NBD in the nucleotide-free state and with complex with adenosine (AMPPNP) was solved by a molecular-replacement method (Shida *et al.*, 2010). They found that nucleotide-free and AMPPNP-bound structures are superimposed, showing that nucleotide-free crystal structure is in "closed form" like AMPPNP-bound structure in this article (Shida *et al.*, 2010). However, Jiang and

colleagues (2005) revealed opened form of bHsc70 in nucleotide free state (Jiang *et al.*, 2005). To combine these findings, it was proposed that NBD structures in equilibrium between closed and opened form in the nucleotide free state (Figure 1.7). According to their findings, T15, K56 and E268 play a role in stabilizing the closed form and the control of IIB subdomain position in NBD (Shida *et al.*, 2010). This means that closed form is controlled by the residues rather than ADP or ATP. Furthermore, the opened form is stabilized by G230 into IIB subdomain and S340 in IIA subdomain and D199 and D206 residues limit the rotation in the opened form of NBD (Shida et al, 2010).

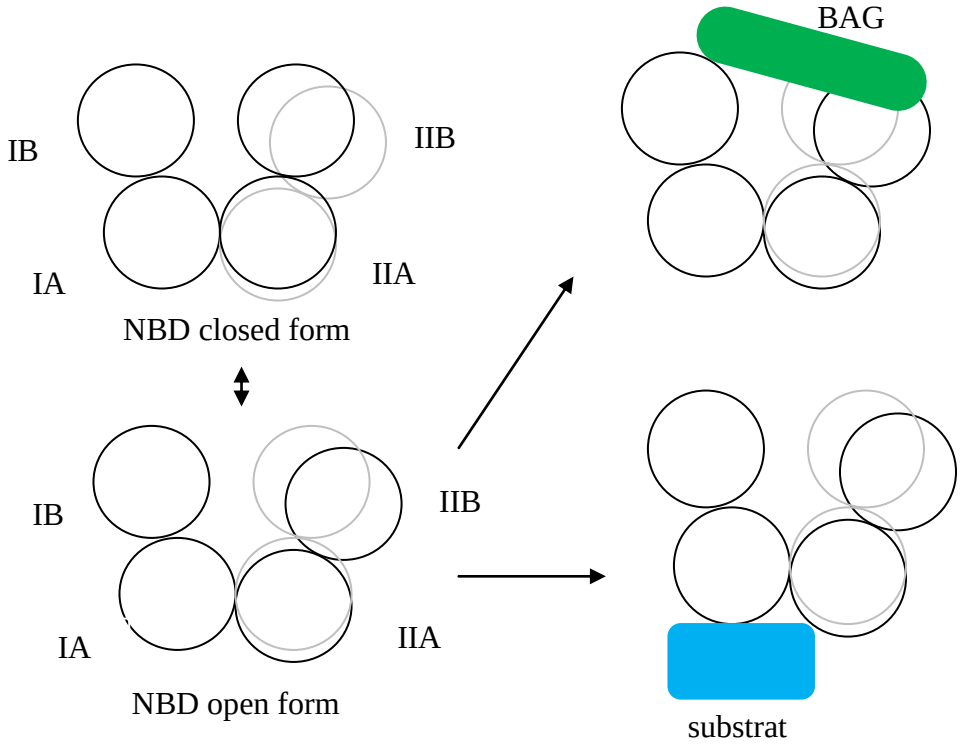

Figure 1.7 : The schematic structures of NBD as closed and open form. Nucleotide exchange factors (Bag-1) and substrates keep the NBD in the open conformation. Figure 1.7 was taken from Shida *et al.*, 2010.

1.2.1.2 The substrate binding domain

The structure of SBD of DnaK lacking 31 residues from C-terminus in the substrate-bound form was determined by X-ray crystallography (Zhu *et al.*, 1996). It contains β-subdomain (393-501) and C-terminal α-helical subdomain (509-607) (Figure 1.8). β-subdomain is arranged in two sheets with four antiparalel β-strand. The bottom sheet (β3, β6, β7, β8) is regular, these β-strands are twisted with hairpin and connected to the successive strands. However, it is notable that top sheet (β5, β4, β1,

β2) is irregular. These β-sheets are connected with each other by loops, loop £$_{1,2}$ between β1 and β2, loop £$_{4,5}$ between β4 and β5, loop £$_{3,4}$ between β3 and β4 and loop £$_{5,6}$ between β5 and β6. The channel between loops £$_{1,2}$ and £$_{3,4}$ is for the substrate binding. α-helical subdomain consists of five α helices, αA, αB, αC, αD and αE. Helices αA and αB are connected to each other by a kink of 72º at the residue N522 (Zhu *et al.*, 1996).

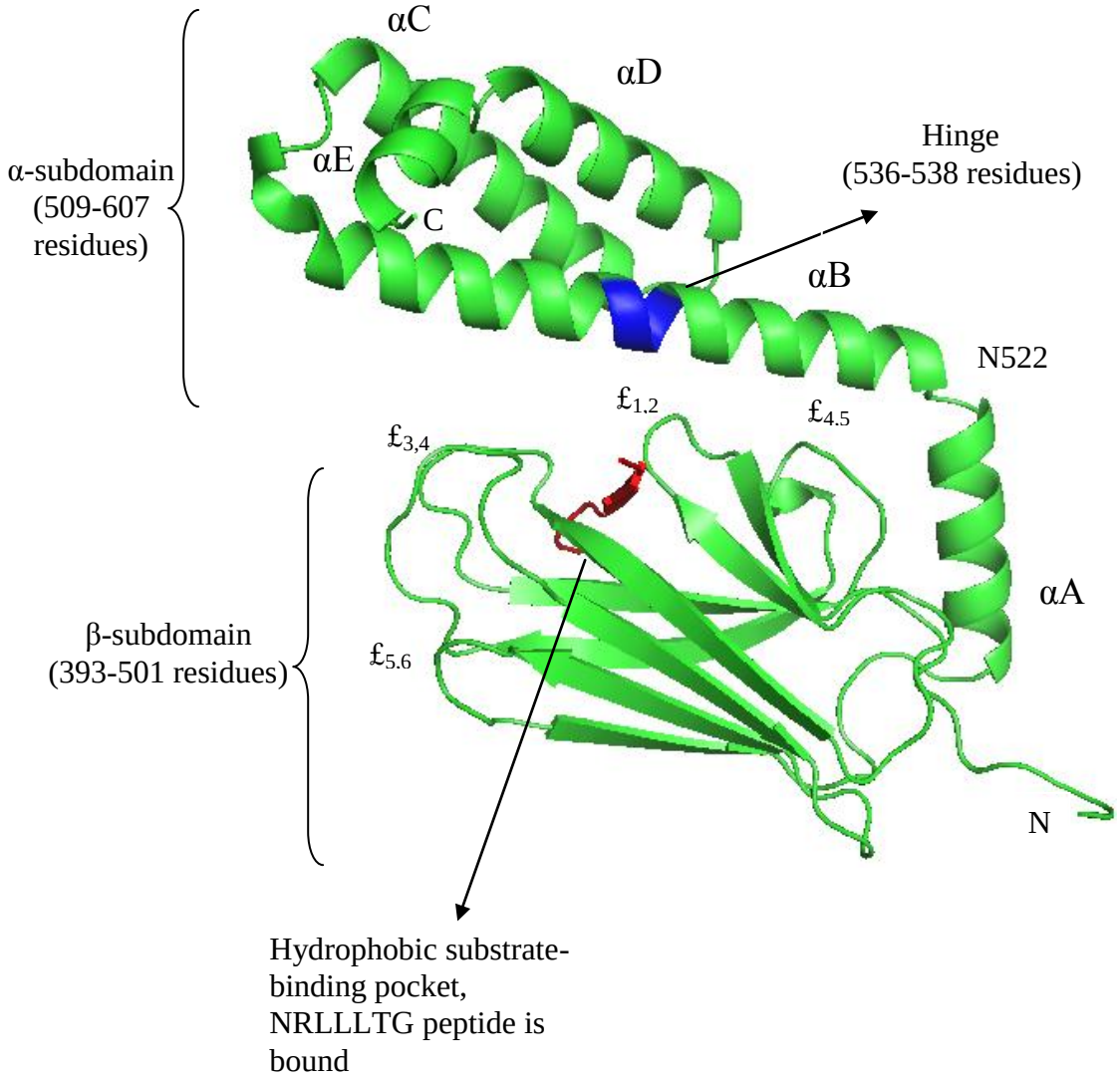

Figure 1.8 : Structure of SBD of DnaK in the peptide-bound form (Zhu *et al.*, 1996). The peptide is shown in red, the hinge region is in blue. (PDB code: 1DKZ)

Helix αB interacts with αC, αD and αE through its C-terminal (Zhu *et al.*, 1996). The α-helical subdomain has more stable conformation than β-subdomain. Helix αA makes hydrophobic contact with loops £$_{4,5}$ and helix αB contacts with all four loops, £$_{1,2}$, £$_{3,4}$, £$_{4,5}$, £$_{5,6}$ (Zhu *et al.*, 1996).

Substrate binds to β-subdomain of SBD and α-subdomain acts as a lid for the binding and release of substrates. NRLLLTG heptapeptide substrate forms many van der Waals interactions and seven hydrogen bonds with the β-subdomain. The central of this peptide (Leu^4) is critical for peptide binding and this residue forms three hydrogen bonds and some van der Waals interaction, forming hydrophobic pocket (Zhu *et al.*, 1996). A hydrophobic arch for the binding channel is the hydrogen bond between M404 and A429 (Zhu *et al.*, 1996). The hinge (residues of 536-538) in the helical lid determines the closed conformation in the ADP-bound state, but open conformation in the ATP-bound state (Zhu *et al.*, 1996).

1.2.2 Mechanism of hsp70s and interdomain coupling

The chaperone activity of Hsp70 is controlled by ATP binding to NBD by transducing a signal to the SBD following by a conformational change. Binding of ATP causes the opening of peptide binding cleft in SBD resulting a high association (k_{on}) and dissociation (k_{off}) rate constants for substrate. Hydrolysis of ATP triggers closing of the peptide binding cleft in SBD causing low on and off rates for substrate and a high affinity for substrate. Rate limiting step is ATP hydrolysis in this mechanism (Mayer *et al.*, 2000).

Proteolysis experiments showed that DnaK has at least 3 distinct conformational states; which are nucleotide-free, ADP and ATP-bound states (Buchberger *et al.*, 1995). In the study of Buchberger and colleagues (1995), T199A mutant (ATPase deficient mutant protein) was used to reveal whether ATP binding or hydrolysis triggers the interdomain communication. It is seen that the conformational change is occurred in T199A mutant, so that binding of ATP causes the allosteric changes in DnaK (Buchberger *et al.*, 1995). It is also proved by tryptophan fluorescence measurements depending on blueshift changes of single tryptophan residue, W102, in DnaK. ATP induces fluorescence changes in the presence of the SBD, so conformational changes in the SBD causes fluorescence changes. In the ADP-bound form, residues of R188, R362 and K387 are protected from trypsin cleavage as compared to that of the nucleotide-free form so that interaction to C-terminal of NBD is altered by ADP binding but these changes do not trigger conformational changes in the SBD and release of substrates (Buchberger *et al.*, 1995).

Mutational and small-angle x-ray scattering (SAXS) analysis revealed that conserved T13 residue is a part of allosteric mechanism in bHsc70 (Sousa and McKay, 1998). Tryptophan intensity analysis showed that T13V and T13G mutants can not indicate a Mg-ATP induced conformational change, therefore the interaction between ATP and hydroxyl group in the position of 13 is essential for ATP-induced conformational change (Sousa and McKay, 1998). Hydroxyl group of threonine at the position of 13 forms hydrogen bond with oxygen of terminal phosphate and it is thought that there is a van der Waals interaction between methyl group of threonine and methylene side chain of K71 (Sousa and McKay, 1998). Also, this study showed that ATP-induced conformation occurs after ATP binding but before hydrolysis, suggesting conformational change governs the slow step of the ATPase cycle rather than the hydrolsis of ATP (Sousa and McKay, 1998).

The details of allosteric mechanism is not clear. Vogel and colleagues (2006a) propounded that the allosteric mechanism contains four element, which are an ATP sensor, a transducer, a switch and a lever (Vogel *et al.*, 2006a). The residues of ATP sensor is located in NBD and a residue of lever in SBD. Kinetic measurements, fluorescence spectra and refolding of denatured proteins analyses in mutant DnaK showed that conserved P143 can be a switch for the interdomain communication between NBD and SBD since this residue increases the enthalpy of activation for ATP hydrolysis (Vogel *et al.*, 2006a). Also, this residue stabilizes the open conformation of substrate binding pocket (Vogel *et al.*, 2006a). Mutation of P143 causes a protein that is nonfunctional (Vogel *et al.*, 2006a). Mutation analysis on R151, so called the transducer, showed that this residue is crucial for allosteric regulation of ATPase activity by the SBD and hydrogen bond formation is important for allosteric communication rather than change of the residue (Vogel *et al.*, 2006a). The residue of P143 contacts K70 and E171, an ATP sensor, for allosteric communication (Vogel *et al.*, 2006a). Binding of ATP sensed by K70 and E171 leads to a conformational change in the location of P143 and the signal is transferred by R151 to the SBD. The overall result of this mechanism is the opening of substrate binding cleft (Vogel *et al.*, 2006a).

Communication between the two domains is essential for chaperone function and is mediated via a conserved, flexible, hydrophobic linker region (^{384}GDVKDVLLL^{392} in DnaK). It was found that ^{389}VLLL^{392} hydrophobic sequence has two

conformations (Zhu *et al.*, 1996). 40% of protein structure showed that ^{389}VLLL^{392} sequence folded into a hydrophobic pocket ("in" conformation), whereas other 60% portion represented that the end of linker region is out a lattice contact ("out" conformation) (Zhu *et al.*, 1996). Mutational analysis revealed that ^{389}AAAA^{392} and ^{389}VDDL^{392} mutant DnaK proteins lacked interdomain communication (Laufen *et al.*, 1999). DnaJ can not stimulate the ATPase rate in the absence or presence of substrate, also these mutants is unlikely to release substrate upon ATP binding (Laufen *et al.*, 1999). TROSY NMR spectra of ADP-bound DnaK(1-388) and DnaK(1-392) showed that the linker is docked in the hydrophobic cleft between IA and IIA in the NBD, especially VLLL sequence is important for interaction (Swain *et al.*, 2007). The residue of L177 is a candidate for the linker binding site (Swain *et al.*, 2007). The linker region is crucial not only to stimulate ATPase rate but also to sense substrate binding (Swain *et al.*, 2007).

Previous studies showed that the linker region is important for allosteric coupling (Vogel *et al.*, 2006b; Swain *et al.*, 2007). Vogel and colleagues (2006b) revealed that basal ATPase rate of truncated DnaK(2-385) is similar to unstimulated full-length DnaK, whereas truncated DnaK(2-393) has basal ATPase rate similar to the stimulated full-length DnaK (Vogel *et al.*, 2006b). Studies displayed that truncated DnaK(1-392), containing the NBD and the entire linker region, mimics the substrate-stimulated form of full-length DnaK, and also similar pH dependent ATPase profiles are observed for both proteins (Swain *et al.*, 2007). However, ATPase activity of truncated DnaK(1-388), containing the NBD and partial linker region (^{384}GDVKD^{388}), is similar to full-length DnaK that is unstimulated by substrate. It is remarkable to note that pH-dependent ATPase activity profiles of DnaK(1-388) and unstimulated full-length DnaK have similar characteristics. To sum up, presence of VLLL sequence stimulates the ATPase activity by 13-fold (Swain *et al.*, 2007).

Circular dichroism (CD) measurements showed that DnaK(1-392) has 3,5ºC higher transition than DnaK(1-388), showing that the linker induces an increase in the stability of NBD (Swain *et al.*, 2007). The charge-state distribution analysis revealed that the linker is important to activate the NBD at neutral pH (Swain *et al.*, 2007). In this study, it was noted that the off-rate of MABA-ADP was slower for DnaK(1-392) than either DnaK(1-388) or full-length DnaK, suggesting that ADP dissociation rate is slower for DnaK(1-392) (Swain *et al.*, 2007). Rate limiting step is the release of

ADP for DnaK(1-392), however ATP hydrolysis for full-length DnaK and DnaK(1-388) (Swain *et al.*, 2007).

1.3 Mutational Studies Done on the Nucleotide Binding Domain of Hsp70 Family

There are many studies involved in mutations of the NBD of Hsp70 to display the roles of residues in phosphorylation, interdomain coupling, peptide dissociation and ATPase activity etc. Understanding the role of each residue will be beneficial for our investigations.

The mutation analysis of T199 in DnaK showed that this site is critical for autophosphorylation and ATPase activity (McCarty and Walker, 1991). Replacement of threonine to alanine, valine and aspartic acid causes an abolished autophosphorylation, and the mutant proteins have weak ATPase activity (McCarty and Walker, 1991). It is noted that the autophosphorylation and ATPase activity depend on temperature changes (McCarty and Walker, 1991). It was observed that the activity is increased at higher temperature (McCarty and Walker, 1991). It can be a strategy to survival in higher temperatures for all the organisms (McCarty and Walker, 1991) (Appendix A).

The replacement of K71 in bHsc70 abolished ATPase activity (O'Brien *et al.*, 1996). K71 was changed to glutamic acid, alanine and methionine, and ATP binding was detected by solving the mutant proteins crystal structures (O'Brien *et al.*, 1996). Three K^+ ions in the active site were detected in the crystals of K71 mutant instead of two K^+ ions (O'Brien *et al.*, 1996). The conserved site of K71 is important for ATP hydrolysis in bHsc70 (O'Brien *et al.*, 1996) (Appendix A).

Vogel and colleagues (2006b) showed that residues of positive K155, R167 in NBD and D393 in the linker region of DnaK are important for allosteric coupling (Vogel *et al.*, 2006b). The mutations of K155A, K155D, R167A, R167D, D393A and D393R in full-length DnaK lack ATP-stimulated substrate release (Vogel *et al.*, 2006b). Tryptophan fluorescence and ATPase activity analysis confirmed that K155, R167 and D393 are important for DnaJ interaction and interdomain communication (Vogel *et al.*, 2006b). Basal ATPase rate of mutants were increased, but synergetically stimulated ATPase rates of K155A and K155D showed a weak reduction when

compared to full-length DnaK (Vogel *et al.*, 2006b). R167A mutant has an extremely reduced ATPase rate when stimulated by DnaJ and substrate but R167D, D393A, D393R mutants have fully lost synergetic stimulation of the ATPase rate (Vogel *et al.*, 2006b). In this study, basal ATPase rate of DnaK(2-385) is similar to that of the full-length unstimulated DnaK, however DnaK(2-393) has basal ATPase rate as high as stimulated ATPase rate of full-length DnaK (Vogel *et al.*, 2006b). The mutant DnaK(2-393) (^{389}AAAA^{392}), whereas, has reduced basal ATPase rate, suggesting that the linker region is responsible for the allosteric coupling (Vogel *et al.*, 2006b). Interestingly, DnaK(2-393) R151A, DnaK(2-393) K155D and DnaK(2-393) R167D have greatly increased ATPase rate (Vogel *et al.*, 2006b) (Appendix A) .

Another study showed that residues of P143, R151, E171D of DnaK are important for the interdomain coupling (Vogel el al., 2006a). ATP binding starts the signal transduction path and the path is continued to substrate binding domain. E171 and K70 sense ATP binding and cause a conformational change of conserved P143 (Vogel el al., 2006a). The residue of R151 relays the signal to the SBD, suggesting that substrate binding pocket is opened (Vogel el al., 2006a). Binding of DnaJ triggers the back transition through R151 (Vogel el al., 2006a). In this mechanism, P143 has a switch role to stabilize two distinct conformational states (Vogel el al., 2006a). Proline residue undertakes switch roles to provide the basal interconversion frequency is to be kept low (Vogel el al., 2006a) (Appendix A).

The mutation analysis and crystal structure of bHsc70 showed that four asidic residues (D10, E175, D199, D206) are important for ATP hydrolysis (Wilbanks *et al.*, 1994). The residue of D10 and D199 form hydrogen bond to two H_2O molecules and E175 seems to form a weak hydrogen bond to one of these H_2O (Wilbanks *et al.*, 1994). The mutations of D206 has the smallest effect on the ATPase activity (Wilbanks *et al.*, 1994). This study showed a group of residues working in corcert is responsible for ATP hydrolysis (Wilbanks *et al.*, 1994) (Appendix A)

There is another study involved in mutational analysis on four conserved hydrophobic residues of linker region (Kumar *et al.*, 2011). They analysed V389D, V389A, L390D, L390A, L391D, L391A, L392D, L392A mutants of full-length DnaK (Kumar *et al.*, 2011). Mutating V389 and L391 resulted in dramatic allosteric coupling defects (Kumar *et al.*, 2011). However, L390 and L392 mutants showed allosteric coupling, but Hsp40 interactions are almost abrogated (Kumar *et al.*, 2011).

V389 and L391 form extensive hydrophobic contacts with the NBD and have essential roles in coupling the two functional domain (Kumar *et al.*, 2011). L390 and L392 are located on the surface and are important for DnaJ interaction (Kumar *et al.*, 2011) (Appendix A).

Important residue for DnaK was found in mutational analysis (Buchberger *et al.*, 1994). The mutant (E171A, E171K, E171K) DnaK proteins have increased V_{max} and K_m for ATP and increased K_d for substrate (Buchberger *et al.*, 1994). Also, the mutants lack the ability to grow at 42ºC, replicate λ DNA and refold denaturated luciferase, suggesting that the replacement of E171 position causes nonfunctional proteins *in vivo* and *in vitro* (Buchberger *et al.*, 1994). It is found that E171 is crucial in the coupling of ATPase activity and substrate release (Buchberger *et al.*, 1994). Substrate can not stimulate the ATPase rate when E171 is mutated (Buchberger *et al.*, 1994). Also, mutants of E171 are defective ATP-dependent release of bound substrate (Buchberger *et al.*, 1994). To combine these findings, the linkage between ATP binding and substrate release is disrupted by the mutation of E171 (Buchberger *et al.*, 1994) (Appendix A).

Recent study in 2010 focused on mutagenesis analysis of DnaK (Chang, 2010). Researchers tested luciferase activity and ATPase activity stimulated by ATP, substrate and GrpE (Chang, 2010). The mutants showing normal luciferase activity but decreased ATPase rate are the "decoupling mutants" (F67L, P90A, F91A, E230Q, D231N and K263A) (Chang, 2010). DnaK(F67L), DnaK(P90A) and DnaK(F91A) showed different digestion patterns than wt, suggesting that these mutations destabilize the $loop_{74-96}$ which is crucial for ATP hydrolysis and cooperation with DnaJ and GrpE during both refolding and heat shock rescue (Chang, 2010). The ATPase rates of DnaK(F67L), DnaK(P90A) and DnaK(F91A) are stimulated by DnaJ in the presence of substrate and K_m values are increased as compared to DnaK. Other "decoupling mutants" which are DnaK(E230Q), DnaK(D231N) have normal responses to DnaJ but GrpE can not stimulate the ATPase rate (Chang, 2010). The residues of E230 and D231 are located at the interface between the IIA and IIB subdomains (Chang, 2010). The interface contains a hinge controlling the rotation of the IIB subdomain upon ATP hydrolysis (Chang, 2010). It was found that a poor correlation between ATPase rate and heat shock

rescue, but the correlation between refolding activity and heat shock rescue has higher R^2 value (Chang, 2010) (Appendix A).

Mutational analysis of bHsc70 revealed I216, D152, K325, V388 and L393 residues as important sites for ATPase activiy, tryptophan quenching and protease resistance by ATP (Jiang *et al.*, 2005). I216 mutation has strong effects on function of bHsc70 in the cell but, interestingly, lesser effects on ATPase activity and tryptophan quencing (Jiang *et al.*, 2005). D152 mutation caused reduced ATP quenching of tryptophan fluorescence and reduced ATP protection of linker proteolysis (Jiang *et al.*, 2005). K325 is important for the function of bHsc70 and it is interesting that K325E mutation causes significantly increased ATP protection of linker proteolysis (Jiang *et al.*, 2005). V388 and L393 mutations on linker region cause reduced reduced ATP quench of tryptophan fluorescence and reduced ATP protection of linker proteolysis (Jiang *et al.*, 2005) (Appendix A).

The crystal structure of Sse1 was solved by X-ray crystallography and mutational effects of DnaK, Sse1 and Ssa1 were studies in this article (Liu and Hendrickson, 2007). *E. coli* cells can survive at high temperatures, whereas the cells can not survive at 40ºC when N170D, T173D, I160D, V389D and E230R mutations are done (Liu and Hendrickson, 2007). On the contrary, the cells containing T173V and D156A mutations can survive at high temperatures (Liu and Hendrickson, 2007). The intriguing point is that the homolog mutations of Sse1 effects are completely different than DnaK mutants (Liu and Hendrickson, 2007). For instance, N173D, T176D and F392D on Sse1 (N170D, T173D, V389D in DnaK, respectively) showed heat resistance phenotype (Liu and Hendrickson, 2007). This shows that DnaK and Sse1 have different characteristics *in vivo*. The replacement of threonine 176 to valine (T175V for Ssa1, T175V for DnaK) and aspartic acid 159 to alanine (D158A for Ssa1, D156A for DnaK) do not affect the resistance for heat for all Sse1, Ssa1 and DnaK (Liu and Hendrickson, 2007). Whereas the replacement of isolucine 163 to aspartic acid (I162D for Ssa1, I160D for DnaK) and arginine 235 to glutamic acid (E228R for Ssa1, E230R for DnaK) showed a loss of heat resistance for all Sse1, Ssa1 and DnaK (Liu and Hendrickson, 2007) (Appendix A).

1.4 Co-chaperones J-domain and Nucleotide Exchange Factors (NEFs) of Hsp70s

ATPase cycle is arranged by two cofactors: J proteins and NEFs. They have important roles in the cycle of Hsp70s (Figure 1.9). J protein holds a non-native protein through its peptide binding domain. The J protein with client protein binds to Hsp70 in ATP-bound state. The client protein interacts 'open' peptide binding cleft and ATP hydrolysis leading to conformational change triggers to stabilize the binding of client protein with closing peptide binding cleft and release the J protein. Nucleotide exchange factor (NEF) binds to ATPase domain of Hsp70 with client protein in ADP-bound state, because of higher affinity to Hsp70-ADP than Hsp70-ATP. Binding of NEF leads to dissociation of ADP, and ATP binds to Hsp70. Client protein releases due to lower affinity to Hsp70-ATP than Hsp70-ADP (Kampinga and Craig, 2010).

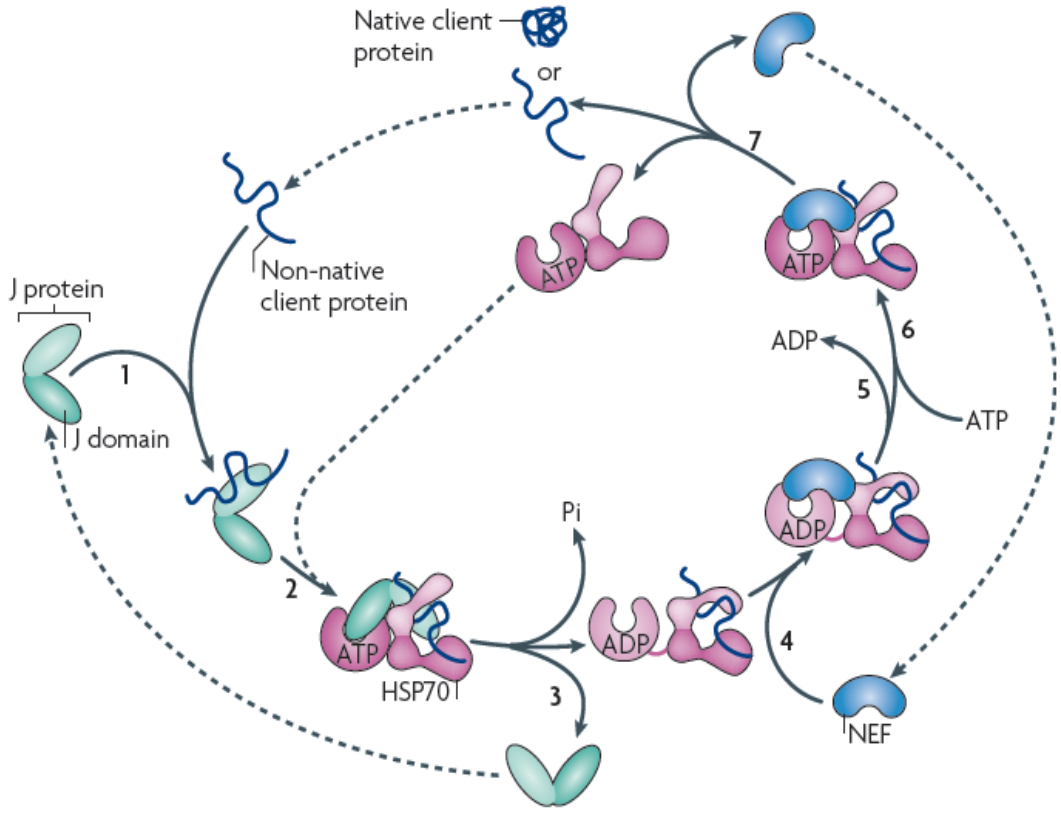

Figure 1.9 : The cycle of Hsp70s with J proteins and NEFs (Kampinga and Craig, 2010).

NEFs are divided into four groups: GrpE in prokaryotes, Bag1, Hsp110 and Hsp-binding protein (HspBP1) in eukaryotes. They have no sequence similarity, so they

are envolved independently. GrpE binds to the cleft located between subdomain IB and IIB of ATPase domain of Hsp70 homolog in *E. coli*, DnaK and the interaction triggers a 14º rotation in subdomain IIB of ATPase domain, causes the opening nucleotide binding cleft (Blatch, 2007). Interaction both GrpE and DnaJ to DnaK induces ATPase activity by 50 fold (Patury *et al.*, 2009). The second class of NEF Bag1, named Bcl-2-associated athanogene-1, is the first identified nucleotide exchange factor in eukaryotes. Similar to GrpE, binding of Bag1 to Hsc70 leads to 14º outward rotation in subdomain IIB of ATPase domain. The third class, Hsp110 have the similar structure to Hsp70, it consists of N-terminal ATPase domain, peptide-binding domain and flexible linker region connecting these domains each other. Though it has ATPase activity, it does not obtain peptide-binding cycle in ATP-dependent manner. Therefore, they act as "holdases" and they prevent aggregation especially in stress conditions. (Kampinga and Craig, 2010). HspBP1 is located in cytosol and ER in eukaryotes and it supports the action of Hsp70 from stress-related proteins.

There are ~6 kinds of J-domain proteins in *E. coli*, ~20 kinds of J-domain proteins in *Sacchoromyces cerevisiae* and ~40 type of J-domain proteins humans (Qiu *et al.*, 2006; Vos *et al.*, 2008). J proteins contain J domain which is the conserved approximate 70 amino acid region. J proteins are named Hsp40, despite most of J proteins are not 40 kDa. They stimulate the ATPase activity by conserved 3 amino acids, His, Pro and Asp, between two main helix (Helix II and Helix III) in their structure. J proteins bind to Hsp70s through HPD motif (Figure 1.10). The J protein family, historically, has been classified into three classes. Class I J proteins, also known Class A, contain N-terminal J domain, a Gly and Phe-rich region, zinc finger motif and extention C-terminal known to bind client proteins. *E. coli* DnaJ is located into this group. Class II J proteins, Class B, have N-terminal J domain and Gly-Phe region but do not consist of zinc-finger motif. And the J proteins, which do not have any similarities to Class I or II, are names Class III J proteins (Class C). It is underlined that this classification depends on structure properties, not biochemical and functional characteristics (Figure 1.11).

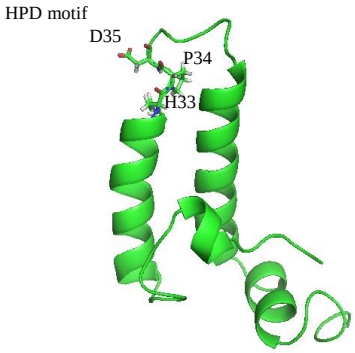

Figure 1.10: The secondary structure of DnaJ protein (PDB code: 1XBL).

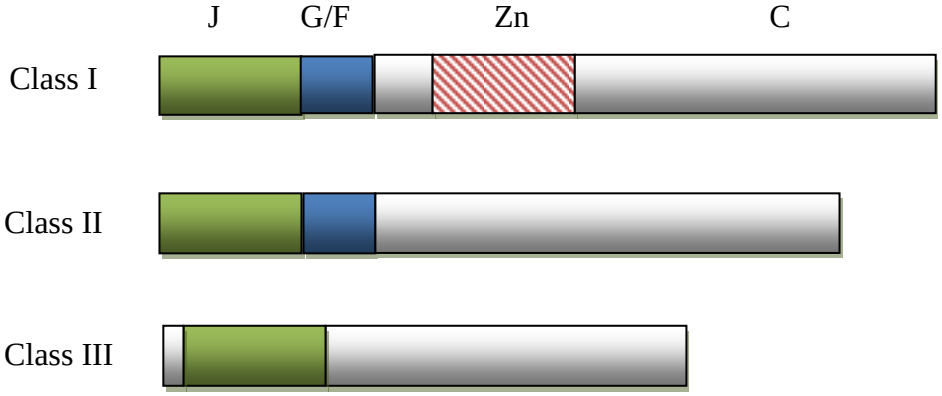

Figure 1.11 : The domains of J protein classification. J, J domain; G/F, Gly/Phe rich region; Zn, zinc finger motif, C, C-terminal domain.

1.5 Aim of the Study

In this study, we aimed to understand the details of allosteric mechanism of Hsp70. In the first step of the allosteric communication of Hsp70, the linker region binds to the hydrophobic cleft between IA and IIA on NBD (Swain *et al*., 2007). The binding leads to conformational changes of ATPase domain. We believe that a signal is conveyed to ATPase domain by substrate binding and this stimulus contains crucial amino acids communicating each other like an allosteric network. To study the signal transduction pathway, we picked a putative network, composed of R71, D85, T225 and H226, in DnaK(1-392) construct and analyzed each site in that network using a mutational analysis. DnaK(1-392) mimics the conformation of the stimulated form of full-length DnaK (Swain *et al*., 2007), thus this construct will be a good model to study linker induced effects on the ATPase domain. The allosteric mechanism is important to reveal new therapeutic strategies for the treatment of neurodegenerative diseases, such as Alzheimer's, Parkinson's and Huntington's diseases, and many

types of cancer, for example, breast, cervix, kidney, lung, leukemia, osteosarcoma and ovary cancers.

Previous study showed that ATPase activity versus pH profile of DnaK(1-392) is bell-shaped (Swain *et al.*, 2007), therefore we proposed that the bell-shaped profile is arised from a histidine residue in the catalytic site. To this purpose, we mutated H226 to alanine and phenylalanine. Also, we changed R71, D85 and T225 to understand the network between H226 and these residues. In addition, we mutated H295 to aspartic acid, although this residue is located far away from active site. We purified DnaK(1-392) and mutant proteins using anion-exchange and affinity chromatography. We obtained ATPase profiles of mutants as a function of pH to analyse mutational effects on ATPase activity. We used native gel electrophoresis to understand tertiary structures of mutants. We revealed secondary structures and protein stability of histidine mutants using CD. In this study, we tried to display the residues in the ATPase domain that are crucial in signal transmission starting linker binding to the cleft between IA and IIA on ATPase domain in the substrate stimulation.

2. MATERIAL AND METHOD

2.1 Materials

Materials are listed in Appendix B.

2.1.1 Laboratory Equipments

Laboratory equipments are listed in Appendix C.

2.2 Methods

2.2.1 Introduction of replacement mutations to DnaK(1-392)

The replacement mutations were made on DnaK(1-392) by Site-Directed mutagenesis Kit (Agilent Technologies, Quikchange Site-Directed Mutagenesis Kit, USA). The primers were listed in Table 2.1.

PCR reaction contained 125 nM primer (forward/reverse), 100 ng pMS plasmid, dNTP mix (dATP, dCTP, dGTP, dTTP), 1 µl Pfu Turbo DNA polymerase and 1x Pfu Buffer in 50 µl total volume. Pfu Turbo DNA polymerase have a high fidelity mismatch repair system with 3'→5' exonuclease activity. PCR condition was set as the following: initial denaturation at 95ºC for 30 sec, is followed by denaturation, anneling, elongation steps 95ºC for 30 sec, 60ºC for 1 min, 68ºC for 7 min, respectively and this cycle was repeated for 18 times. Degradation of methylated (parental) DNA with DpnI was obtained by the thermal cycler at 37ºC for 1 hour. The PCR reaction was purified by High Pure PCR Product Purification Kit (Roche, Switzerland) and was controlled in the 1% agarose gel. The sample was transformed to XL1-blue supercompetent cells. 1 µl of sample was added to 25 µl of XL1-blue cells and the mix was incubated on ice for 30 min. The heat-shock was applied by 42ºC for 45 sec and 0ºC for 2 min. 250 µl of Luria Bertani (LB) medium was added and the mixture was incubated at 37ºC for 1 hour. The mixture was spread to the selective LB-agar medium with 100 µg/mL ampicillin and incubated at 30ºC for overnight. One selected colony was picked and grown at LB medium with 100

μg/mL ampicillin at 30ºC for overnight. The plasmid isolation was done by High Pure Plasmid Isolation Kit (Roche, Switzerland) and replacement mutation control was analyzed after sequencing (Iontek Biotechnology Incorporated Company).

Table 2.1 : Primers used for replacement mutations. The changed codons are underlined.

Mutation	Forward primer	Reverse Primer
R71A	5'-CGC AAA ACA CTC TGT TTG CGA TTA AAG CCC TGA TTG GTC GCC-3'	5'-GGC GAC CAA TCA GGG CTT TAA TCG CAA ACA GAG TGT TTT GCG-3'
D85A	5'-CGA AGA AGT ACA GCG TGC TGT TTC CAT CAT GCC GT-3'	5'-ACG GCA TGA TGG AAA CAG CAC GCT GTA CTT CTT CG-3'
D85E	5'-GAA GAA GTA CAG CGT GAG GTT TCC ATC ATG CCG TT-3'	5'-AAC GGC ATG ATG GAA ACC TCA CGC TGT ACT TCT TC-3'
T225A	5'-GCA ACC AAC GGT GAT GCC CAC CTG GGG G-3'	5'-CCC CCA GGT GGG CAT CAC CGT TGG TTG C-3'
T225D	5'-GGC AAC CAA CGG TGA TGA CCA CCT GGG GGG TG-3'	5'-CAC CCC CCA GGT GGT CAT CAC CGT TGG TTG CC-3'
H226F	5'-GGC AAC CAA CGG TGA TAC CTT CCT GGG GGG TGA AGA-3'	5'-TCT TCA CCC CCC AGG AAG GTA TCA CCG TTG GTT GCC-3'
H226A	5'-GGC AAC CAA CGG TGA TAC CGC CCT GGG GGG TGA AGA-3'	5'-TCT TCA CCC CCC AGG GCG GTA TCA CCG TTG GTT GCC-3'
H295D	5'-CGC GAC CGG TCC GAA AGA CAT GAA CAT CAA AGT GAC TCG-3'	5'-CGA GTC ACT TTG ATG TTC ATG TCT TTC GGA CCG GTC GCG-3'

2.2.2 Protein expression

The plasmids were transformed in to *E. coli* BB1553 strain (*ΔdnaK*) and colonies were grown at the selective LB medium with ampicilin (100 μg/mL) and chloramphenicol (25 μg/mL) overnight. One colony was picked and diluted in 1 L LB medium containing 100 μg/mL ampicilin and 25 μg/mL chloramphenicol. When optical density (OD) at 600 nm was reached to 1, IPTG induction was done to a final concentration of 0.2 mM. After 4 hours of induction, the culture was centrifuged at

2800xg for 30 min and the pellet was resuspended in the solution containing 20 mM Tris, 50 mM NaCl, 0.1 mM EDTA, pH 7.4, using 3 mL buffer/gram cells of resuspended cells. The cells were stored at -80 ºC until further use. Later induction control was done by SDS-PAGE.

2.2.3 Isolation of mutant proteins

Cells were lysed using a mix of; lysozyme (0.5 mg/ml), PMSF (0.5 mM), aprotinin (2.5 g/ml), pepstatin A (1 µg/ml), leupeptin (5 µg/ml) and DNAse I (0.15 mg/ml) and with an inoculation on ice for 30 min. For complete lysis, sonication was done for 5 min on ice (15 sec burst, 10 sec interval between the burst). The samples were centrifuged at 17,400 xg for 40 min at 4ºC. Supernatant was loaded to the DEAE Sephacel column equilibrated with 20 mM Tris-HCl, 1 mM EDTA, pH 7.4. The gradient was generated by the solution containing 20 mM Tris-HCl, 1 mM EDTA, 1 M NaCl, pH 7.4. The fractions containing DnaK protein were pooled and dialyzed in 20 mM Hepes, 100 mM KCl, 5 mM $MgCl_2$, pH 7.4 for at least 3 hours. The sample was, later, loaded to ATP-agarose column which is N-6 linked ATP-agarose resin (Sigma A9264). The elution of target protein was done by the solution containing 20 mM Hepes, 10 mM EDTA, 100 mM KCl, pH 7.4. The eluted proteins were concentrated by Millipore, Amicon Centrifugal Filter Tube, USA and dialyzed in 20 mM Hepes, 100 mM KCl, 5 mM $MgCl_2$, pH 7.4 for at least 3 hours. The purity of protein was tested by SDS-PAGE.

2.2.4 ATPase measurement

Steady-state ATPase activity measurements were performed using the method involved in ATP hydrolysis by DnaK. The principles of the enzyme coupled colorimetric ATPase assay (Norby, 1988) was described in Figure 2.1. ATP is hyrolyzed to ADP by DnaK. The reaction of ADP and PEP generates pyruvate. In the other step, NADH is oxidized by pyruvate.

The decrease of NADH concentration was monitored in transmission (%T) mode at 340 nm on Bio-Rad Benchmark Plus, Microplate Spectrophometer in UV mode for 30 min at 30ºC. The final concentrations of reagents were 40 mM Hepes, 50 mM KCl, 11 mM $Mg(OAc)_2$, 0.3 mM ATP, 50 mM DTT, 6 mM PEP, 2 mM β-NADH and 1 µM DnaK protein in total 200 µl and ~2,6 unit PK and LDH enzymes was

used. The reaction was performed in a 96 well plate (Costar 3361, flat bottom, sterile, polystyrene).

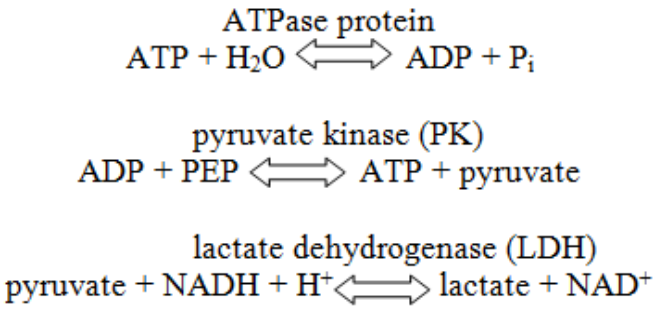

Figure 2.1 : The reactions of ATPase assay.

The graph was plotted using the data and the slope was determined. The linear regression was used to define the ATPase rate. The correct slope was stated by taking out the autohydrolysis slope. Finally, the equation was used to normalize for protein concentration to give units of mol ATP (mol DnaK)$^{-1}$.min^{-1}**(2.1)**.

$$\frac{dATP}{dt} = -6220\frac{dA340}{dt} \qquad \textbf{(2.1)}$$

The last result was corrected by the article (Kiianitsa *et al.*, 2003) to adapt the NADH-coupled ATPase assay for a 96-well microplate reader.

2.2.5 Circular dichroism (CD)

Circular Dichroism measurements were performed by Jasco J-810 spectrapolarimeter in TUBITAK, Marmara Research Center. The CD scans were acquired in the scale between 200 nm and 250 nm and the conditions were 1 nm step size, 1 nm band width, 100 nm/min speed, 2 sec response time and 25 ºC. CD melts measuments were obtained between 25ºC and 90ºC and were controlled and were by a peltier temperature controller (Jasco, PTC-34801). The conditions were set as 0.1 ºC step size, 2 sec response time and 1.0 nm band wind. The protein concentration was 10-15 µM in 20 mM Hepes, 100 mM KCl, 5 mM $MgCl_2$, pH 7.4 and pH values were adjusted by NaOH and HCl. The equation (2.2) was used to convert the ellipticity values, θ (in milidegrees), to mean residue weight ellipticity, [θ] (in degree.cm^2/decimol) **(2.2)**.

$$[\theta] = \frac{\theta}{10 \times C \times I \times N} \qquad \textbf{(2.2)}$$

I is the path length in centimeters, C is the molar protein concentration, N is the number of peptide bonds in the protein.

3. RESULTS

3.1 Introduction of Replacement Mutations to DnaK(1-392)

The PCR products were loaded to 1% agarose gel and the results are shown in Figures 3.1-3.2. H226F indicates that histidine amino acid in the position of 226 was substituted to phenylalanine and similarly D85A, D85E, R71A, T225D and T225A are shown in Figures 3.1-3.2. It was not necessary to observe the product of PCR in a 1% agarose gel. For example, we did not detect the PCR product of D85E mutant because of its low concentration, but sequencing analysis showed that mutation of D85E was successfully obtained (Figure 3.1).

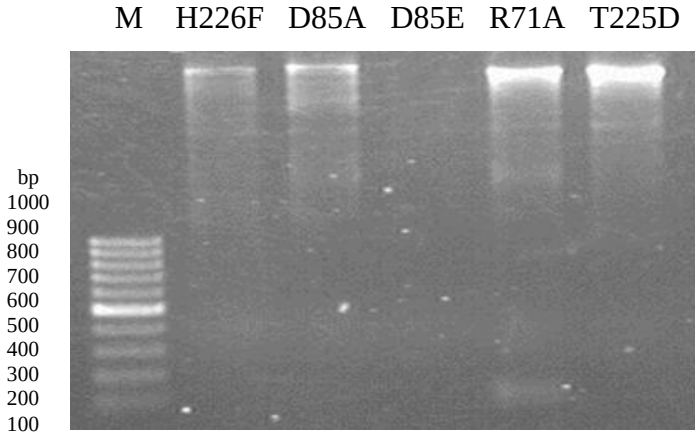

Figure 3.1 : PCR products of mutants. M: 100 bp DNA ladder.

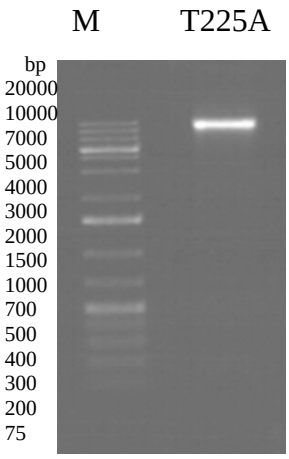

Figure 3.2 : PCR product of T225A mutant. M: 1kb DNA ladder.

DNA sequencing of mutants was done by Iontek Biotechnology Incorporated Company and the alignment analysis was done by EMBL-EBI, Pairwise Sequence Alignment. Wild type DnaK sequence was shown as wtDnaK and the changed codons were in yellow in Figures 3.3A-H. The raw data of sequencing results for each mutant were given in Appendix C. The alignment analysis in Figure 3.3A showed that the CGC codon coding arginine (R) in the position of 71 amino acid was changed with GCC codon coding for alanine (A). GAT codon coding aspartic acid (D) in the position of 85 was changed with both GCT codon coding for alanine (A) and GAG codon coding for glutamic acid (E) (Figures 3.3B-C). ACC codon coding threonine (T) in the position of 225 was replaced with both GCC codon coding for alanine amino acid (A) and GAC codon coding for aspartic acid (D) (Figures 3.3D-E). The replacement of CAC codon coding histidine (H) in the position of 226 to TTC codon coding for phenylalanine (F) and GCC codon coding for alanine (A) were shown in Figures 3.3F-G, respectively. The alignment analysis in Figure 3.3H showed that the CAC codon coding histidine (H) in the position of 295 was changed to GAC codon coding aspartic acid (D). The plasmids containing H226A and H295D mutations were obtained from Assist. Prof. Dr. Gizem Dinler Doğanay.

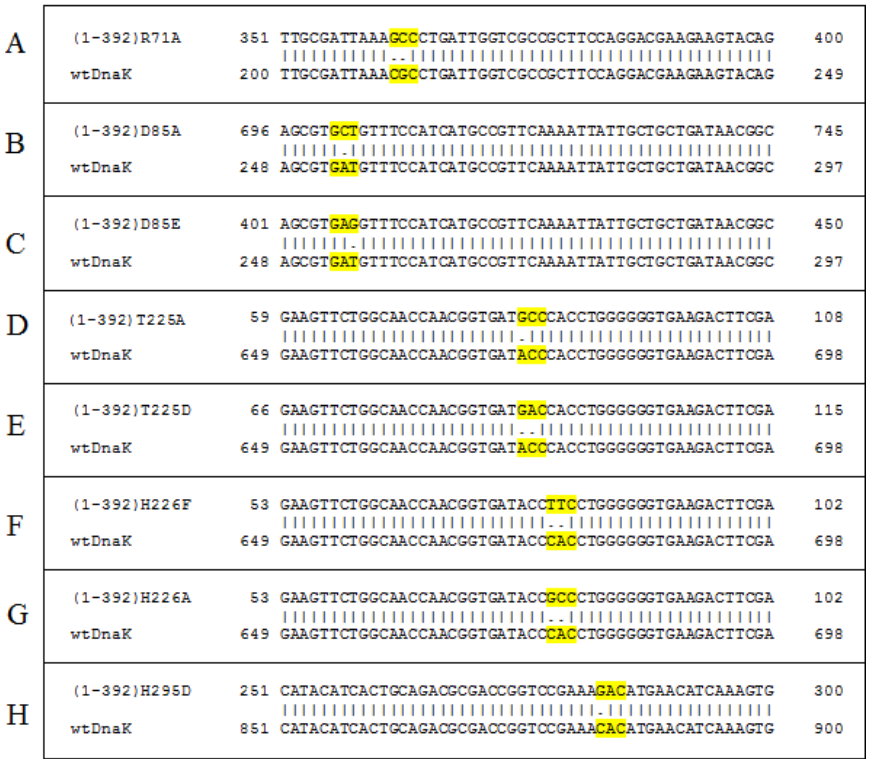

Figure 3.3 : Alignment of mutants with wtDnaK. Changed codon is shown in yellow. A) R71A, B) D85A, C)D85E, D)T225A, E) T225D, F) H226F, G)H226A, H)H295D.

3.2 Protein Expression

Vectors carrying target gene were transformed into *E. coli* BB1553 (*ΔdnaK*) cells by heat-shock transformation. Although, the optimum growth temperature of *E. coli* is 37ºC, *E. coli* BB1553 (*ΔdnaK*) cells were grown at 30ºC because of the lack of chaperone gene in the genome, thus cells survive better at the lower growth temperature.

IPTG is a molecular mimic of allolactose. The lactose metabolite called allolactose, which is a combination of glucose and galactose, binds to the repressor of *lac* operon and causes a change in its shape. Therefore, the repressor is unable to bind to the operator due to the altered shape, allowing transcription of the *lac* genes. Mutant *dnaK* genes (*dnaK*(1-392) H226F, H226A, H295D, T225D, D85E, D85A, R71A and T225A) were induced by IPTG in 1 L of LB medium. Uninduced (-) and induced (+) proteomes were loaded to SDS-PAGE and the overexpression of the target protein was detected in the correct size at 45 kDa (Figures 3.4-3.6).

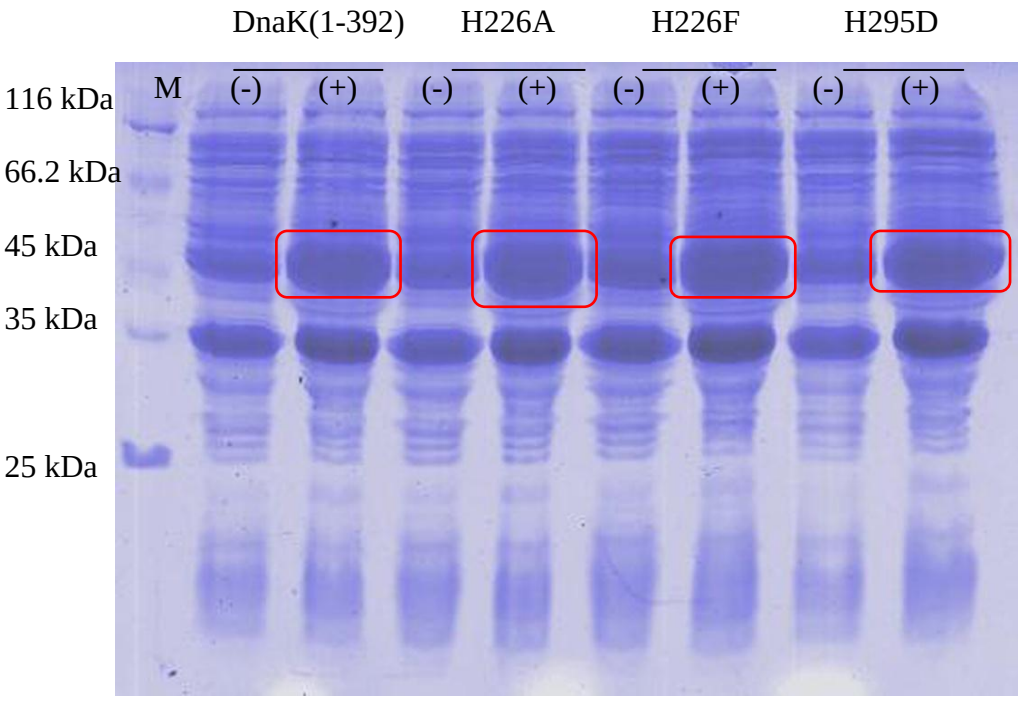

Figure 3.4 : Induction control of DnaK(1-392), DnaK(1-392) H226A, DnaK(1-392) H226F and DnaK(1-392) H295D mutants by SDS-PAGE. M: Protein marker, (-): uninduced proteome, (+): induced proteome by IPTG.

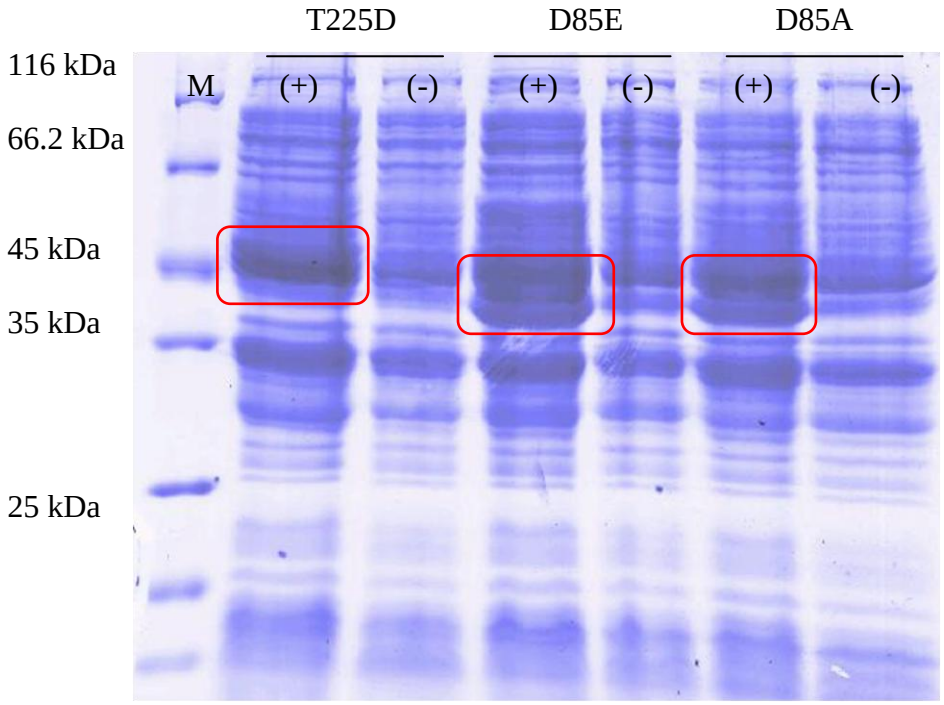

Figure 3.5 : Induction control of DnaK(1-392) T225D, DnaK(1-392) D85E and DnaK(1-392) D85A mutants by SDS-PAGE. M: Protein marker, (-): uninduced proteome, (+): induced proteome by IPTG.

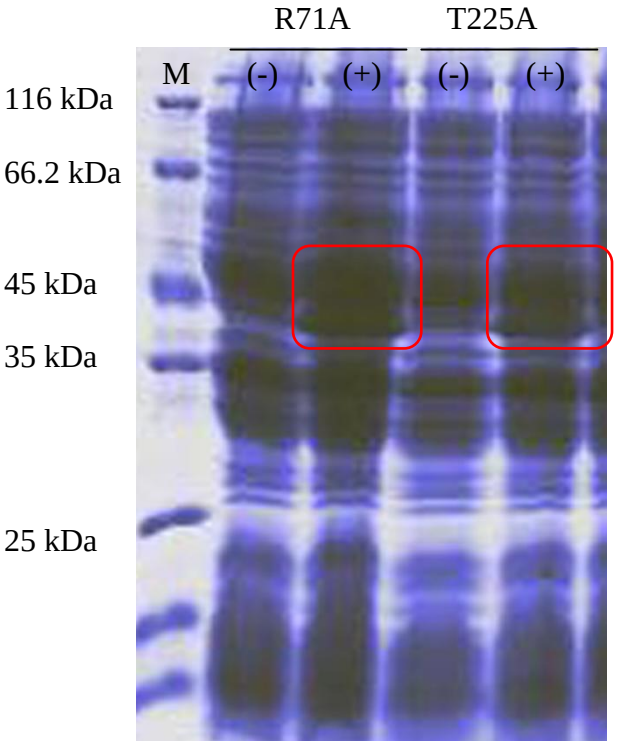

Figure 3.6 : Induction control of DnaK(1-392) R71A and DnaK(1-392) T225A mutants by SDS-PAGE. M: Protein marker, (-): uninduced proteome, (+): induced proteome by IPTG.

3.3 Isolation of Mutant Proteins

Isolation of mutant proteins was done by the replication of two tandem chromatography techniques: DEAE Sephacel anion exchange ion chromatography and ATP-agarose chromatography. First, DEAE Sephacel anion exchange chromatography was applied. Negatively charged proteins could bind to DEAE Sephacel anion exchange column and NaCl gradient was used to elute proteins having different pIs as fractions. Collected fractions later were analyzed on the SDS-PAGE to detect the fractions enriched by DnaK(1-392) and mutant DnaK(1-392) proteins (Figure 3.7).

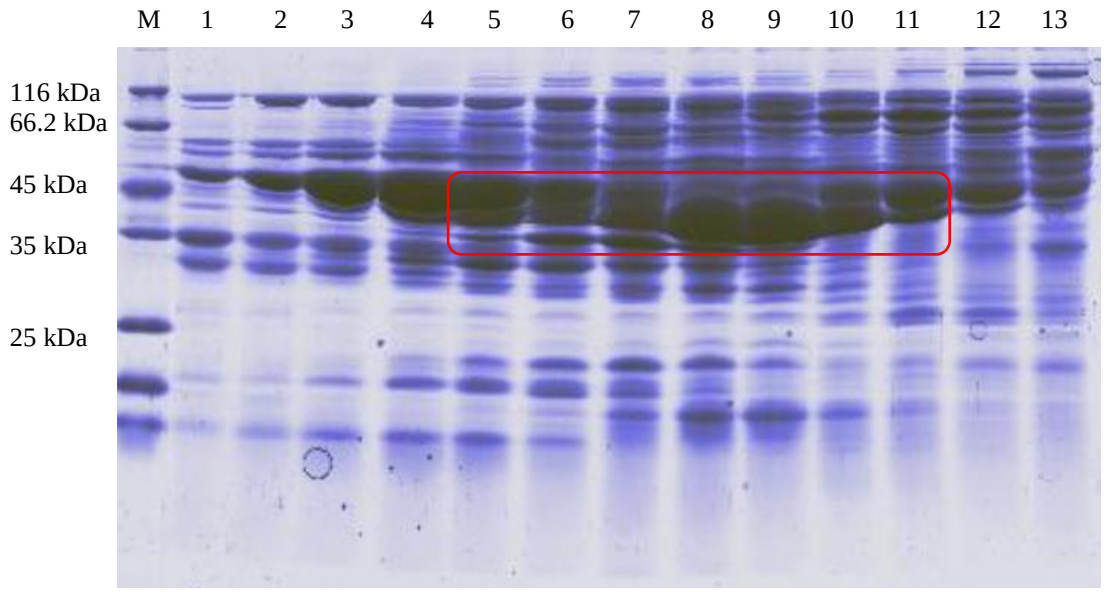

Figure 3.7 : DEAE anion exchange column fractions of DnaK(1-392) by SDS-PAGE. M: Protein Marker, Numbers: the fraction numbers.

It was detected that the fractions of 5, 6, 7, 8, 9, 10 and 11 were enriched by DnaK(1-392) protein and second step, ATP agarose column, was produced with these fractions. The purity of the isolated protein was controlled by SDS-PAGE (Figure 3.8). The procedure was repeated for all the mutants but their corresponding gel images of DEAE Sephacel column fractions were not shown. One single band was detected by SDS-PAGE as shown Figures 3.8-3.11, suggesting that we obtained purified proteins. The concentrations were varying in the range of 20 to 100 μM.

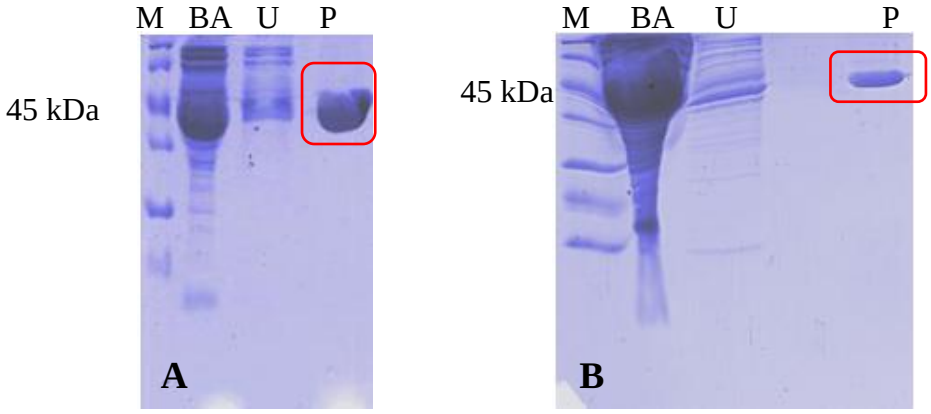

Figure 3.8 : Purified DnaK(1-392) and DnaK(1-392) R71A proteins. A) DnaK, B) DnaK(1-392) R71A, M: Protein marker, BA: The fraction before loading to ATP-agarose column , U: The proteins which were not bind ATP-agarose column, P: Purified proteins

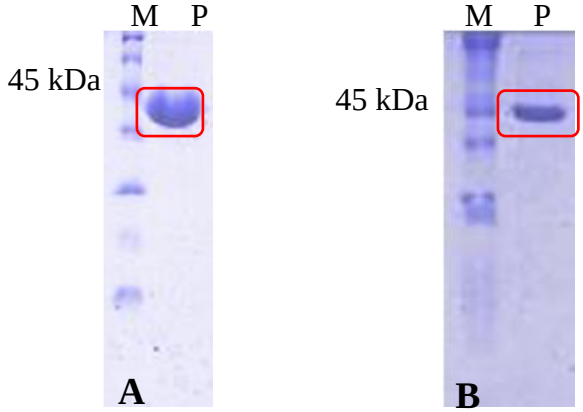

Figure 3.9 : Purified DnaK(1-392) D85A and DnaK(1-392) D85E proteins. A) DnaK(1-392) D85A, B) DnaK(1-392) D85E. M: Protein marker, P: Purified protein

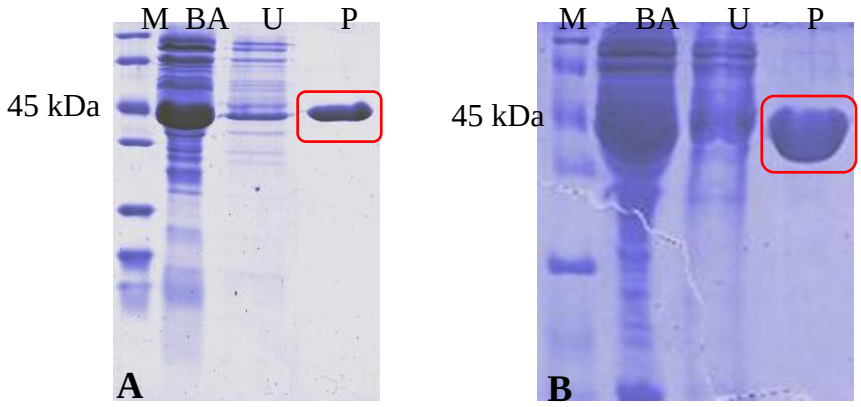

Figure 3.10 : Purified DnaK(1-392) T225D and DnaK(1-392) H226F proteins. A) DnaK(1-392) T225D, B) DnaK(1-392) H226F. M: Protein marker, BA: The fraction before loading to ATP-agarose column , U: The proteins which were not bind ATP-agarose column, P: Purified proteins.

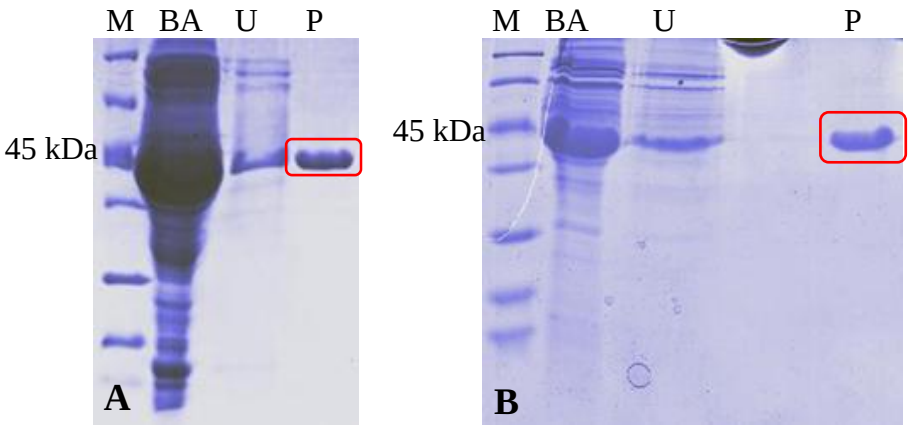

Figure 3.11 : Purified DnaK(1-392) H226A and DnaK(1-392) H295D proteins. A) DnaK(1-392) H226A, B) DnaK(1-392) H295D. M: Protein marker, BA: The fraction before loading to ATP-agarose column, U: The proteins which were not bind ATP-agarose column, P: Purified proteins.

3.4 Native Gel Electrophoresis

Native gel electrophoresis is an electrophoretic separation method based on protein, size, shape and native charge. This method is performed without using denaturating agent SDS and reducing agent DTT, unlike SDS-PAGE electrophoresis. In-non denaturating conditions, the proteins migrate due to their net negative charge and shape in alkaline running buffer and they remain in their native states. Since we would like to understand the structure of Hsp70, we used native gel electrophoresis to determine polymerization of proteins.

We loaded different protein concentrations to the native gel in the presence and absence of ATP. 0.3 mM of ATP was used for 1 µM of DnaK. We observed one band for DnaK(1-392) and its mutants, suggesting that DnaK(1-392) and the mutants remain as monomers. They do not interact with each other, therefore they do not polymerize in the native state. Higher and lower mobility were detected for DnaK(1-392) H295D, DnaK(1-392) D85A mutants respectively, these differences may be arised from changed net negative charge or altered tertiary conformation.

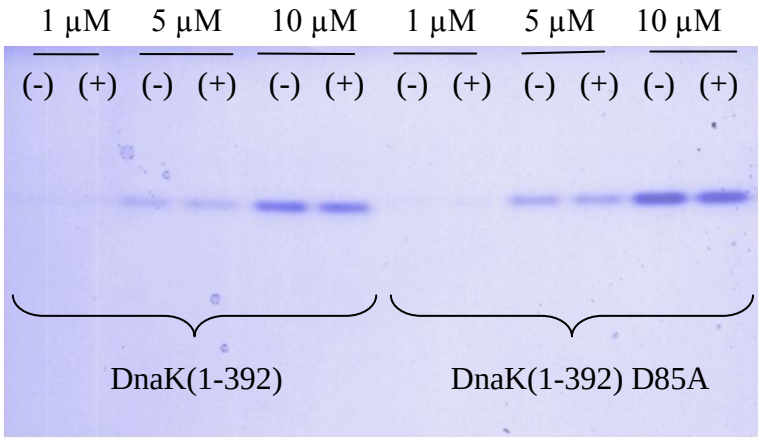

Figure 3.12 : DnaK(1-392) and DnaK(1-392) D85A in native conditions.

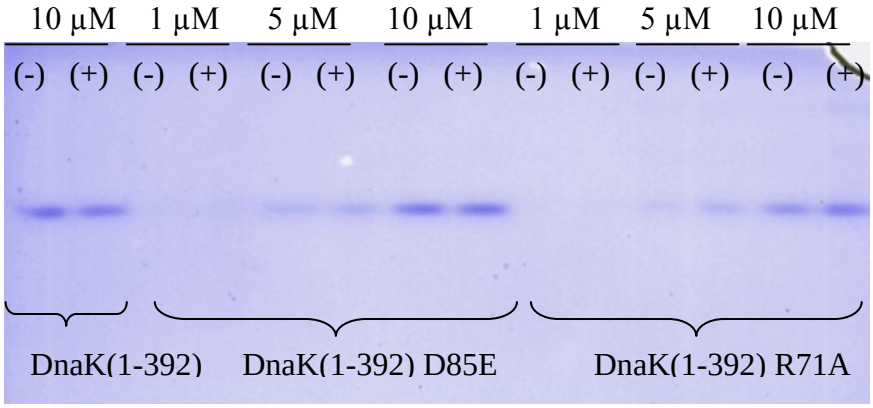

Figure 3.13 : DnaK(1-392), DnaK(1-392) D85E and DnaK(1-392) R71A in native conditions.

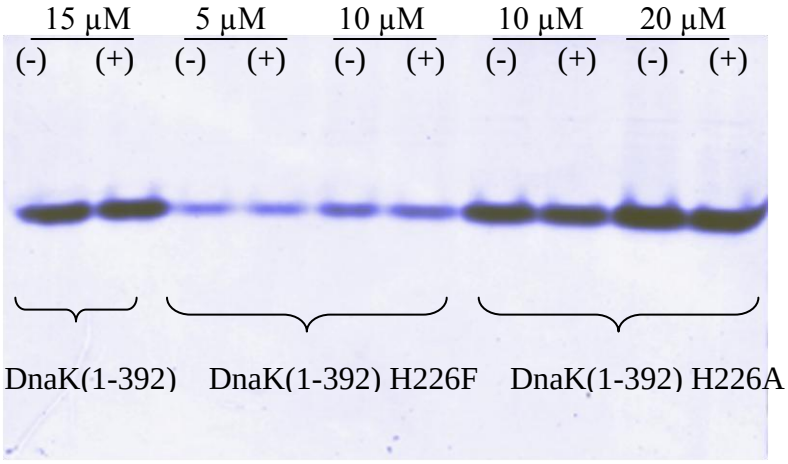

Figure 3.14 : DnaK(1-392), DnaK(1-392) H226F and DnaK(1-392) H226A in native conditions.

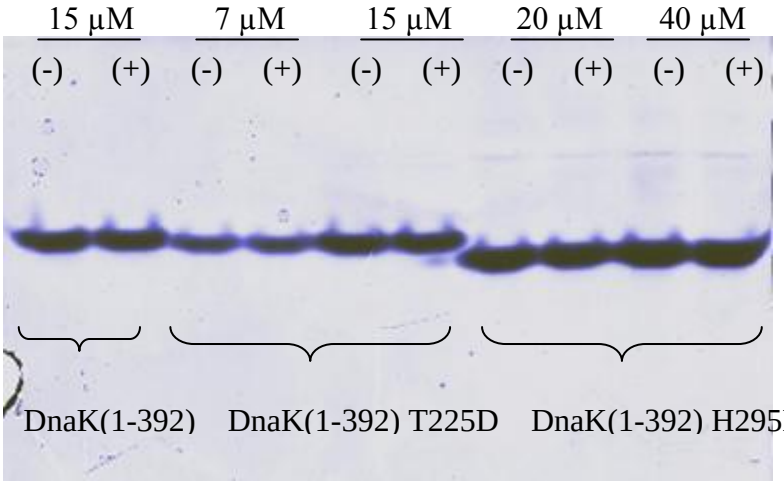

Figure 3.15 : DnaK(1-392), DnaK(1-392) D225D and DnaK(1-392) H295D in native conditions.

3.5 ATPase Measurement

The ATPase rates of mutant proteins were measured depending on pH values. In this experiment, the concentration of DnaK was calculated by absorbance at 280 nm with respect to the equation **(3.1)**. The molar extinction coefficient value is 18607 M^{-1} cm^{-1} for DnaK(1-392).

$$A = \varepsilon \times c \times l \qquad \textbf{(3.1)}$$

A is absorbans, ε is extinction coefficient ($M^{-1}cm^{-1}$), c is concentration (M), l is path length (cm).

Data from Swain *et al.*, 2007; Vogel *et al.*, 2006b and recent findings of Zhuravleva and Gierasch, 2011 confirmed that DnaK(1-392) construct can be a model protein of Hsp70 mimicking the substrate stimulated form of the full-length protein. Since the conformation of the ATPase domain in this construct is similar, we further used this protein in our studies to understand linker induced effects to the domain (as if linker transmits substrate binding signals to the ATPase domain). We reproduced the ATPase activity results of DnaK(1-392) and we observed asymmetric bell-shaped ATPase profile contained a peak at pH around 7.5 as it was observed in the article of Swain *et al.*, 2007. Bell-shaped activity versus pH is arised from two separate ionizable groups. First ionizable group which act as acid is deprotonated at lower pH. On the other hand, second group which act as base is deprotonated as pH is increased. The asymmetric bell-shaped ATPase profile of DnaK(1-392) indicates that

the activity is maximum at pH 7.5 where acidic amino acids in the active site are deprotonated, whereas the basic amino acids in the catalytic site are protonated. Since the basic part of ATPase profile is above compared acidic part of ATPase profile, the catalytic site of DnaK(1-392) contains much more acidic amino acids than the number of basic ones. In this study, we would like to understand the crucial amino acids in the catalytic site which are responsible to convey the linker-induced signal. To this purpose, we revealed the effects of mutant proteins, DnaK(1-392) R71A, DnaK(1-392) D85E, DnaK(1-392) D85A, DnaK(1-392) T225D, DnaK(1-392) H226F, DnaK(1-392) H226A and DnaK(1-392) H295D on ATPase activity as pH is increased.

We measured the ATPase rate of DnaK(1-392) R71A in the pH range of 5.5 and 8.5. We observed that the ATPase rate is increased by 1.5 fold with a bell-shaped ATPase profile similar to DnaK(1-392) (Figure 3.16). We thought that this residue may be important due to its localization as a neighbour of K70 which is catalytic residue. But we need further analysis to reveal whether it is important for the transmission of substrate stimulation.

We measured the ATPase rate of the mutation DnaK(1-392) D85E and DnaK(1-392) D85A. ATPase rates of these mutants are significantly decreased with the loss of bell-shaped ATPase profile, similar to DnaK(1-388) construct whose ATPase rate and ATPase profile are similar to unstimulated full-length DnaK (Swain *et al.* 2007). Swain and colleagues (2007) showed that truncated DnaK(1-388) has unstimulated ATPase rate and ATPase profile of DnaK(1-388) has a plateau as a function of pH. The effects of the mutants D85 are similar to DnaK(1-388), suggesting that the signal transmission path after substrate stimulation may be blocked by the replacement mutation of D85 (Figure 3.17).

We started this project to answer the question: “Which residue(s) is(are) important for bell-shaped ATPase profile of DnaK(1-392)?”. Since a histidine residue is located in the catalytic site in many proteins, we thought H226 located near catalytic site of DnaK can be a candidate for this aim. We changed the histidine to alanine and phenylalanine and examined the ATPase rate. These mutations caused 3-fold increased ATPase rate, and the bell-shaped ATPase profile was kept similar to the DnaK(1-392). We concluded that the histidine is not responsible for the bell-shaped ATPase profile as observed for DnaK(1-392). However, 3-fold increased ATPase

rate for histidine mutations may refer to the enhanced rate in the opening and closing of the ATPase domain. Afterwards, we mutated T225 which is a neighbour of H226. We changed threonine to aspartic acid and measured ATPase rate. Interestingly, we observed that the mutation caused an increased in the ATPase rate by 3-fold and the pH-dependent ATPase profile has a peak at 7.5 similar to that of DnaK(1-392). Since the effects of H226 and T225 mutations are similar, we thought there may be an interaction between H226 and T225 (Figures 3.18-3.19).

We changed the other histidine on the position of 295 with an aspartic acid. We did not observe an important change on the ATPase rate when compared to that of DnaK(1-392), but the bell-shaped ATPase profile is slightly disrupted (Figure 3.20). The analysis of the mutation is work in progress, we need to understand the mutation effect by further experiments.

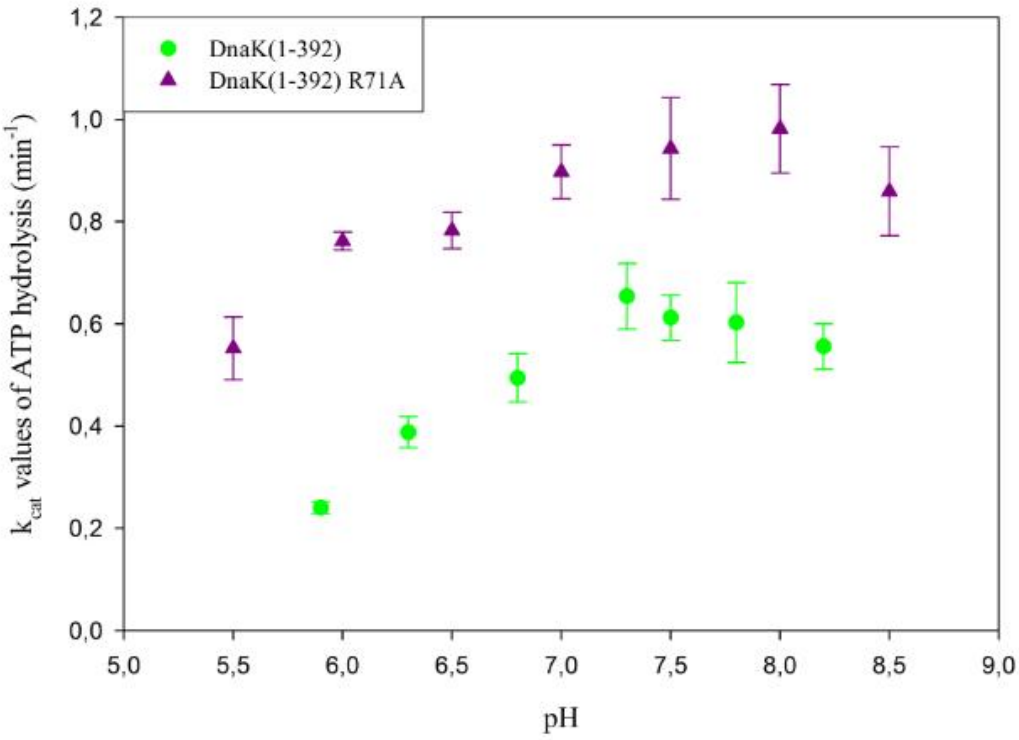

Figure 3.16 : ATPase activity profiles of DnaK(1-392) and DnaK(1-392) R71A.

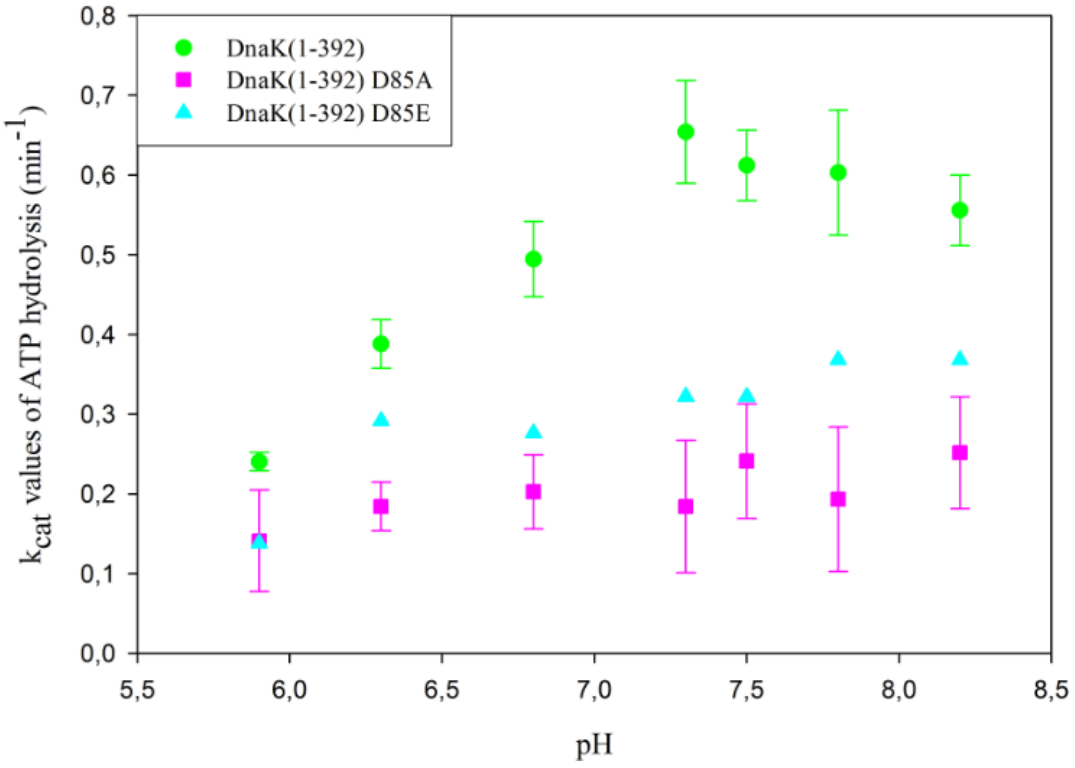

Figure 3.17 : ATPase activity profiles of DnaK(1-392), DnaK(1-392) D85A and DnaK(1-392) D85E.

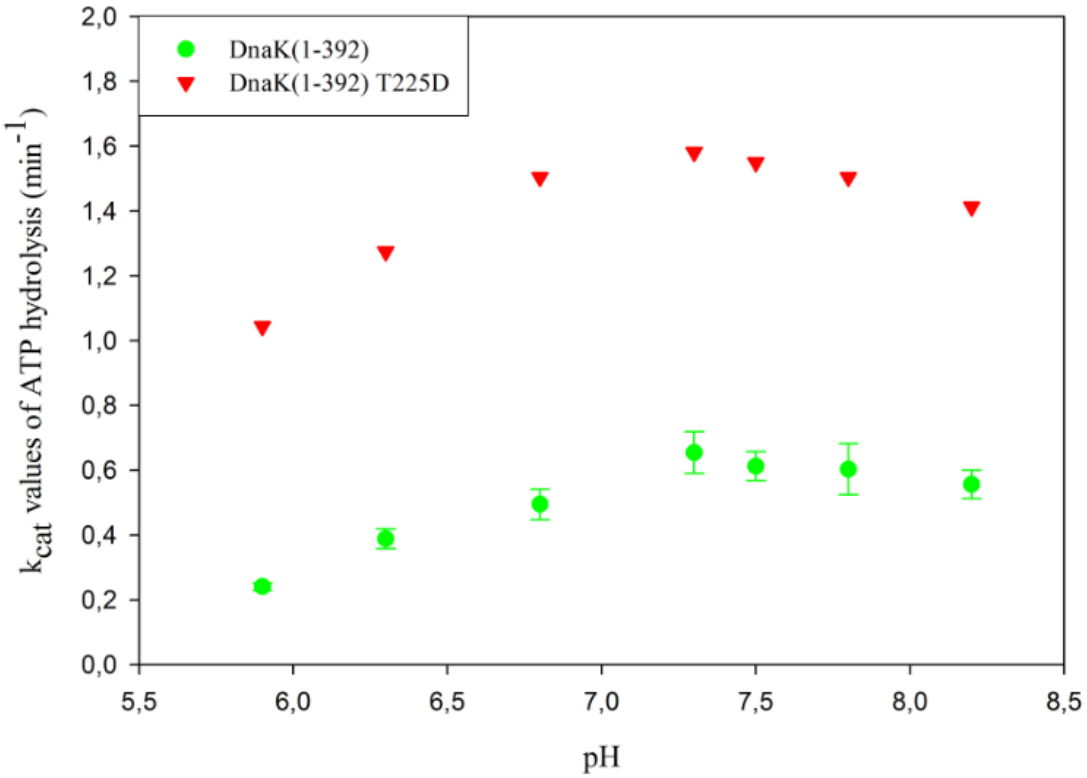

Figure 3.18 : ATPase activity profiles of DnaK(1-392) and DnaK(1-392)T225D.

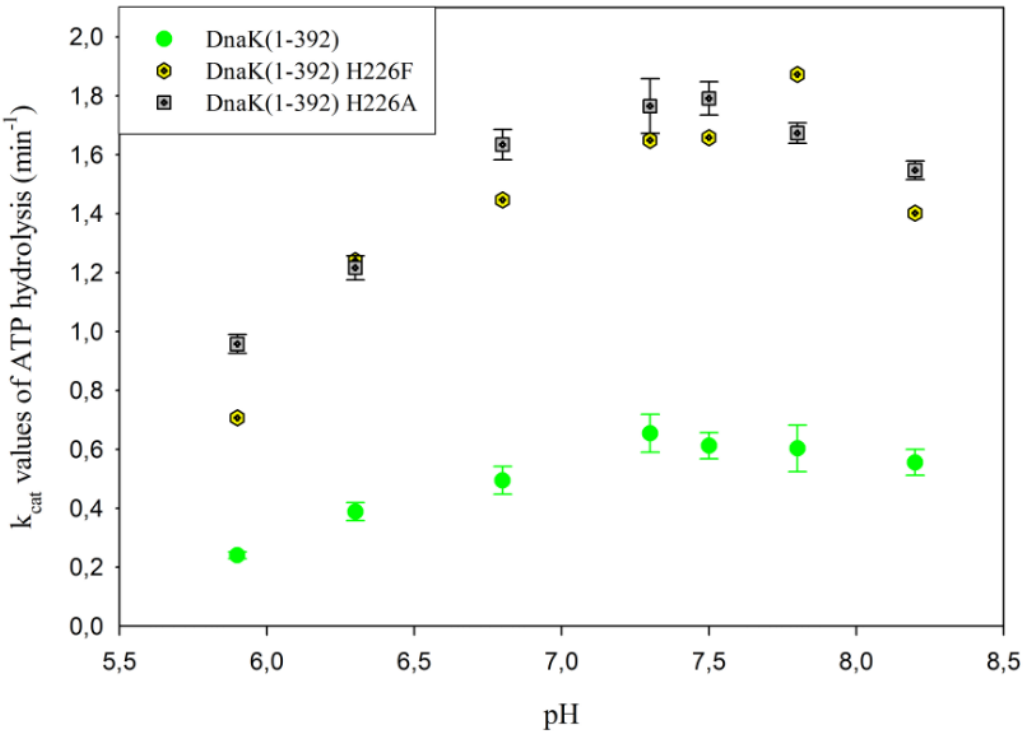

Figure 3.19 : ATPase activity profiles of DnaK(1-392), DnaK(1-392)H226F and DnaK(1-392) H226A.

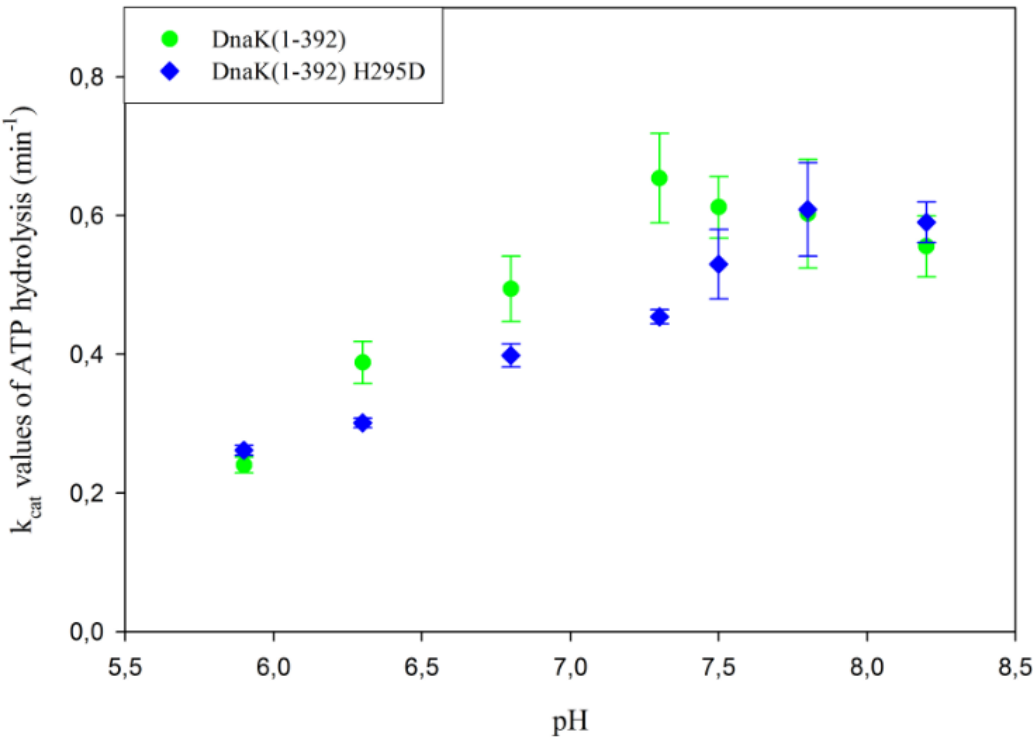

Figure 3.20 : ATPase activity profiles of DnaK(1-392), DnaK(1-392) H295D.

3.6 Secondary Structure Analysis

Since the secondary structure of protein absorb the circulary polarized lights, the differences in the absorption of left-handed and right-handed polarized light were measured by CD spectroscopy. The chromophore is amide bond in the far-UV wavelength (below 250 nm). The three regular secondary structures, α helices, β sheets and random coils have different characteristic in CD spectra. The CD spectrum of α helix shows negative peak at 222 nm and 208 nm and a positive peak at 192 nm. The spectrum of typical β sheet is characterized a negative peak near 215 nm and a positive peak near 198 nm. The CD spectrum of random coil has a weak peak near 226 nm and a strong negative peak near 206 nm. The characterictics of CD spectra of α helices, β sheets and random coils inform the secondary structure of proteins.

We measured the ellipticity for the proteins of DnaK(1-392), DnaK(1-392) H226F and DnaK(1-392) H226A in the range between 200 and 250 nm and calculated mean residue weight ellipticity using the equation (2.2). The graphs of proteins in Figure 3.21 were not overlapping with each other, therefore the secondary structures of proteins were not similar according to this figure. We thought that there might be a pipetting error (~5-10% pipetting error for DnaK(1-392) H226A and DnaK(1-392), respectively), therefore we calculated the mean residue weight again and we superimposed the graphs by adjusting the molar protein concentration (Figure 3.22). We detected that the secondary structures of mutants are almost same as DnaK(1-392) at pH 7. The ellipticity values as a function of wavelength at pH 8 were determined as shown in Figure 3.23. Since the graphs of pH 8 are overlapped, we understood that there was no pipetting error. It was obvious that the graphs of mutants DnaK(1-392) H226A and DnaK(1-392) H226F shifted to the left on the y axis, therefore moving to 208 nm on the graphs showed that their secondary structures of histidine mutants are more helical.

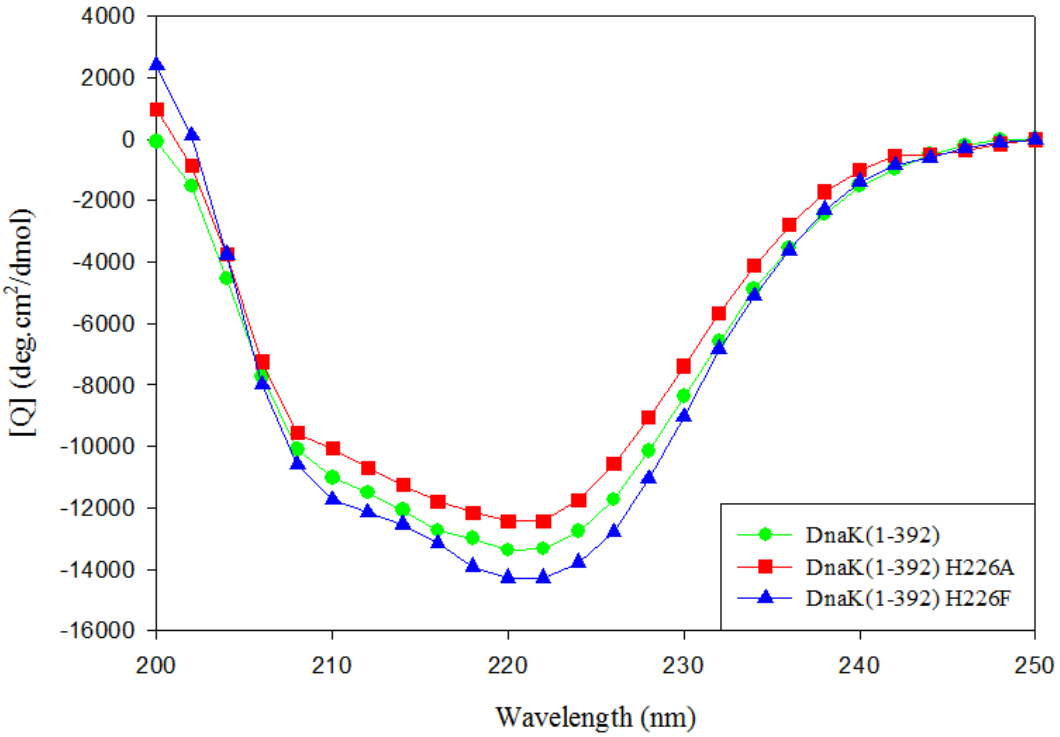

Figure 3.21 : CD spectra of DnaK(1-392), DnaK(1-392) H226A and DnaK(1-392) H226F at pH 7.

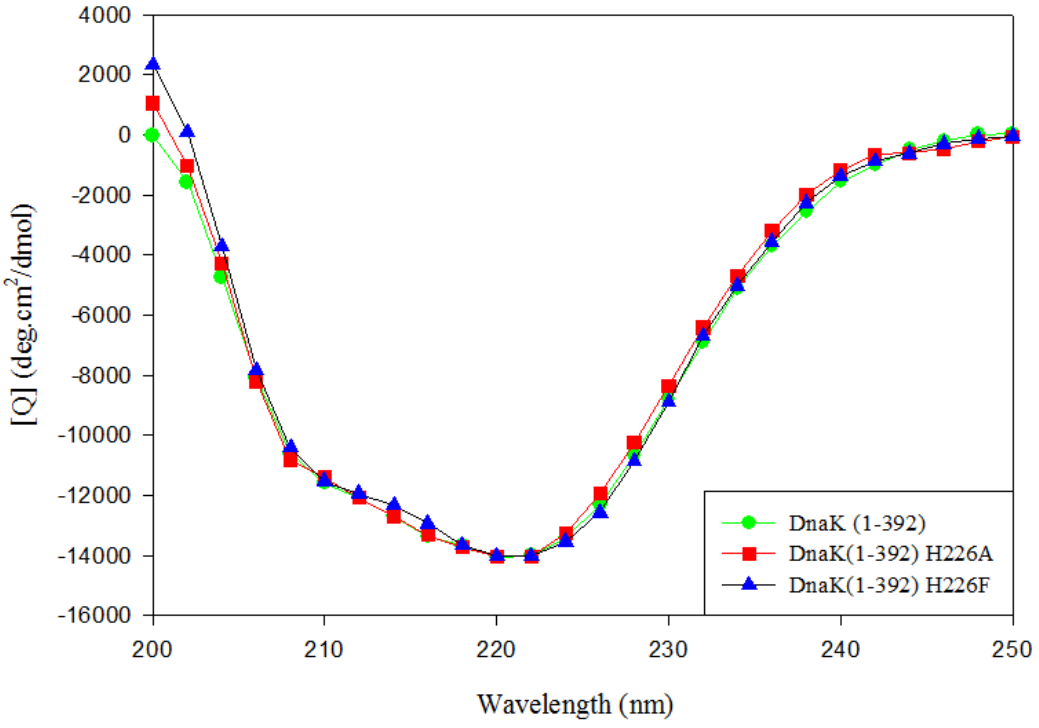

Figure 3.22 : Superimposition of CD spectra of DnaK(1-392), DnaK(1-392) H226A and DnaK(1-392) H226F at pH 7.

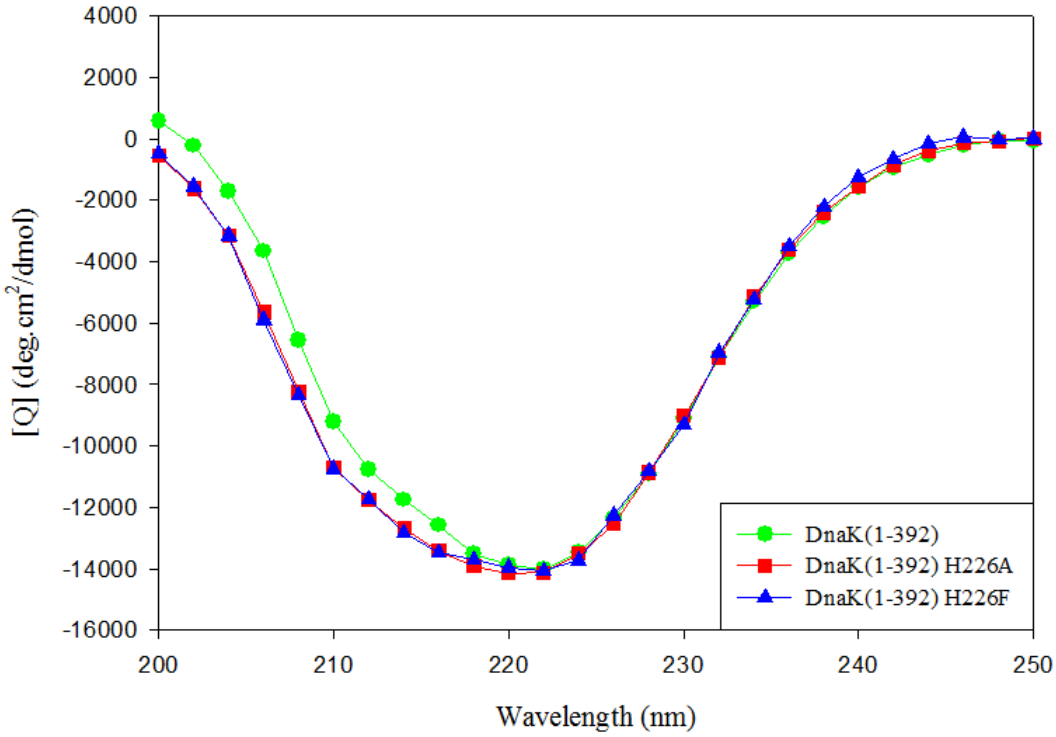

Figure 3.23 : CD spectra of DnaK(1-392), DnaK(1-392) H226A and DnaK(1-392) H226F at pH 8.

3.7 Protein Stability Analysis

We demanded to understand the effects of mutations on the stability of DnaK. Secondary structure of proteins were disrupted by increasing temperature monitoring by CD spectroscopy. The proteins are denatured by breaking hydrogen bonds, hydrophobic interactions and salt linkages. We used the scale from 25ºC to 90ºC in this experiment. The conformational stability of proteins depending on temperature was searched at 222 nm.

We measured the ellipticity of DnaK(1-392), DnaK(1-392) H226F and DnaK(1-392) H226A as a function of temperature at pH values 7 and 8. We observed that the first transition of DnaK(1-392) is shifted to the right on the y axis indicating temperature at pH 7, therefore DnaK(1-392) is more stable at pH 7 than pH 8 (Figure 3.24). However, histidine mutants did not show stability differences at pH 7 and 8 (Figures 3.25-3.26). The first transitions of the mutants were shifted to the left on the y axis represented temperature at both pH 7 and pH 8 as shown in the table of T_m values (Table 3.1). Stability differences between pH 7 and 8 were shown on DnaK(1-392), however CD measurement showed that stability of histidine mutants were similara at

both pH 7 and 8, suggesting that H226 is responsible for the stability difference. Decreased protein stability shifts the open and closed conformational equilibrium to a more open state correlating well with the shifting to the left on graphs confirmed 3-fold enhanced ATPase activity of mutants DnaK(1-392) H226A and H226F where an easier ADP release can occur.

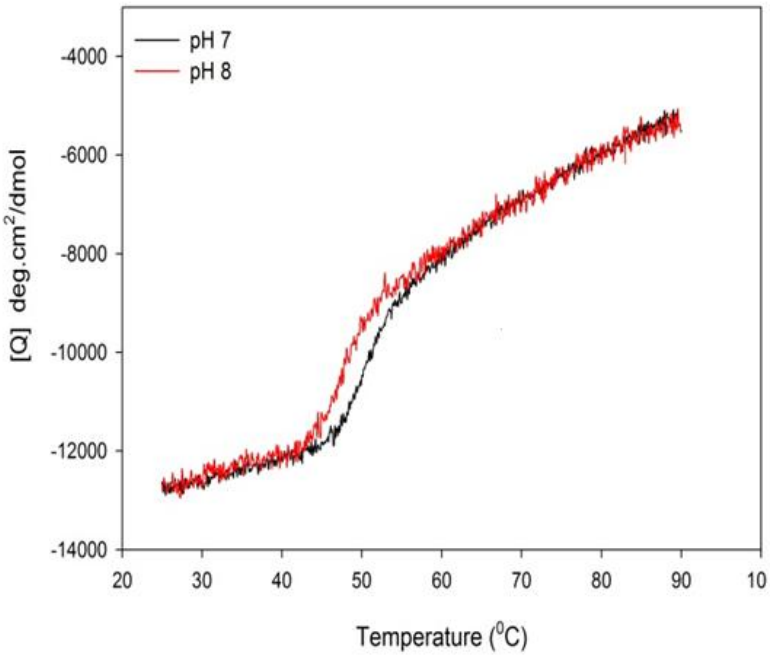

Figure 3.24 : CD thermal melt of DnaK(1-392) in the comparison of pH 7 and 8.

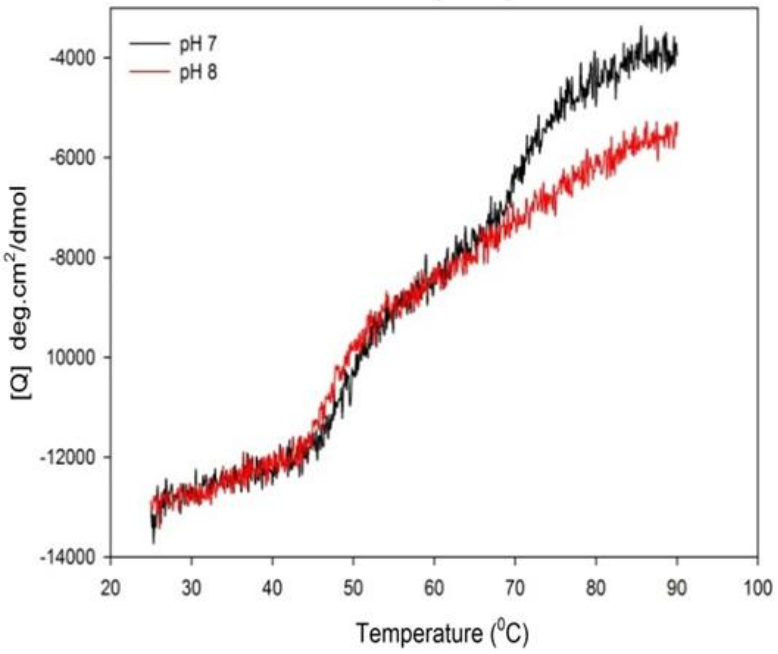

Figure 3.25 : CD thermal melt of DnaK(1-392) H226A in the comparison of pH 7 and 8.

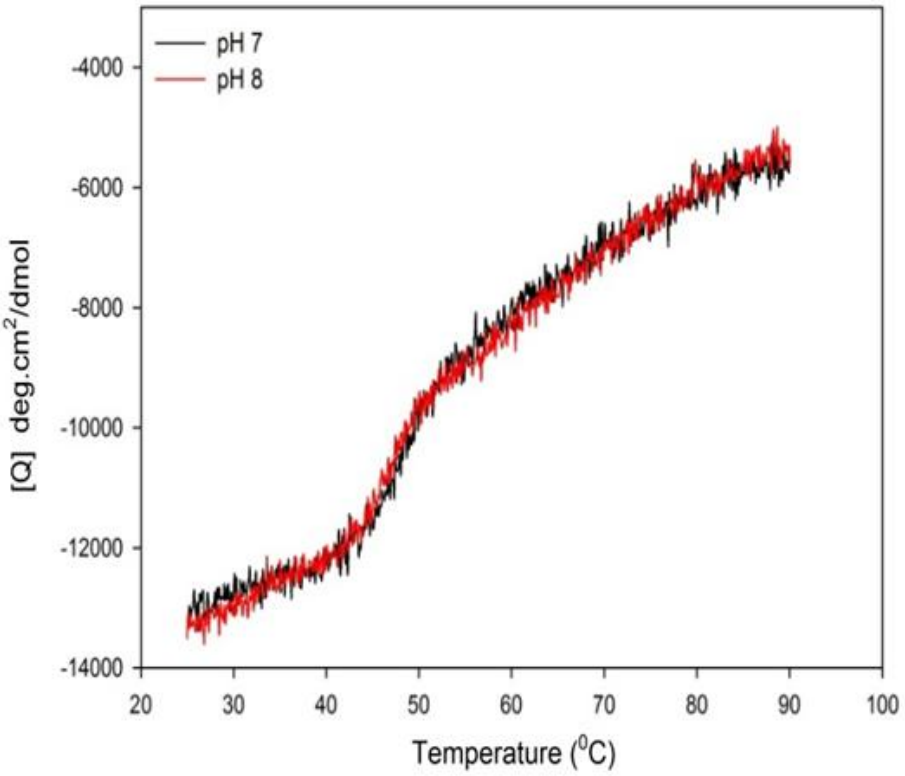

Figure 3.26 : CD thermal melt of DnaK(1-392) H226F in the comparison of pH 7 and 8.

Table 3.1 : T_m values of first transition at pH 7.0 and 8.0

	T_m values at pH 7.0	**T_m values at pH 8.0**
DnaK(1-392)	50.4ºC	47.7 ºC
DnaK(1-392) H226A	48.2ºC	46.7ºC
DnaK(1-392) H226F	47.4ºC	46.8ºC

4. DISCUSSION AND CONCLUSION

The conformational changes of Hsp70s are important for function of Hsp70s. Allosteric communication of Hsp70 is controlled by some residues and we tried to understand the crucial amino acids in ATPase activation upon substrate binding which is the mechanism regulating Hsp70 function.

The studies revealed that the linker has a role in the allosteric control between the domains of Hsp70s (Laufen *et al.*, 1999, Swain *et al.*, 2007, Vogel *et al.*, 2006b). It was noted that the mutations on the linker region (^{389}AAAA^{392} and ^{389}VDDL^{392}) cause a loss of interdomain coupling (Laufen *et al.*, 1999). Other study showed the importance of linker in the stimulation of ATPase domain (Vogel *et al.*, 2006b). They compared the basal ATPase rates of truncated DnaK(2-385) and DnaK(2-393) (Vogel *et al.*, 2006b). It was found that DnaK(2-385) has the ATPase rate as the unstimulated full-length DnaK, although basal ATPase rate of DnaK(2-393) is similar to that of the stimulated full-length DnaK (Vogel *et al.*, 2006b). Swain and colleagues (2007) revealed additional knowledge about the importance of linker. They showed that DnaK(1-392), containing NBD and the entire linker, has stimulated ATPase rate, also exhibits pH dependent ATPase profile as substrate stimulated full-length DnaK (Swain *et al.* 2007). For this reason, we used DnaK(1-392) construct in this study as a model of substrate stimulated full-length DnaK.

The first step of allosteric mechanism is that NBD senses the signal of substrate binding. In this step, linker region connects the hydrophobic cleft between subdomains of IA and IIA on NBD (Swain *et al.*, 2007). We aimed to reveal the important amino acids conveying the signal to ATPase domain upon substrate binding. In our strategy, we mutated the putative network residues which are of 71, 85, 225, 226 and 295 (Figure 4.1).

In this study, we purified DnaK(1-392) and analysed the ATPase rate as a function of pH. We obtained the peak at pH 7.5 on ATPase rate as was shown previously (Swain *et al.*, 2007). This pH-dependent ATPase profile shows that there may be a catalytic residue/residues which is/are titratable upon change in pH. The asymmetric ATPase

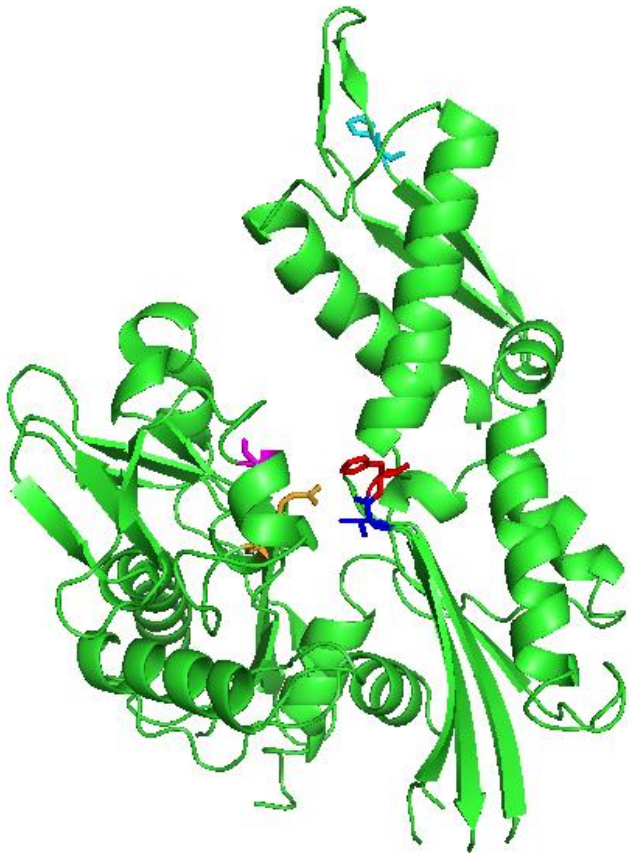

Figure 4.1 : Mutated residues on NBD of DnaK. R71 is shown in orange, D85 in magenta, T225 in blue, H226 in red and H295 in cyan. (PDB code: 1DKG).

profile indicates that the asidic amino acids may be much more than basic amino acids in the catalytic site. For example, there may be two asidic amino acids, whereas one basic amino acid in the controlling of the ATPase rate. To understand the crucial amino acids in the active site, we mutated H226 located near the catalytic region. We changed histidine to alanine and phenylalanine and measured the ATPase rate. The replacement mutations caused to increase ATPase rate by 3-fold without changing ATPase profile which has the peak at pH 7.5. Interestingly, the replacement mutation threonine to aspartic acid on the position of 225 caused 3-fold increased ATPase rate and the peak around pH 7.5 observed in the pH-dependent ATPase profile is similar to that of DnaK(1-392), suggesting that the mutations of H226 and T225 have similar effects on the ATPase rate and pH-dependent ATPase profile. Since, mutants of histidine and threonine showed asymmetric bell-shaped pH-dependent ATPase profile similar to that of DnaK(1-392), H226 and T225 are not the residues which are titrated as a function of pH. Histidine and threonine mutations may cause an increase in the opening and closing rate of the ATPase domain. We observed the same pattern

of ATPase profile to be compared with DnaK(1-392), revealing that the limiting step is ADP release as measured for DnaK(1-392) (Swain *et al.* 2007). We obtained almost the same effects when the residues are mutated separately, suggesting that there may be an interaction between T225 and H226, and these residues may have a similar role in the allosteric communication (Figure 4.2). CD analysis showed that DnaK(1-392) is more stable at pH 7 than pH 8, however there is no difference for DnaK(1-392) H226F and DnaK(1-392) H226A mutants, both showed lower stability as observed like pH 8.0 for DnaK(1-392). Since the first transition of histidine mutants were shifted to the left on the axis of temperature at both pH 7 and 8, histidine mutants are less stable when compared to that of DnaK(1-392). Lower stability of histidine mutants indicated that ATPase domains show open conformation to compared DnaK(1-392). This open conformation may facilitate release of ADP, resulting high ATPase activity. Also, secondary structures of DnaK(1-392) H226F and DnaK(1-392) H226A were analysed by CD. It was observed that DnaK(1-392) and histidine mutants show almost the same secondary structure at pH 7, however DnaK(1-392) H226F and DnaK(1-392) H226A mutants are more helical at pH 8. We need further experiments to understand the difference of secondary structures of histidine mutants.

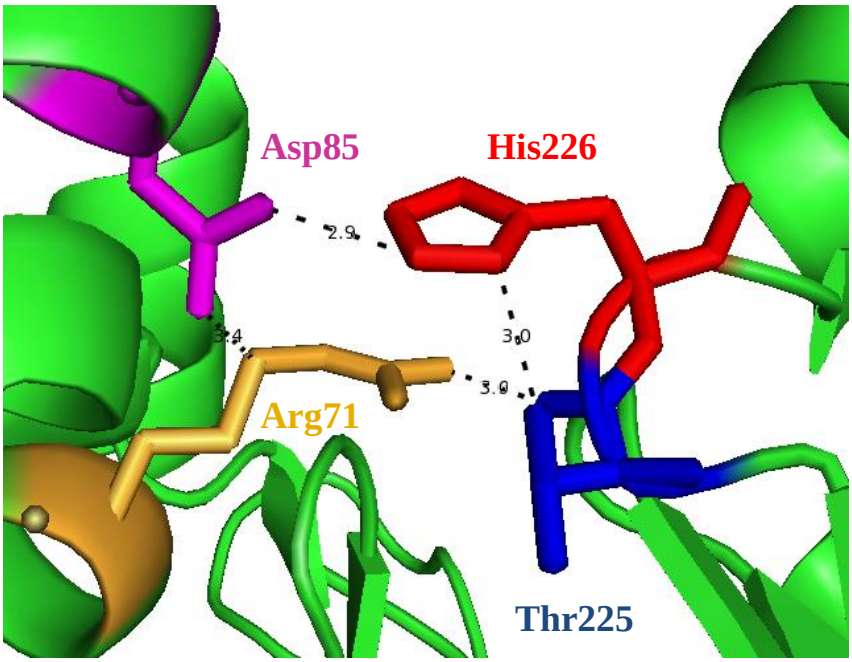

Figure 4.2 : The putative interactions between Arg71, Asp85, Thr225 and His226 in bHsc70 (complexed with Bag) structure. The stick representations of the Arg71 (bHsc70: Arg72), Asp85 (bHsc70: Asp86), Thr 225 (Hsc70: Thr 226), His 226 (bHsc70: His 227) are shown in orange, magenta, blue and red, respectively (PDB code: 1HX1). The distance between the residues was measured in terms of Å.

We found that H226F and H226A mutants affect the ATPase rate similarly, suggesting that the positive charged histidine is importand for ATPase activity, rather than molecule size.

The replacement mutation of D85 caused a dramatic decrease in the ATPase rate revealing a steady rate as a function of pH, similar to that of DnaK(1-388), which is linkerless version of DnaK (Swain et al., 2007). ATPase profiles of DnaK(1-392) D85A and DnaK(1-392) D85E are alike to truncated DnaK(1-388) which is the similar conformation of unstimulated full-length DnaK (Swain *et al.*, 2007). The mutation of D85 disrupted the stimulated conformation of DnaK(1-392) and interrupted transmission the signal to the ATPase domain by substrate binding, showing that D85 may be a catalytic residue for ATPase activation. Also, mutational analysis of D85 on full-length DnaK confirms our results (Chang *et al*., 2010). Chang and colleagues (2010) showed that D85A mutation on full-length DnaK disrupts substrate stimulation (Chang *et al*., 2010).

Furthermore, the mutations to glutamic acid and alanine on the position of 85 caused a similar effect on DnaK(1-392), suggesting that not only the charge of amino acid on the position 85 but also the size of amino acid is crucial for delivering signal to the ATPase domain upon substrate binding.

We changed arginine residue to alanine on the position of 71 which is a neighbour of the catalytic residue, K70 (O'Brien *et al.*, 1996). We thought that arginine may stabilize the position of K70 by electrostatic interactions and it may interact with the flexible loop at which G196, G197 and G198 are located. The flexible loop is important for positioning T199, which is the site of autophosphorylation (McCarty and Walker, 1991). We think that the replacement mutation from arginine to alanine cause to disrupt the repulsion between lysine and arginine. We observed that the mutation caused to increase ATPase rate by 1.5 fold by bell-shaped ATPase profile. We need further experiments to identify the mechanism of R71.

We would like to understand the effect of histidine residues on bell-shaped ATPase profile, we analysed the mutational effects of other histidine which is at the 295th position. We mutated this histidine to aspartic acid and measured the ATPase rate as afunction of pH. It was seen that the ATPase profile is slightly shifted with similar values of ATPase rate to compared DnaK(1-392). Intriguingly, the replacement mutation on the position of 295 affects the ATPase profile, although this residue is

solvent exposed according to crystal structures. In my opinion, it can not affect the environment of catalytic site, since it is far away from the catalytic site of the protein. The mechanism needs to be revealed by other experiments.

We would like to understand the structures of mutants in their native state. To this purpose, we used the native gel electrophoresis to observe that the mutant proteins remain as a monomer or form polymers in non-denaturating conditions. We observed no polymerization for all mutants, but the H295D and D85A mutants exhibited higher and lower mobility, respectively, with respect to DnaK(1-392) and other mutants. Higher migration of H295D may arise due to its more compact conformation or its increased net negative charge. Since the residue of 295 is solvent exposed, replacement mutation to aspartic acid might increase the net negative charge on protein. On the other hand, the replacement of negatively charged aspartic acid on the position of 85 caused lower mobility due to decreased negative charge on protein. According to our hypothesis, the groove between IA and IIA is important for polymerization. In DnaK(1-388), the positively charged groove is opened and exposed to interact a negative residue. The polymerization was detected in some mutants of DnaK(1-388) (data not shown). However, In DnaK(1-392), we think that carboxylate at the C-terminus L392 interacts with a positively charged residue on the groove between IA and IIA subdomains. Since the positively charged groove is already been occupied by the linker, no polymerization could be detected for the mutants of DnaK(1-392).

Our study with moleculer modeling analysis showed that there can be a network between R71, D85, E230, T225 and H226. In this interconnection, there can be two major catalytic activation path; one is by the correct positioning of T199 and the other is by again correct positioning of K70 for catalysis. The salt bridge interaction of R71 and E230 may affect the positioning of T225, H226 and E81 and D85, in this network, the ATPase activity can be determined by the correct positioning of T199 and G196, G197, G198. The salt bridge of R71 and E230, also, may affect the correct positioning of catalytic residue of K70. In the way of our thinking, the alteration of IIB subdomain orientation can be determined by the interactions of R71. Distrupting substrate stimulation on full-length DnaK by mutating E230 and R71 confirms the importance of these residue on signal transduction to ATPase domain by substrate binding (Chang *et al.*, 2010). We suggest that E230 and R71 play the

main role and regulate the interactions of D85, E81, T225 and H226 on interdomain coupling upon substrate binding. Our future experiments will include a mutational analysis governing both E81 and E230. By this way, we will be able to complete our investigations on our putative network while studying linker induced or substrate stimulated allosteric signaling in the ATPase domain of Hsp70s.

REFERENCES

Bertelsen, E. B., Chang, L., Gestwicki, J. E., & Zuiderweg, E. R. (2009). Solution conformation of wild-type E. coli Hsp70 (DnaK) chaperone complexed with ADP and substrate. *Proceedings of the National Academy of Sciences of the United States of America, 106*(21), 8471-8476.

Blatch G.L. (2007). *The Networking of Chaperones by Co-chaperones*. Springer, New York, USA.

Buchberger, A., Valencia, A., McMacken, R., Sander, C., Bukau, B. (1994). The chaperone function of DnaK requires the coupling of ATPase activity with substrate binding through residue E171. *The EMBO Journal, 13(7),* 1687 – 1695.

Buchberger, A., Theyssen, H., Schroder, H., McCarty, J. S., Virgallita, G., Milkereit, P., Reinstein J., Bukau, B. (1995). Nucleotide-induced conformational changes in the ATPase and substrate binding domains of the DnaK chaperone provide evidence for interdomain communication, *The Journal of Biological Chemistry, 270(28),* 16903-16910.

Chang, L., Thompson, A. D., Ung, P., Carlson, H. A., & Gestwicki, J. E. (2010). Mutagenesis reveals the complex relationships between ATPase rate and the chaperone activities of Escherichia coli heat shock protein 70 (Hsp70/DnaK). *The Journal of Biological Chemistry,* 285.

Chai, Y., Koppenhafer, S. L., Bonini, N. M., & Paulson, H. L. (1999). Analysis of the role of heat shock protein (Hsp) molecular chaperones in polyglutamine disease. *The Journal of Neuroscience, 19*(23), 10338-10347.

Ciocca, D. R., & Calderwood, S. K. (2005). Heat shock proteins in cancer: diagnostic, prognostic, predictive, and treatment implications. *Cell Stress Chaperones, 10*(2), 86-103.

Dou, F., Netzer, W. J., Tanemura, K., Li, F., Hartl, F. U., Takashima, A., Gouras G. K., Greengard P., Xu, H. (2003). Chaperones increase association of tau protein with microtubules. *Proceedings of the National Academy of Sciences of the United States of America, 100*(2), 721-726.

Flaherty, K. M., Wilbanks, S. M., DeLuca-Flaherty, C., & McKay, D. B. (1994). Structural basis of the 70-kilodalton heat shock cognate protein ATP hydrolytic activity. II. Structure of the active site with ADP or ATP bound to wild type and mutant ATPase fragment. *The Journal of Biological Chemistry, 269*(17), 12899-12907.

Flaherty K. M., DeLuca-Flaherty C., McKay D. B., (1990), Three-dimensional structure of the ATPase fragment of a 70K heat-shock cognate protein, *Nature,* 346, 623-628.

Harrison, C. J., Hayer-Hartl, M., Di Liberto, M., Hartl, F., & Kuriyan, J. (1997). Crystal structure of the nucleotide exchange factor GrpE bound to the ATPase domain of the molecular chaperone DnaK. *Science, 276*(5311), 431-435.

Hartl, F. U., & Hayer-Hartl, M. (2002). Molecular chaperones in the cytosol: from nascent chain to folded protein. *Science, 295*(5561), 1852-1858.

Jiang, J., Prasad, K., Lafer, E. M., & Sousa, R. (2005). Structural basis of interdomain communication in the Hsc70 chaperone. *Molecular Cell, 20*(4), 513-524.

Jaattela M., (1999), Escaping Cell Death: Survival Proteins in Cancer, *Experimental Cell Research*, *248*, 30-43.

Jolly C., Morimoto R. I., (2000), Role of the Heat Shock Response and Molecular Chaperones in Oncogenesis and Cell Death, *The Journal of the National Cancer Institute,* Vol. 92, No. 19, 1564-1572.

Kampinga, H. H., & Craig, E. A. (2010). The HSP70 chaperone machinery: J proteins as drivers of functional specificity. *Nature Reviews Molecular Cell Biology, 11*(8), 579-592.

Kiianitsa, K., Solinger, J. A., & Heyer, W. D. (2003). NADH-coupled microplate photometric assay for kinetic studies of ATP-hydrolyzing enzymes with low and high specific activities. *Analytical Biochemistry, 321*(2), 266-271.

Kumar, D. P., Vorvis, C., Sarbeng, E. B., Cabra Ledesma, V. C., Willis, J. E., & Liu, Q. (2011). The four hydrophobic residues on the Hsp70 inter-domain linker have two distinct roles. *Journal of Molecular Biology, 411*(5), 1099-1113.

Labrador-Garrido, A., Bertoncini, C.W. and Roodveldt C. (2011). The Hsp70 Chaperone System in Parkinson's Disease. In Rana A.Q. (ed.), *Etiology and Pathophysiology of Parkinson's Disease* (pp. 221–246). ISBN: 978-953-307-462-7, InTech.

Laufen, T., Mayer, M. P., Beisel, C., Klostermeier, D., Mogk, A., Reinstein, J., & Bukau, B. (1999). Mechanism of regulation of hsp70 chaperones by DnaJ cochaperones. *Proceedings of the National Academy of Sciences of the United States of America, 96*(10), 5452-5457.

Liu Q., Hendrickson W. A., (2007) Insights into Hsp70 Chaperone Activity from a Crystal Structure of the Yeast Hsp110 Sse1. *Cell, 131*, 106-120.

Mayer, M. P., Schroder, H., Rudiger, S., Paal, K., Laufen, T., & Bukau, B. (2000). Multistep mechanism of substrate binding determines chaperone activity of Hsp70. *Nature Structural&Molecular Biology, 7*(7), 586-593.

Mayer, M. P., & Bukau, B. (2005). Hsp70 chaperones: cellular functions and molecular mechanism. *Cellular and Molecular Life Science, 62*(6), 670-684.

McCarty, J. S., & Walker, G. C. (1991). DnaK as a thermometer: threonine-199 is site of autophosphorylation and is critical for ATPase activity, *Biochemistry, 88*, 9513-9517.

Norby, J. G. (1988). "Coupled assay of Na+,K+-ATPase activity." *Methods in Enzymology*, *156*,116-9.

O'Brien M. C., Flaherty K. M., , McKay D. B., (1996) Lysine 71 of the Chaperone Protein Hsc70 Is Essential for ATP Hydrolysis. *The Journal of Biological Chemistry*, *271(27)*, 15874–15878.

Patury, S., Miyata, Y., & Gestwicki, J. E. (2009). Pharmacological targeting of the Hsp70 chaperone. *Current Topics in Medicinal Chemistry, 9*(15), 1337-1351.

Qiu, X. B., Shao, Y. M., Miao, S., & Wang, L. (2006). The diversity of the DnaJ/Hsp40 family, the crucial partners for Hsp70 chaperones. *Cellular and Molecular Life Sciences, 63*(22), 2560-2570.

Saleh, A., Srinivasula, S. M., Balkir, L., Robbins, P. D., & Alnemri, E. S. (2000). Negative regulation of the Apaf-1 apoptosome by Hsp70. *Nature Cell Biology, 2*(8), 476-483.

Schlesinger M. J. (1990). Heat shock proteins. *The Journal of Biological Chemistry*, 265(7), 12111-12114

Schmid, D., Baici, A., Gehring, H., & Christen, P. (1994). Kinetics of molecular chaperone action. *Science, 263*(5149), 971-973.

Shida, M., Arakawa, A., Ishii, R., Kishishita, S., Takagi, T., Kukimoto-Niino, M., . . . Yokoyama, S. (2010). Direct inter-subdomain interactions switch between the closed and open forms of the Hsp70 nucleotide-binding domain in the nucleotide-free state. *Acta Crystallographic a Section D Biological Crystallography, 66*(Pt 3), 223-232.

Sondermann, H., Scheufler, C., Schneider, C., Hohfeld, J., Hartl, F. U., & Moarefi, I. (2001). Structure of a Bag/Hsc70 complex: convergent functional evolution of Hsp70 nucleotide exchange factors. *Science, 291*(5508), 1553-1557.

Sousa, M. C., & McKay, D. B. (1998). The hydroxyl of threonine 13 of the bovine 70-kDa heat shock cognate protein is essential for transducing the ATP-induced conformational change. *Biochemistry, 37*(44), 15392-15399.

Sriram, M., Osipiuk, J., Freeman, B., Morimoto, R., & Joachimiak, A. (1997). Human Hsp70 molecular chaperone binds two calcium ions within the ATPase domain. *Structure*, 5, 403-413.

Swain, J. F., Dinler, G., Sivendran, R., Montgomery, D. L., Stotz, M., & Gierasch, L. M. (2007). Hsp70 chaperone ligands control domain association via an allosteric mechanism mediated by the interdomain linker. *Molecular Cell, 26*(1), 27-39.

Vogel, M., Bukau, B., & Mayer, M. P. (2006a). Allosteric regulation of Hsp70 chaperones by a proline switch.*Molecular Cell, 21*(3), 359-367.

Vogel, M., Mayer, M. P., & Bukau, B. (2006b). Allosteric regulation of Hsp70 chaperones involves a conserved interdomain linker. *Journal of Biological Chemistry, 281*(50), 38705-38711.

Vos, M. J., Hageman, J., Carra, S., & Kampinga, H. H. (2008). Structural and functional diversities between members of the human HSPB, HSPH, HSPA, and DNAJ chaperone families. *Biochemistry, 47*(27), 7001-7011.

Warrick, J. M., Chan, H. Y., Gray-Board, G. L., Chai, Y., Paulson, H. L., & Bonini, N. M. (1999). Suppression of polyglutamine-mediated neurodegeneration in Drosophila by the molecular chaperone HSP70. *Nature Genetics, 23*(4), 425-428.

Wilbanks, S. M., DeLuca-Flaherty, C., & McKay, D. B. (1994). Structural basis of the 70-kilodalton heat shock cognate protein ATP hydrolytic activity. I. Kinetic analyses of active site mutants. *The Journal of Biological Chemistry, 269*(17), 12893-12898.

Wilbanks, S. M., & McKay, D. B. (1995). How Potassium Affects the Activity of the Molecular Chaperone Hsc70. *The Journal of Biological Chemistry, 270*(5), 2251-2257.

Zhu, X., Zhao, X., Burkholder, W. F., Gragerov, A., Ogata, C. M., Gottesman, M. E., & Hendrickson, W. A. (1996). Structural analysis of substrate binding by the molecular chaperone DnaK. *Science, 272*(5268), 1606-1614.

Zhuravleva, A., & Gierasch, L. M. (2011). Allosteric signal transmission in the nucleotide-binding domain of 70-kDa heat shock protein (Hsp70) molecular chaperones. *Proceedings of the National Academy of Sciences of the United States of America, 108*(17).

APPENDICES

APPENDIX A: Details of Mutant Effects on Hsp70s

APPENDIX B: Materials

APPENDIX C: Laboratory Equipments

APPENDIX D: Sequence Analysis of Mutants

APPENDIX A : **Details of Mutant Effects on Hsp70s**

Table A : Details of mutant effects on Hsp70s**.** The comparative adjectives, such as "similar", "lower" and "higher", are used to compare mutants with wild type protein activity.

Mutation	Homolog of Hsp70	Length of Hsp70	Effect	Publication
E171A	DnaK	Full-length	Inability to grow at 42ºC, lack of λ DNA replication, inability to refold of denatured luciferase, 6.5 fold increased K_m for ATP, 4 fold higher V_{max}, 6 fold increased K_d for peptide, no ATP hydrolysis stimulation by peptide, defective in ATP-dependent release of bound peptides, trypsin cleavage pattern did not change in the addition of ATP	(Buchberger *et al.*, 1994)
E171L	DnaK	Full-length	Inability to grow at 42ºC, lack of λ DNA replication, inability to refold of denatured luciferase, 12 fold increased K_m for ATP, 2.5 fold higher V_{max}, 4 fold increased K_d for peptide, no ATP hydrolysis stimulation by peptide, defective in ATP-dependent release of bound peptides, different trypsin cleavage pattern,	(Buchberger *et al.*, 1994)
E171K	DnaK	Full-length	Inability to grow at 42ºC, lack of λ DNA replication, inability to refold of denatured luciferase, 18 fold increased K_m for ATP, 13 fold higher V_{max}, 4 fold increased K_d for peptide, no ATP hydrolysis stimulation by peptide, defective in ATP-dependent release of bound peptides, different trypsin cleavage pattern	(Buchberger *et al.*, 1994)
E171S	DnaK	Full-length	Normal holdase activity, 0.7 fold intrinsic ATPase rate, no DnaJ, GrpE and substrate stimulation on ATPase rate	(Chang *et al.*, 2010)
T199A	DnaK	Full-length	Normal holdase activity, 0.3 fold intrinsic ATPase rate, no DnaJ, GrpE and substrate stimulation on ATPase rate	(Chang *et al.*, 2010)
L177A	DnaK	Full-length	1.5 fold holdase activity, 1.8 fold intrinsic ATPase rate, slightly reduced	(Chang *et al.*, 2010)

Table A (continued) : Details of mutant effects on Hsp70s. The comparative adjectives, such as "similar", "lower" and "higher", are used to compare mutants with wild type protein activity.

Mutation	Homolog of Hsp70	Length of Hsp70	Effect	Publication
			DnaJ stimulation on ATPase rate, reduced GrpE stimulation on ATPase rate, normal substrate stimulation on ATPase rate	
V192A	DnaK	Full-length	Normal holdase activity, 2.2 fold intrinsic ATPase rate, reduced DnaJ stimulation on ATPase rate, increased GrpE stimulation on ATPase rate, slightly reduced substrate stimulation on ATPase rate	(Chang *et al.*, 2010)
Y193A	DnaK	Full-length	Normal holdase activity, 3 fold intrinsic ATPase rate, increased DnaJ stimulation on ATPase rate, increased GrpE stimulation on ATPase rate, increased substrate stimulation on ATPase rate	(Chang *et al.*, 2010)
I373A	DnaK	Full-length	1.3 fold holdase activity, 2.1 fold intrinsic ATPase rate, no DnaJ stimulation on ATPase rate, reduced GrpE stimulation on ATPase rate, no substrate stimulation on ATPase rate	(Chang *et al.*, 2010)
T12A	DnaK	Full-length	2 fold holdase activity, 1.7 fold intrinsic ATPase rate, increased DnaJ stimulation on ATPase rate, reduced GrpE stimulation on ATPase rate, increased substrate stimulation on ATPase rate	(Chang *et al.*, 2010)
K55A	DnaK	Full-length	1.5 fold holdase activity, 1.4 fold intrinsic ATPase rate, increased DnaJ stimulation on ATPase rate, no GrpE stimulation on ATPase rate, no substrate stimulation on ATPase rate	(Chang *et al.*, 2010)
R56A	DnaK	Full-length	2 fold holdase activity, 1.8 fold intrinsic ATPase rate, increased DnaJ, GrpE and substrate stimulation on ATPase rate	(Chang *et al.*, 2010)
F67L	DnaK	Full-length	1.7 fold holdase activity, 0.8 fold intrinsic ATPase rate, no DnaJ, GrpE	(Chang *et al.*, 2010)

Table A (continued) : Details of mutant effects on Hsp70s. The comparative adjectives, such as "similar", "lower" and "higher", are used to compare mutants with wild type protein activity.

Mutation	Homolog of Hsp70	Length of Hsp70	Effect	Publication
			and substrate stimulation on ATPase rate, different trypsin digestion pattern, the ATPase rate stimulated by DnaJ in the presence substrate, increased K_m value	
R71A	DnaK	Full-length	1.5 fold holdase activity, 1.4 fold intrinsic ATPase rate, no DnaJ, GrpE and substrate stimulation on ATPase rate	(Chang *et al.*, 2010)
D85A	DnaK	Full-length	1.3 hold holdase activity, 1.7 fold intrinsic ATPase rate, increased DnaJ stimulation on ATPase rate, reduced GrpE stimulation on ATPase rate, no substrate stimulation on ATPase rate	(Chang *et al.*, 2010)
M89A	DnaK	Full-length	2 fold holdase activity, 2 fold intrinsic ATPase rate, increased DnaJ stimulation on ATPase rate, reduced GrpE stimulation on ATPase rate, increased substrate stimulation on ATPase rate	(Chang *et al.*, 2010)
P90A	DnaK	Full-length	1.5 fold holdase activity, normal intrinsic ATPase rate, increased DnaJ stimulation on ATPase rate, reduced GrpE stimulation on ATPase rate, no substrate stimulation on ATPase rate, different trypsin digestion pattern, the ATPase rate stimulated by DnaJ in the presence substrate, increased K_m value	(Chang *et al.*, 2010)
F91A	DnaK	Full-length	1.5 fold holdase activity, normal intrinsic ATPase rate, no DnaJ, GrpE and substrate stimulation on ATPase rate, different trypsin digestion pattern, the ATPase rate stimulated by DnaJ in the presence substrate, increased K_m value	(Chang *et al.*, 2010)
K106A	DnaK	Full-length	2 fold holdase activity, 3 fold intrinsic ATPase rate, increased DnaJ stimulation on ATPase rate, normal	(Chang *et al.*, 2010)

Table A (continued) : Details of mutant effects on Hsp70s. The comperative adjectives, such as "similar", "lower" and "higher", are used to compare mutants with wild type protein activity..

Mutation	Homolog of Hsp70	Length of Hsp70	Effect	Publication
			GrpE stimulation on ATPase rate, normal substrate stimulation on ATPase rate	
D233A	DnaK	Full-length	1.7 fold holdase activity, 3.3 fold intrinsic ATPase rate, increased DnaJ stimulation on ATPase rate, no GrpE stimulation on ATPase rate, no substrate stimulation on ATPase rate	(Chang *et al.*, 2010)
K263A	DnaK	Full-length	1.5 fold holdase activity, 2 fold intrinsic ATPase rate, no DnaJ, GrpE and substrate stimulation on ATPase rate	(Chang *et al.*, 2010)
G198A	DnaK	Full-length	1.2 fold holdase activity, 1.3 fold intrinsic ATPase rate, normal DnaJ stimulation on ATPase rate, no GrpE stimulation on ATPase rate, no substrate stimulation on ATPase rate	(Chang *et al.*, 2010)
I202A	DnaK	Full-length	1.2 fold holdase activity, 0.9 fold intrinsic ATPase rate, increased DnaJ stimulation on ATPase rate, no GrpE stimulation on ATPase rate, no substrate stimulation on ATPase rate	(Chang *et al.*, 2010)
S203A	DnaK	Full-length	1.3 fold holdase activity, 2.3 fold intrinsic ATPase rate, no DnaJ stimulation on ATPase rate, reduced GrpE stimulation on ATPase rate, no substrate stimulation on ATPase rate	(Chang *et al.*, 2010)
E217A	DnaK	Full-length	1.2 fold holdase activity, 0.7 fold intrinsic ATPase rate, no DnaJ, GrpE and substrate stimulation on ATPase rate	(Chang *et al.*, 2010)
G223A	DnaK	Full-length	1.2 fold holdase activity, 0.3 fold intrinsic ATPase rate, no DnaJ, GrpE and substrate stimulation on ATPase rate	(Chang *et al.*, 2010)
L227A	DnaK	Full-length	1.3 fold holdase activity, 0.6 fold intrinsic ATPase rate, no DnaJ, GrpE and substrate stimulation on ATPase	(Chang *et al.*, 2010)

Table A (continued) : Details of mutant effects on Hsp70s. The comperative adjectives, such as "similar", "lower" and "higher", are used to compare mutants with wild type protein activity.

Mutation	Homolog of Hsp70	Length of Hsp70	Effect	Publication
			rate	
E230A	DnaK	Full-length	2 fold holdase activity, 1.9 fold intrinsic ATPase rate, increased DnaJ stimulation on ATPase rate, reduced GrpE stimulation on ATPase rate, no substrate stimulation on ATPase rate, GrpE can not stimulate the ATPase rate	(Chang *et al.*, 2010)
E230Q	DnaK	Full-length	Normal holdase activity, 0.3 fold intrinsic ATPase rate, increased DnaJ stimulation on ATPase rate, no GrpE stimulation on ATPase rate, no substrate stimulation on ATPase rate	(Chang *et al.*, 2010)
G228A	DnaK	Full-length	1.3 fold holdase activity, 1.4 fold intrinsic ATPase rate, no DnaJ, GrpE and substrate stimulation on ATPase rate	(Chang *et al.*, 2010)
D231N	DnaK	Full-length	0.6 fold holdase activity, 0.3 fold intrinsic ATPase rate, no DnaJ, GrpE and substrate stimulation on ATPase rate, GrpE can not stimulate the ATPase rate	(Chang *et al.*, 2010)
S234A	DnaK	Full-length	0.6 fold holdase activity, 0.3 fold intrinsic ATPase rate, normal DnaJ stimulation on ATPase rate, no GrpE stimulation on ATPase rate, no substrate stimulation on ATPase rate	(Chang *et al.*, 2010)
D152C	bHsc70	Full-length	1.5 fold increased ATPase rate, similar blueshift upon ATP binding, significantly decreased protease resistance by ATP	(Jiang *et al.*, 2005)
D152K	bHsc70	Full-length	2 fold increased ATPase rate, lower blueshift changes upon ATP, significantly decreased protease resistance by ATP	(Jiang *et al.*, 2005)
I216T	bHsc70	Full-length	The same ATPase rate, lower blueshift changes upon ATP, decreased protease	(Jiang *et al.*, 2005)

Table A (continued) : Details of mutant effects on Hsp70s. The comperative adjectives, such as "similar", "lower" and "higher", are used to compare mutants with wild type protein activity.

Mutation	Homolog of Hsp70	Length of Hsp70	Effect	Publication
			resistance by ATP	
I216C	bHsc70	Full-length	Almost the same ATPase rate, similar blueshift upon ATP binding, significantly decreased protease resistance by ATP	(Jiang *et al.*, 2005)
I216H	bHsc70	Full-length	Almost the same ATPase rate, similar blueshift upon ATP binding, decreased protease resistance by ATP	(Jiang *et al.*, 2005)
K325E	bHsc70	Full-length	Slightly decreased ATPase rate, similar blueshift upon ATP binding, significantly increased protease resistance by ATP	(Jiang *et al.*, 2005)
K325C	bHsc70	Full-length	Almost the same ATPase rate, similar blueshift upon ATP binding, significantly decreased protease resistance by ATP	(Jiang *et al.*, 2005)
V388C	bHsc70	Full-length	Almost the same ATPase rate, very low blueshift changes upon ATP, significantly decreased protease resistance by ATP	(Jiang *et al.*, 2005)
L393C	bHsc70	Full-length	Almost the same ATPase rate, very low blueshift changes upon ATP, significantly decreased protease resistance by ATP	(Jiang *et al.*, 2005)
I216C/ G229S	bHsc70	Full-length	0.5 fold decreased ATPase rate, lack of blueshift changes upon ATP	(Jiang *et al.*, 2005)
V388C/ L393C	bHsc70	Full-length	One third of wt ATPase rate, very low blueshift changes upon ATP, significantly decreased protease resistance by ATP	(Jiang *et al.*, 2005)
I216C/ V388C	bHsc70	Full-length	The same ATPase rate, lower blueshift changes upon ATP, significantly decreased protease resistance by ATP	(Jiang *et al.*, 2005)
V389D	DnaK	Full-length	No growth at 37ºC, no effect on intrinsic ATPase activity and intrinsic	(Kumar *et al.*, 2011)

Table A (continued) : Details of mutant effects on Hsp70s. The comperative adjectives, such as "similar", "lower" and "higher", are used to compare mutants with wild type protein activity.

Mutation	Homolog of Hsp70	Length of Hsp70	Effect	Publication
			peptide binding affinity, no blueshift changes upon ATP, very low fold of stimulation over the range of the peptide concentration, no fold of stimulation by DnaJ, SRP signal on DnaK-DnaJ interaction is 10% that of the wt DnaK protein	
V389A	DnaK	Full-length	No growth at 37ºC, no effect on intrinsic ATPase activity and intrinsic peptide binding affinity, no blueshift changes upon ATP, very low fold of stimulation over the range of the peptide concentration, no fold of stimulation by DnaJ, SRP signal on DnaK-DnaJ interaction is similar to the wt DnaK protein	(Kumar *et al.*, 2011)
L390D	DnaK	Full-length	No growth at 37ºC, no effect on intrinsic ATPase activity and intrinsic peptide binding affinity, similar blueshift changes to wt, fold of stimulation over the range of peptide concentration, no fold of stimulation by DnaJ, no SRP signal on DnaK-DnaJ interaction	(Kumar *et al.*, 2011)
L390A	DnaK	Full-length	No growth at 37ºC, no effect on intrinsic ATPase activity and intrinsic peptide binding affinity, similar blueshift changes to wt, fold of stimulation over the range of peptide concentration, DnaJ can stimulate ATPase activity, SRP signal on DnaK-DnaJ interaction is 10% that of the wt DnaK protein	(Kumar *et al.*, 2011)
L391D	DnaK	Full-length	No growth at 37ºC, no effect on intrinsic ATPase activity and intrinsic peptide binding affinity, no blueshift changes upon ATP, very low fold of stimulation over the range of the peptide concentration, no fold of stimulation by	(Kumar *et al.*, 2011)

Table A (continued) : Details of mutant effects on Hsp70s. The comperative adjectives, such as "similar", "lower" and "higher", are used to compare mutants with wild type protein activity.

Mutation	Homolog of Hsp70	Length of Hsp70	Effect	Publication
			DnaJ, no SRP signal on DnaK-DnaJ interaction	
L391A	DnaK	Full-length	Significant defect in growth at 37ºC, no effect on intrinsic ATPase activity and intrinsic peptide binding affinity, small degree of blueshift upon ATP binding, very low fold of stimulation over the range of the peptide concentration, no fold of stimulation by DnaJ, SRP signal on DnaK-DnaJ interaction is 10% that of the wt DnaK protein	(Kumar *et al.*, 2011)
L392D	DnaK	Full-length	No growth at 37ºC, no effect on intrinsic ATPase activity and intrinsic peptide binding affinity, similar blueshift changes to wt, fold of stimulation over the range of peptide concentration, no fold of stimulation by DnaJ, no SRP signal on DnaK-DnaJ interaction	(Kumar *et al.*, 2011)
L392A	DnaK	Full-length	No growth at 37ºC, no effect on intrinsic ATPase activity and intrinsic peptide binding affinity, similar blueshift changes to wt, fold of stimulation over the range of peptide concentration, no fold of stimulation by DnaJ, no SRP signal on DnaK-DnaJ interaction	(Kumar *et al.*, 2011)
N173D	Sse1	Full-length	Ability to grow at 37-40ºC	(Liu and Hendrickson, 2007)
T176D	Sse1	Full-length	Ability to grow at 37-40ºC	(Liu and Hendrickson, 2007)
T176V	Sse1	Full-length	Ability to grow at 37-40ºC	(Liu and Hendrickson, 2007)
F392D	Sse1	Full-length	Ability to grow at 37-40ºC	(Liu and Hendrickson, 2007)

Table A (continued) : Details of mutant effects on Hsp70s. The comperative adjectives, such as "similar", "lower" and "higher", are used to compare mutants with wild type protein activity.

Mutation	Homolog of Hsp70	Length of Hsp70	Effect	Publication
D159A	Sse1	Full-length	Ability to grow at 37-40ºC	(Liu and Hendrickson, 2007)
I163D	Sse1	Full-length	Inability to grow at 37-40ºC	(Liu and Hendrickson, 2007)
R235E	Sse1	Full-length	Inability to grow at 37-40ºC	(Liu and Hendrickson, 2007)
N172D	Ssa1	Full-length	Inability to grow at 37-40ºC	(Liu and Hendrickson, 2007)
T175D	Ssa1	Full-length	Inability to grow at 37-40ºC	(Liu and Hendrickson, 2007)
T175V	Ssa1	Full-length	Ability to grow at 37-40ºC	(Liu and Hendrickson, 2007)
L388D	Ssa1	Full-length	Inability to grow at 37-40ºC	(Liu and Hendrickson, 2007)
D158A	Ssa1	Full-length	Ability to grow at 37-40ºC	(Liu and Hendrickson, 2007)
I162D	Ssa1	Full-length	Inability to grow at 37-40ºC	(Liu and Hendrickson, 2007)
E228R	Ssa1	Full-length	Inability to grow at 37-40ºC	(Liu and Hendrickson, 2007)
N170D	DnaK	Full-length	Inability to grow at 37-40ºC	(Liu and Hendrickson, 2007)
T173D	DnaK	Full-length	Inability to grow at 37-40ºC	(Liu and Hendrickson, 2007)
T173V	DnaK	Full-length	Ability to grow at 37-40ºC	(Liu and Hendrickson, 2007)
V389D	DnaK	Full-length	Inability to grow at 37-40ºC	(Liu and Hendrickson, 2007)

Table A (continued) : Details of mutant effects on Hsp70s. The comperative adjectives, such as "similar", "lower" and "higher", are used to compare mutants with wild type protein activity.

Mutation	Homolog of Hsp70	Length of Hsp70	Effect	Publication
D156A	DnaK	Full-length	Ability to grow at 37-40ºC	(Liu and Hendrickson, 2007)
I160D	DnaK	Full-length	Inability to grow at 37-40ºC	(Liu and Hendrickson, 2007)
E230R	DnaK	Full-length	Inability to grow at 37-40ºC	(Liu and Hendrickson, 2007)
T199D, T199A, T199V	DnaK	Full-length	The site of autophosphorylation	(McCarty and Walker, 1991)
K71E,K71A, K71M	bHsc70	Full-length	ATP binding is detected, but the mutants are devoid of ATPase activity	(O'Brien *et al.*, 1996)
T13G, T13S, T13V	bHsc70	Full-length	Loss of ability for interdomain coupling except T13S, the hydroxyl group of Thr is important on the position of 13.	(Sousa and McKay, 1998)
P143A	DnaK	Full-length	Decreased basal ATPase rate, stimulation ATPase rate by substrate or a combination of DnaJ and substrate, the rate for ATP stimulated substrate release was only one fifth of the wild-type rate, had an emission maximum at a similar wavelength as DnaKwt in the nucleotide- free state, but one third of blueshift upon ATP to compare wtDnaK, in the absence of peptide the blueshift is similar to wtDnaK, K_d is increased by 4 fold according to wtDnaK, decreased the enthalpy of activation strongly by 30%	(Vogel *et al.*, 2006a)
P143G	DnaK	Full-length	Lack of refolding denaturated luciferase, decreased basal	(Vogel *et al.*, 2006a)

Table A (continued) : Details of mutant effects on Hsp70s. The comperative adjectives, such as "similar", "lower" and "higher", are used to compare mutants with wild type protein activity.

Mutation	Homolog of Hsp70	Length of Hsp70	Effect	Publication
			rate, stimulation ATPase rate by substrate or a combination of DnaJ and substrate, similar to wtDnaK for peptide dissociation rate, had an emission maximum at a similar wavelength as DnaKwt in the nucleotide- free state, but very small blueshift upon addition of ATP, K_d is increased by 9 fold according to wtDnaK, decreased the enthalpy of activation strongly by 30%	
R151A	DnaK	Full-length	Lack of refolding denaturated luciferase, increased basal ATPase rate, but lack of stimulation of ATPase rate by substrate or DnaJ, lack of stimulation of peptide stimulation rate by ATP, had an emission maximum at a similar wavelength as DnaKwt in the nucleotide-free state, lack of blueshift of tryptophan fluorescence upon ATP, K_d is almost the same to wtDnaK, decreased the enthalpy of activation strongly by 20%	Vogel *et al.*, 2006a)
R151K	DnaK	Full-length	Increased basal ATPase rate, but lack of stimulation of ATPase rate by substrate or DnaJ, had an emission maximum at a similar wavelength as DnaKwt in the nucleotide- free state, almost lack of blueshift upon ATP, one third of blueshift upon ATP to compare wtDnaK	(Vogel *et al,*, 2006a)
E171D, E171Q	DnaK	Full-length	Lack of refolding denaturated luciferase, decreased basal ATPase rate, stimulation ATPase rate by substrate or a combination of DnaJ and substrate, had an emission maximum at a similar wavelength as DnaKwt in the nucleotide- free state, the rates for ATP stimulated substrate release were almost one third of the wild-type rate, one third of	(Vogel *et al.*, 2006a)

Table A (continued) : Details of mutant effects on Hsp70s. The comperative adjectives, such as "similar", "lower" and "higher", are used to compare mutants with wild type protein activity.

Mutation	Homolog of Hsp70	Length of Hsp70	Effect	Publication
			blueshift upon ATP to compare wtDnaK	
R167A	DnaK	Full-length	Sensitive to elevated temperature, first transition $T_m$value is 3ºC higher in CD measurement, lack of ATP stimulated substrate release, lack of substrate release in the absence of nucleotide, peptide dissociation rate increases in the presence of ATP, no blueshift in the absence of nucleotide but ATP induces blueshift of tryptophan fluorescence, increased basal ATPase rate and DnaJ stimulation is very low, substrate stimulation for ATPase rate is normal, reduced synergistically stimulated ATPase rate	(Vogel *et al.*, 2006b)
R167D	DnaK	Full-length	Sensitive to elevated temperature, first transition $T_m$value is 4ºC higher in CD measurement, lack of ATP stimulated substrate release, lack of blueshift of tryptophan fluorescence, increased basal ATPase rate, increased basal ATPase rate and DnaJ stimulation is very low, lack of substrate stimulation for ATPase rate, lack of synergistically stimulated ATPase rate	(Vogel *et al.*, 2006b)
D393A	DnaK	Full-length	Sensitive to elevated temperature, first transition $T_m$value is similar to wt, lack of blueshift of tryptophan fluorescence, increased basal ATPase rate and DnaJ stimulation is very low, lack of substrate stimulation for ATPase rate, lack of synergistically stimulated ATPase rate	(Vogel *et al.*, 2006b)
D393R	DnaK	Full-length	Sensitive to elevated temperature, first transition $T_m$value is 4ºC higher in CD measurement, lack of ATP stimulated substrate release, lack of blueshift of tryptophan fluorescence, increased basal ATPase rate and DnaJ stimulation is very low, lack of substrate stimulation for ATPase rate	(Vogel *et al.*, 2006b)

Table A (continued) : Details of mutant effects on Hsp70s. The comperative adjectives, such as "similar", "lower" and "higher", are used to compare mutants with wild type protein activity.

Mutation	Homolog of Hsp70	Length of Hsp70	Effect	Publication
D388R	DnaK	Full-length	Not sensitive to elevated temperature, ATPase stimulated substrate release, tryptophan fluorescence blushift and ATPase rate are similar to full-length DnaK but DnaJ stimulation for ATPase rate is higher to compare wt	(Vogel *et al.*, 2006b)
R151A, K155D, R167D	DnaK	(2-393)	Greatly increased basal ATPase rate	(Vogel *et al.*, 2006b)
D393A, D393R	DnaK	(2-393)	Increased basal ATPase rate	(Vogel *et al.*, 2006b)
K155A	DnaK	Full-length	Sensitive to elevated temperature, first transition Tmvalue is 2ºC higher in CD measurement, lack of substrate release in the absence of nucleotide, peptide dissociation rate increases in the presence of ATP, no blueshift in the absence of nucleotide but ATP induces blueshift of tryptophan fluorescence, increased basal ATPase rate, DnaJ stimulation for ATPase rate is higher than wt, substrate stimulation for ATPase rate is normal, reduced synergistically stimulated ATPase rate	(Vogel et al., 2006b)
K155D	DnaK	Full-length	Sensitive to elevated temperature, first transition Tmvalue is 6ºC higher in CD measurement, lack of ATP stimulated substrate release, no blueshift in the absence of nucleotide but ATP induces blueshift of tryptophan fluorescence, increased basal ATPase rate, substrate stimulation for ATPase rate is normal, reduced synergistically stimulated ATPase rate,	(Vogel *et al.*, 2006b)
D199N, D199S	bHsc70	Full-length	The most severe effect on $k_{cat,}$, reducing it 2 orders of magnitude form wt, have no signicifant effect on K_m	(Wilbanks *et al.*, 1994)

Table A (continued) : Details of mutant effects on Hsp70s. The comperative adjectives, such as "similar", "lower" and "higher", are used to compare mutants with wild type protein activity.

Mutation	Homolog of Hsp70	Length of Hsp70	Effect	Publication
E175Q, E175S	bHsc70	Full-length	An order of magnitude decrease in k_{cat}, 2 orders of magnitude increase in K_m	(Wilbanks *et al.*, 1994)
D206N, D206S	bHsc70	Full-length	Has similar K_m and $k_{cat,}$ to wt	(Wilbanks *et al.*, 1994)
4A (V389A, L390A, L391A, L392A)	DnaK	(2-392)	Completely loss of increaes basal ATPase rate which DnaK (2-392) has	(Vogel *et al.*, 2006b)
D10N, D10S	bHsc70	Full-length	The most severe effect on $k_{cat,}$, reducing it 2 orders of magnitude form wt, an order of magnitude increase in K_m	(Wilbanks *et al.*, 1994)

APPENDIX B : Materials

Luria Bertani (LB) Medium

10g tryptone (Fluka), 5g yeast extract (Himedia Laboratories), 10g NaCl (Merck) were dissolved in distilled water and completed up to 1 lt. It was sterilized for 15 minutes under 1.5 atm at 121°C. The medium was stored at room temperature.

LB Agar Medium

10 g tryptone (Fluka), 5 g yeast extract (Himedia Laboratories), 10 g NaCl (Merck), 15 g agar (Merck) were dissolved in distilled water and completed up to 1 lt. And sterilized for 15 minutes under 1.5 atm at 121 °C. The medium was poured to the plates

SDS-PAGE

To prepare the running gel, 2.41 ml H_2O, 3.04 ml 40% acryl-bisacrylamide, 1.9 ml 1.5 M Tris pH 8.8, 75 µl 10% SDS were dissolved, afterwards 75 µl 10% APS and 3 µl TEMED were added just before pouring the solution into the gel cassette. The 1-2 mm of isopropanol was overlayed to ensure a flat interface between the running and stacking gels and it was required 30 min to polymerize the gel. To prepare the stacking gel, 1.46 ml ml H_2O, 0.27 ml 40% acryl-bisacrylamide, 0.25 ml 1.5 M Tris pH 6.8, 20 µl 10% SDS, 20 µl 10% APS and 2 µl TEMED were dissolved and the cassette was filled with the mixture. The comb was inserted to the gel before polymerization.

Native Gel Electrophoresis

The running gel contains 3.96 ml H_2O, 2 ml 40% acryl-bisacrylamide, 2 ml 1.5 M Tris pH 8.8. Since dissolved oxygen prevents to polymerization, this mixture is degassed before adding 40 µl 10% APS and 4 µl TEMED. The 1-2 mm of isopropanol was overlayed to ensure a flat interface between the running and stacking gels and it was required approximately 30 min to polymerize the gel. The stacking gel consists of 1.295 ml H_2O, 0.187 ml 40% acryl-bisacrylamide, 0.5 ml 0,5 M Tris pH 6.8 and again degassing should be done before adding 16.67 µl 10% APS and 2.5 µl TEMED. Electrophoresis buffer is composed of 3 g Tris-base and 14.4 g glycine into 1 L of distilled water and final pH is adjusted to 8.3.

Table B : The chemicals used in this study.

Chemical	Company	Country
DTT	Applicem	Germany
TEMED	Sigma	Germany
Coomassie brilliant blue	Molecula	UK
Glycin	Sigma	Germany
APS	Molekula	UK
40% Acrylamide/Bis	BioRad	USA
SDS	Molekula	UK
ATP	Sigma	Germany
$Mg(OAc)_2$	Merck	Germany
PEP	Sigma-Aldrick	Germany
B-NADH	Sigma	Germany
PK/LDH	Sigma	Germany
Glycerol	Merck	Germany
Ethanol	Merck	Germany
Methanol	Emboy	Turkey
Acetic acid	Merck	Germany
Lysozyme	Fluka	Germany
Ampicilin	Roth	Germany
Chloramphenicol	Applichem	Germany
IPTG	Peqlab	Germany
PMSF	Molekula	UK
Leupeptin	Roth	Germany
Pepstatin A	Roth	Germany
DEAE Sephacel	GE Heathcare	UK
Adenosine 5-diphosphate Agarose	Sigma	Germany
Agarose	Peqlab	Germany
$MgCl_2$	Merck	Germany
KCl	Carlo Erba Reagents	Italy
Hepes	Fisher Scientific	UK
Tris(hydroxymetyl) aminomethane; 99%	ABCR	Germany

Table B (continued) : The chemicals used in this study.

Chemical	Company	Country
EDTA	Molekula	UK
NaCl	Merck	Germany

APPENDIX C: Laboratory Equipments

Autoclave	**:** Systec GmbH Labor-Systemtechnik, Germany
Centrifuges	**:** Thermo Scientific, MicroCL 17, USA**;** Beckman Coulter; AvantiJ30I, USA; Bechman Coulter, Allegra 25R Centrifuge, USA
Deep freezers and refrigerators	**:** -80ºC New Brunswick Scientific, Ultra low Temperature Freezer, U410 Premium, USA; -20ºC and +4ºC Bosch Refrigerator, Germany
Electrophoresis Equipments	**:** GE Healthcare, UK
Gel Documentation System	**:** BioRad GS-800 Calibrated Densitometer, USA
Gel Dryer	**:** BioRad, Model 583, USA
Ice Machine	**:** Scotsman, AF 80, USA
Laminar Flow Cabinet	**:** Faster BH-EN2003, Italy
Magnetic Stirrer	**:** Dragon Lab, MS-H-S, China
Orbital Shaker	**:** BioLab Certolab SII
Flat shaker	**:** Heidolph, Duomax 1030, Germany
pH meter	**:** Mettler Toledo, Five Easy, Switzerland
Micropipets	**:** Gilson pipette, USA
Thermal Cycler	**:** Applied Biosystems, GeneAmp, PCR System 2700, USA
Vortex	**:** Dragon Lab MX-F, China
UV-Visible Spectrophometer	**:** Shimadzu UV-1700, Japan; Thermo Scientific, NanoDrop 2000 Spectrophometer, USA
Multiplate Spectrophotometer	**:** BioRad Benchmark Plus, UK
FPLC	**:** BioRad Biologic DuaFlow, UK
Water bath	**:** Nüve, BM 302, Turkey

Ultrasonicator	**:** Bandelin, Sonoplus
Ultrasonic bath	**:** Elma, TranssonicTP690, Germany
Balances	**:** Precisa XB 220A, Switzerland; Precisa BJ610C, Switzerland
Circular Dichroism	**:** Jasco J-815 spectrapolarimeter, USA

APPENDIX D: Sequence Data of Mutants

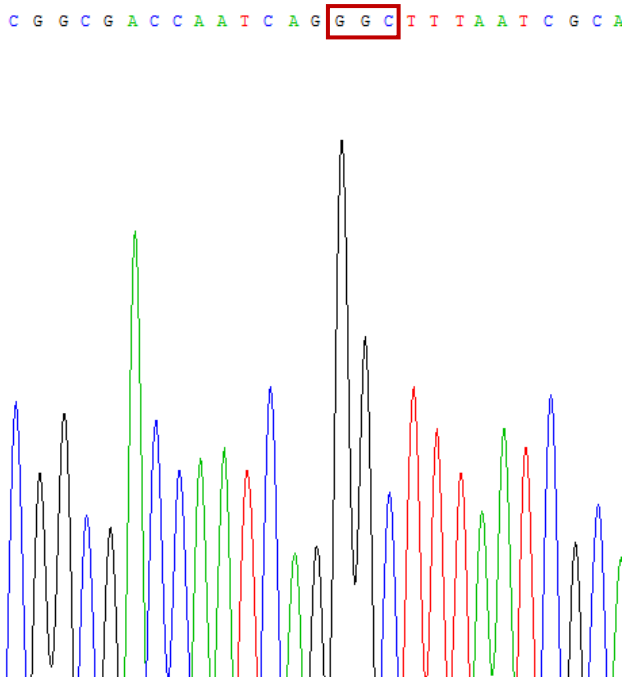

Figure D.1 : Sequence analysis of R71A. The changed codon in red regtangle is shown as reverse complement of alanine codon (GCC).

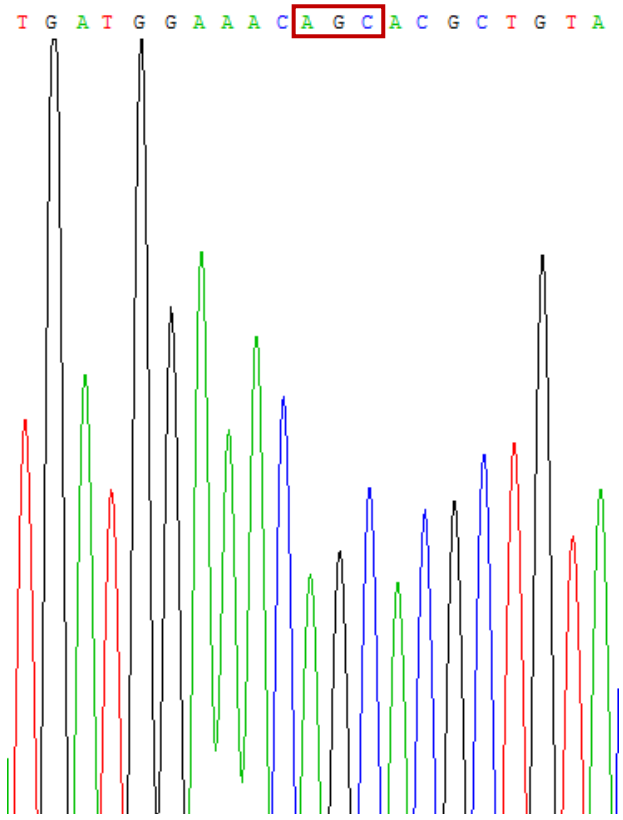

Figure D.2 : Sequence analysis of D85A. The changed codon in red regtangle is shown as reverse complement of alanine codon (GCT).

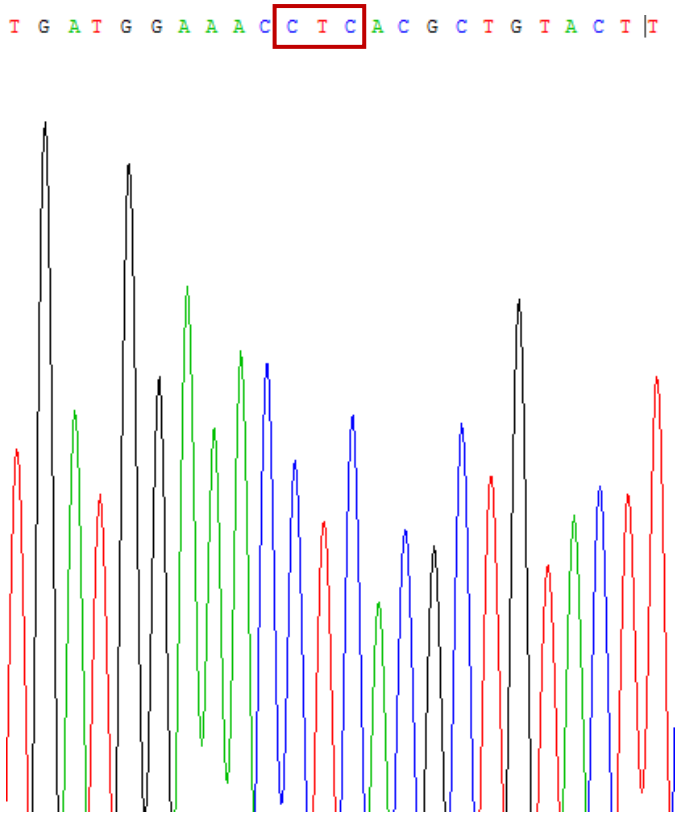

Figure D.3 : Sequence analysis of D85E. The changed codon in red regtangle is shown as reverse complement of glutamic acid codon (GAG).

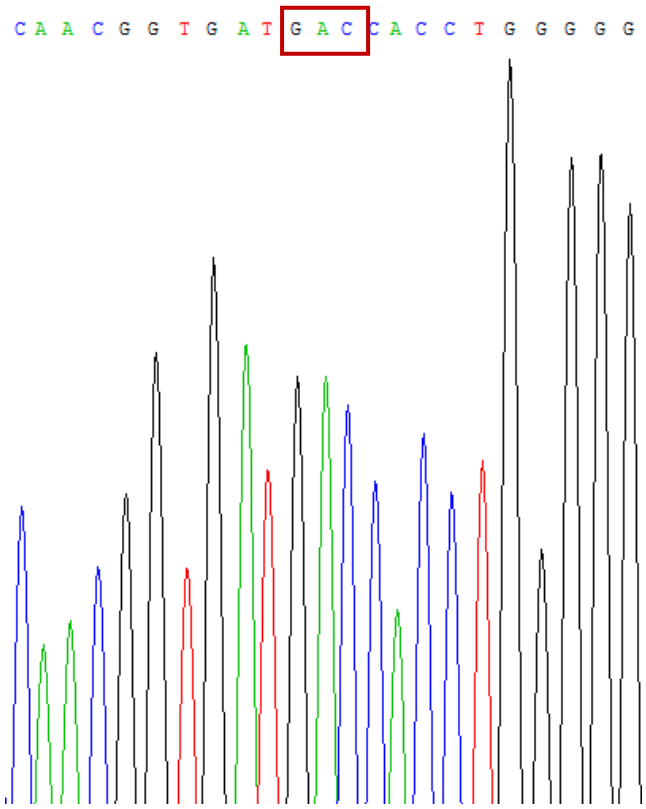

Figure D.4 : Sequence analysis of T225D. The changed codon is shown in red regtangle.

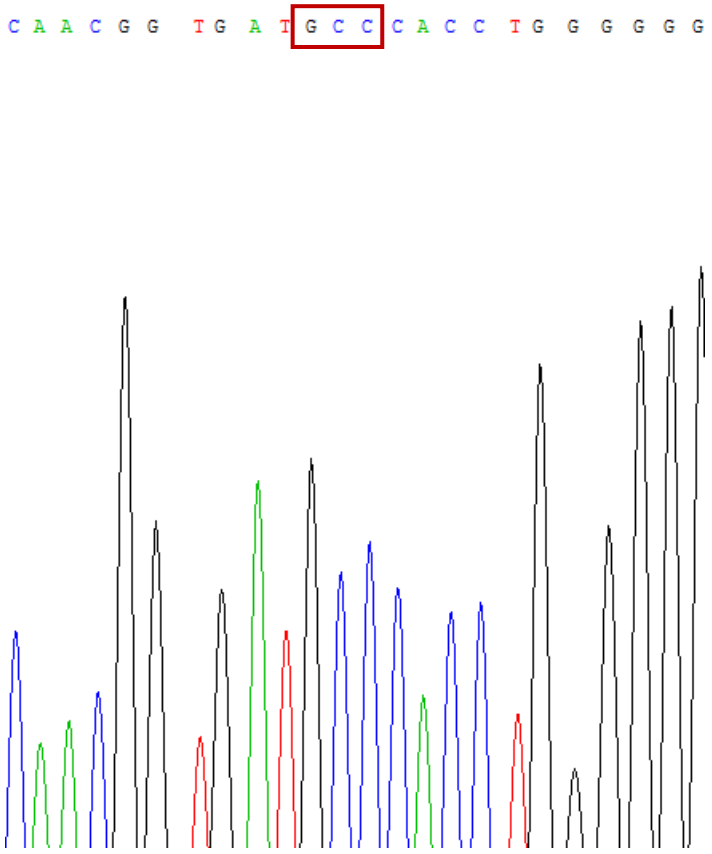

Figure D.5 : Sequence analyis of T225A. The changed codon is shown in red regtangle.

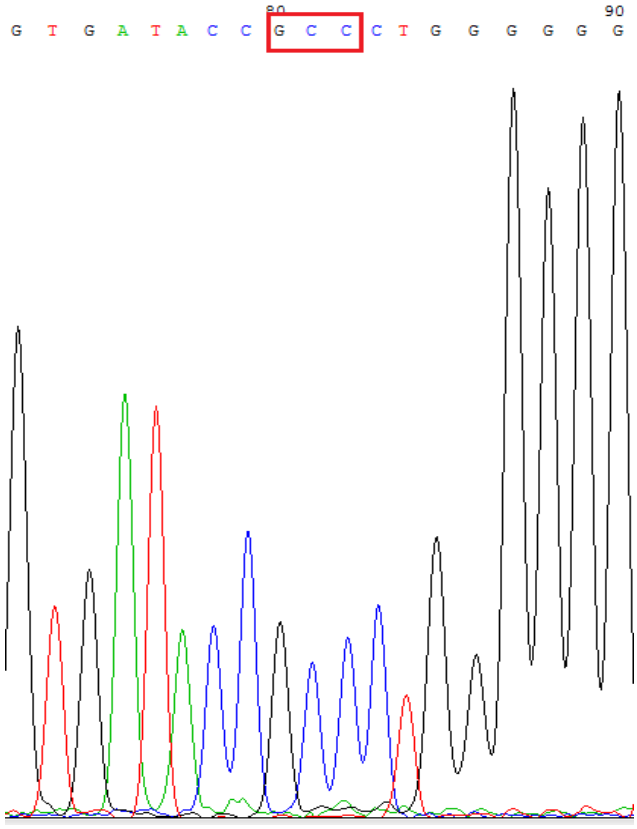

Figure D.6 : Sequence analysis of H226A. The changed codon is shown in red regtangle.

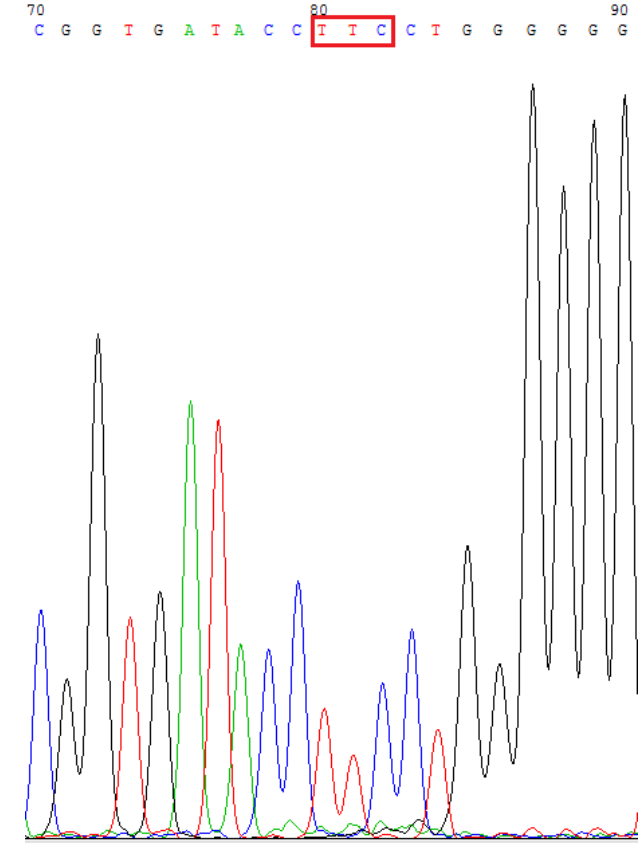

Figure D.7: Sequence analysis of H226F. The changed codon is shown in red regtangle

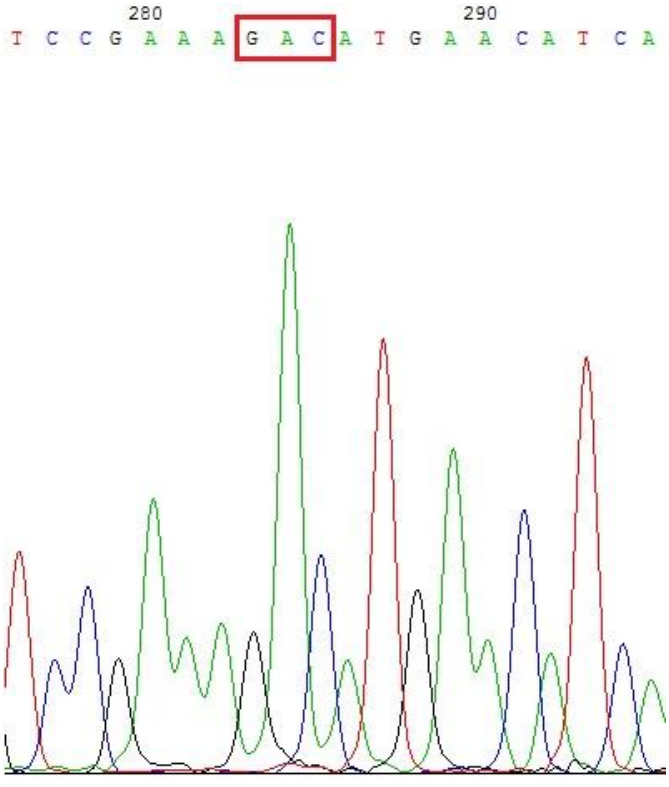

Figure D.8 : Sequence analysis of H295D. The changed codon is shown in red regtangle

CURRICULUM VITAE

Name Surname: İrem AVCILAR

Place and Date of Birth: Adapazarı - 02.05.1987

Address: Gülbahar mah. Çulluk sok. No:38 D:7 Şişli/İstanbul

E-Mail: iremavcilar@hotmail.com

B.Sc.: Department of Molecular Biology and Genetics

Istanbul University

PUBLICATIONS/PRESENTATIONS ON THE THESIS

- **İ. Avcılar**, U. Günsel, A. Kıçik, G. Gün, G. Dinler-Doğanay (2011), Investigating allosteric sites that are critical for ATPase activation in Hsp70 molecular chaperone, DnaK, when stimulated by a substrate, FEBS Journal, Volume 278, pp 93.
- **İ. Avcılar**, U. Günsel, A. Kıçik, G. Gün, G. Dinler-Doğanay (2011), Identificaton of allosteric residues in the ATPase domain of Hsp70 molecular chaperones upon substrate binding, In vivo, Volume 25, pp 512.